VNIVERSITAT DE VALÈNCIA

Doctorado en BIOMEDICINA Y FARMACIA

Analysis of the molecular mechanisms that mediate the therapeutic actions of glucocorticoids in skin

Tesis doctoral presentada por:

Elena Carceller Zazo

Directores

Dra. Paloma Pérez Sánchez

Dra. Pilar D'Ocon Navaza

Valencia, 2017

VNIVERSITAT DE VALÈNCIA

INSTITUTO DE BIOMEDICINA DE VALENCIA CSIC

Doctorado en Biomedicina y Farmacia

Dña. Paloma Pérez Sánchez del Instituto de Biomedicina de Valencia (CSIC) y Dña. Pilar D'Ocon Navaza de la Facultad de Farmacia (Universidad de Valencia)

CERTIFICAN:

Que el trabajo presentado por la Lda. Elena Carceller Zazo, titulado "Analysis of the molecular mechanisms that mediate the therapeutic actions of glucocorticoids in skin", para obtener el grado de Doctor, ha sido realizado en el Instituto de Biomedicina de Valencia (CSIC), bajo nuestra dirección y asesoramiento.

Concluido el trabajo experimental y bibliográfico, autorizamos la presentación de la Tesis, para que sea juzgado por el tribunal correspondiente.

Lo que firmamos en Valencia a 4 de mayo de 2017

Dra. Paloma Pérez Sánchez Dra. Pilar D'Ocon Navaza

La presente tesis doctoral ha sido realizada con el apoyo económico de los proyectos de investigación que se enumeran a continuación

SAF2011-28115

SAF2014-59474-R

Elena Carceller Zazo ha disfrutado de una beca predoctoral de Formación de Profesorado Universitario (FPU) (AP2010-6094) otorgada por el Ministerio de Educación, Cultura y Deporte y de una beca concedida para la realización de estancia breve con referencia EST14/00508.

Este estudio se ha realizado en el Instituto de Biomedicina de Valencia (IBV-CSIC), bajo la dirección de la Dra. Paloma Pérez Sánchez y la Dra. Pilar D'Ocon Navaza.

Table of Contents

Chapter II: Aims of the study

Chapter III: Material and Methods

Summary

Synthetic glucocorticoids (GCs) have been widely used for the treatment of autoimmune and inflammatory diseases and exert their actions through binding to the GC receptor (GR) (Ramamoorthy and Cidlowski, 2016). GR is a transcription factor (TF) belonging to the nuclear receptor (NR) superfamily that mediates a wide range of important physiological processes (Sacta *et al.*, 2016). Upon ligand binding, GR translocates to the nucleus and exert its actions either through binding to DNA or interacting with other TFs. Direct transcriptional regulation by GR involves its binding to specific DNA regulatory sequences called GC responsive elements or GREs.

For a long time, it was postulated that GR induced their anti-inflammatory effects exclusively through transrepression by inhibiting known inflammatory pathways, including NF-κB, AP-1 and MAPKs (Weikum *et al.*, 2017). However, it is now accepted that transcriptional induction of several classic GRE-containing targets is also key for the anti-inflammatory actions of the GR (De Bosscher and Haegeman, 2009). Continuous treatment or high doses of GCs may lead to unwanted side effects (skin atrophy), which may have a big impact in population (Sacta *et al.*, 2016). Therefore it is important to understand the mechanisms by which GR regulates transcription in skin and their impact on the therapeutic and adverse effects of GCs.

In part I of this dissertation, we studied the regulation of *GC-induced leucine zipper (Gilz/Tsc22d3)* and *Zinc Finger Protein 36/Tristetraprolin* (*Zfp36/Ttp)*, two primary transcriptional GR targets containing GRE binding motifs, in epidermal keratinocytes. These and other GC-targets were previously identified in our laboratory by GR ChIP-seq assays in which GRE, Krüppel-like factor (KLF), and AP-1 were the most overrepresented binding motifs. Given the relevance of GR and Krüppel-like factor 4 (KLF4) in skin, we have analysed the

functional interactions between these TFs and their impact on *Gilz/Tsc22d3* and *Zfp36/Ttp* gene expression.

Loss of function experiments of GR and KLF4 demonstrated total GR but partial KLF4 requirement for full gene induction in response to dexamethasone (Dex). In calcium-induced terminally differentiatied keratinocytes, GR and KLF4 protein expression increased concomitant with *Gilz/Tsc22d3* and *Zfp36/Ttp* up-regulation. However, GR-deficient cells failed to differentiate or fully induce *Gilz, Zfp36* and *Klf4* correlating with an augmented expression of *Trp63,* a known transcriptional repressor of KLF4 which is epithelium-specific. The identified transcriptional cooperation between GR and KLF4 may determine cell-type specific regulation and have implications for developing therapies for skin diseases.

In part II of this dissertation, we have investigated GILZ, which has been shown to act as anti-inflammatory mediator in several cell types similar to GCs but without producing the GC-associated side effects. In contrast, little is known about the role of GILZ in skin function. Thus, we decided to study consequences of GILZ overexpression in psoriasis, an autoimmune inflammatory skin disease, where keratinocytes and immune cells play an important role. For this purpose we used an Imiquimod (IMQ)-induced psoriasis model in mice with generalized overexpression of GILZ (GILZ-Tg). Unexpectedly, GILZ-Tg showed more susceptibility to the IMQ-induced psoriasis, displaying more severe skin alterations shown by histological (increased epidermal hyperplasia and parakeratosis), and biochemical analysis (increased cytokine levels in serum and skin). Importantly, these alterations correlated with skin-specific overactivation of the TGF-β/SMAD signaling, which was recapitulated in cultured keratinocytes. Overall, these findings show that GILZ acts as a pro-inflammatory protein in skin

in an IMQ-induced model of psoriasis and thus caution is advised in its therapeutic use.

Resumen

Los glucocorticoides (GCs) sintéticos han sido ampliamente utilizados para el tratamiento de las enfermedades autoinmunes e inflamatorias y ejercen sus acciones mediante la unión al receptor de GCs (GR en inglés) (Ramamoorthy y Cidlowski, 2016). GR es un factor de transcripción (TF en inglés) que pertenece a la superfamilia de receptores nucleares que media importantes procesos fisiológicos (Sacta *et al.*, 2016). Tras la unión del ligando, GR se transloca al núcleo y ejerce sus acciones mediante la unión a DNA o interaccionando con otros factores de transcripción. La regulación transcripcional directa por GR implica su unión a secuencias reguladoras de ADN específicas llamadas elementos de respuesta a GC o GREs.

Durante mucho tiempo, se postuló que GR inducía sus efectos antiinflamatorios exclusivamente a través de la transrepresión mediante la inhibición de las vías inflamatorias conocidas, incluyendo NF-κB, AP-1 y MAPKs (Weikum et al., 2017). Sin embargo, ahora se acepta que la inducción transcripcional de varias dianas clásicas que contienen GRE también es clave para las acciones anti-inflamatorias de GR (De Bosscher and Haegeman, 2009). El tratamiento continuo o altas dosis de GCs pueden producir efectos secundarios no deseados (atrofia de la piel), lo que puede tener un gran impacto en la población (Sacta et al., 2016). Por lo tanto, es importante comprender los mecanismos por los que GR regula la transcripción en la piel y su impacto en los efectos terapéuticos y adversos de los GCs.

En la parte I de esta tesis se estudió la regulación de *GC-induced leucine zipper* (*Gilz/Tsc22d3*) y *Zinc Finger Protein 36/Tristetraprolin* (*Zfp36/Ttp*), dos dianas transcripcionales primarias de GR que contienen motivos de unión GRE, en queratinocitos epidérmicos. Éstas y otras dianas de GCs se han identificado previamente en el laboratorio mediante ensayos GR ChIP-seq en los que GRE, Krüppel-like factor

(KLF), y AP-1 eran los motivos de unión más sobre-representados. Dada la relevancia de GR y KLF4 en la piel, hemos analizado las interacciones funcionales entre estos factores de transcripción y su impacto en la expresión de los genes *Gilz/Tsc22d3* y *Zfp36/Ttp*.

Los experimentos de pérdida de función de GR y KLF4 mostraron un requisito total de GR pero parcial de KLF4 para la completa inducción de genes en respuesta a dexametasona (Dex). En los queratinocitos terminalmente diferenciados inducidos por calcio, la expresión de la proteína GR y KLF4 aumentó coincidiendo con el aumento de *Gilz/Tsc22d3* y *Zfp36/Ttp*. Sin embargo, las células deficientes en GR no lograron diferenciar o inducir completamente *Gilz*, *Zfp36* y *Klf4*, correlacionando con el aumento de la expresión de *Trp63*, un conocido represor transcripcional de KLF4 que es específico del epitelio. La cooperación transcripcional identificada entre GR y KLF4 puede que determine la regulación específica del tipo celular y tiene implicaciones para el desarrollo de terapias para enfermedades de la piel.

En la parte II de esta tesis, hemos investigado GILZ, que se ha demostrado que actúa como mediador antiinflamatorio en varios tipos celulares de manera similar a los GCs pero sin producir los efectos secundarios asociados a GC. Por el contrario, poco se sabe sobre el papel de GILZ en la función de la piel. Por tanto, decidimos estudiar las consecuencias de la sobreexpresión de GILZ en la psoriasis, una enfermedad autoinmune inflamatoria de la piel, en la que los queratinocitos y las células inmunitarias desempeñan un papel importante. Para ello, utilizamos un modelo de psoriasis inducido por Imiquimod (IMQ) en ratones con sobreexpresión generalizada de GILZ (GILZ-Tg). Inesperadamente, GILZ-Tg mostró más susceptibilidad a la psoriasis inducida por IMQ, mostrando alteraciones cutáneas más

severas mostradas mediante histología (aumento de la hiperplasia epidérmica y paraqueratosis) y análisis bioquímico (niveles de citoquinas en suero y piel). Es importante destacar que estas alteraciones se correlacionaron con la sobreactivación de la señalización TGF-β/SMAD específica en la piel, que se recapituló en queratinocitos en cultivo. En general, estos hallazgos muestran que la GILZ actúa como una proteína pro-inflamatoria en la piel en un modelo de psoriasis inducido por IMQ y por lo tanto conviene tener precaución a la hora de considerar su uso terapéutico.

Abbreviations

aa	Aminoacids
AP-1	Activator protein 1
CASP-14	Caspase-14
cDNA	Complementary DNA
ChIP	Chromatin immunoprecipitation
CO	Control
CRH	Corticotropin-releasing hormone
d	Day
Dex	Dexamethasone
DNA	Deoxyribonucleic Acid
EDTA	Ethylenediaminetetraacetic acid
GBS	GR binding sites
GCs	Glucocorticoids
GILZ	Glucocorticoid-induced leucine zipper
GR	Glucocorticoid receptor
GRE	Glucocorticoid response elements
GR^{EKO}	GR epidermal knockout
h	Hour
H&E	Hematoxylin and eosin
Hipk2	Homeodomain-interacting protein kinase 2
HPA	Hypothalamic-pituitary-adrenal
IL	Interleukin
IMQ	Imiquimod
K	Keratin
KLF	Krüppel-like factor
KO	Knockout
MAPK	Mitogen-activated protein kinase
min	Minutes
MPKs	Mouse primary keratinocytes
mRNA	Messenger RNA
NF-kB	Nuclear factor kappa B
NR3C1	Nuclear receptor subfamily3, group C, member 1
P	Postpartum
PBS	Phosphate Buffered Saline
QPCR	Quantitative PCR

RNA	Ribonucleic acid
rpm	Revolutions per minute
RT-PCR	Real Time PCR
siRNA	Small interfering RNA
SPRRs	Small proline-rich repeat proteins
SD	Standard deviation
SMAD	Small mothers against decapentaplegic
Stat3	Signal transducers and activators of transcription 3
t	Time
TFs	Transcription factors
Tg	Transgenic
TGF-β	Transforming growth factor-β
Th17	T helper 17
TLR	Toll-like receptor
TNF-α	Tumor Necrosis Factor alpha
trp63	Transformation related protein 63
TSC22D	Transforming growth factor β-stimulated clone 22 domain
TSS	Transcriptional start site
TTP	Tristetraprolin
Wt	Wild type
Zfp36	Zinc finger protein 36

Chapter I

Introduction

1. The skin

1.1. Skin structure and function

Skin is the largest and outermost organ of the body, which not only forms a physical barrier between the internal organs and the surrounding environment but it also has an active role in maintaining organism homeostasis. Skin has a pivotal role in protecting the body from the harmful microbes, chemical agents and acts as an insulator for the body to maintain the internal body temperature. Skin is a part of the integumentary system, which also comprises hair and nails (Fuchs and Horsley, 2008; Menon, 2002).

The physiology of the skin is complex and made up of different layers, namely from inner to outside hypodermis, dermis and epidermis.

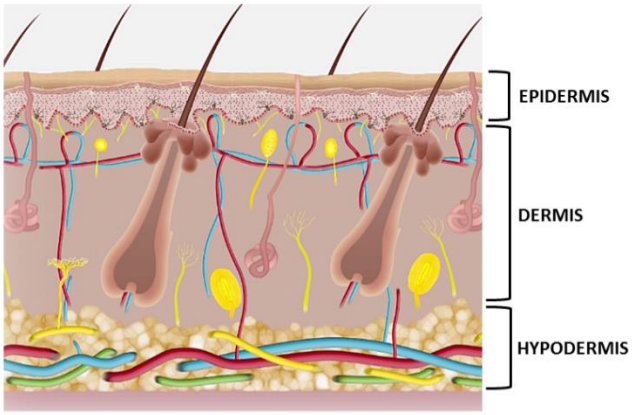

Figure 1. Organization of the skin. Skin contains three major layers namely hypodermis, dermis and epidermis. Hypodermis consists of the lowermost layer and is comprised of adipocytes, fibroblasts and macrophages, as well as connective tissue and elastine. Dermis is the middle layer consists of elastic fibers, collagen, lymphatic and blood vessels, sensory structures, as well as hair follicles and sebaceous and sweat glands and fibroblasts. Finally, epidermis, the outermost layer of the skin, includes mainly keratinocytes and melanocytes. Appendages: hair follicles and sebaceous glands from dermis. This image has been captured from http://www.clinuvel.com/

Hypodermis is the inner layer of the skin and lies beneath the dermis. It is mostly constituted by adipocytes, fibroblasts and macrophages, connective tissue and elastin (**Figure 1**).

The dermis is derived from mesoderm and contains elastic fibers, collagen, lymphatic and blood vessels, as well as sensory structures (Fuchs and Raghavan, 2002). The major cell type is the fibroblast. Hair follicles and sebaceous and sweat glands are appendages localized in this layer, although they are epidermal derivatives. Dermis is connected to the next outer layer by the basement membrane and provides tensile strength and elasticity to the skin (**Figure 1**).

The epidermis, the outermost layer of the skin, is derived from the ectoderm and is mainly composed of keratinocytes. Other cell types, such as melanocytes and antigen-presenting cells termed Langerhans cells are also present. Epidermis is composed of different layers that are explained below (Fuchs and Raghavan, 2002; **Figure 1**).

1.2. Epidermal structure and formation

The epidermis is a self-renewing stratified and keratinized epithelium, which consists of five different layers of cells known as the *stratum basale* or basal layer, *stratum spinosum, stratum granulosum*, *stratum lucidum* (only present in human palms and soles) and *stratum corneum* (Fuchs and Horsley, 2008; **Figure 2**). The epidermis is constantly renewing, as cells of the outer layers are continuously shed and replaced by the inner cells, which move up to the surface. The keratinocytes present in the basal layer of the epidermis have the ability to divide continuously. The newly formed cells migrate towards the more superficial layers of the skin and start the differentiation. In the *stratum granulosum* keratinocytes continue to flatten, lose their nuclei and their cytoplasm looks granular. Finally in the *stratum corneum*, the

exterior layer of the epidermis, keratinocytes become non-viable cornified cells (flattened dead cells filled with keratin filaments and water), namely corneocytes. These cells are surrounded by lipid layers and by a protein envelope filled with water-retaining keratin proteins (Fuchs and Horsley, 2008). The *stratum corneum* provides the first barrier against external insults (Fuchs and Horsley, 2008). It is also composed of structural proteins, including involucrin, loricrin and small proline-rich repeat proteins (SPRRs), all being part of the epidermal differentiation complex encoded by genes localized on human chromosome 1q21 (Jackson *et al.*, 2005).

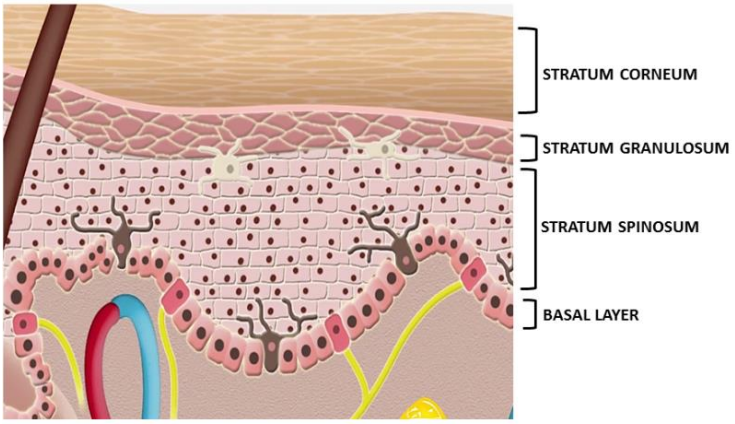

Figure 2. Epidermis structure is formed by different layers named *stratum basale* or basal layer, *stratum spinosum, stratum granulosum* and *stratum corneum*. This image has been captured from http://www.clinuvel.com/

There is an extracellular calcium gradient in the epidermis, which is a very important factor in the regulation of epidermal differentiation and cell-cell adhesion. In fact, the addition of calcium to *in vitro* primary keratinocytes recapitulates the *in vivo* differentiation by inducing morphological changes and formation of cell-cell contacts along with the expression of differentiation markers, such as SPRRs and loricrin, among others (Hennings *et al*., 1980; Sen *et al*., 2008).

1.3. Skin pathologies

Immune and inflammatory responses protect us from external pathogens. However, when the skin protection mechanisms fail or are not sufficient, humans can develop distinct pathologies. Inflammation is a necessary part of the response, but it is unhealthy when it becomes chronic.

Skin can be affected by external insults such as UV radiation, microbes, mechanical damage and chemicals. For a normal epidermal function it is required a tight control of keratinocyte proliferation, differentiation and death. A dysregulation among these processes may lead to an aberrant barrier function and subsequently to skin diseases, such as atopic dermatitis, psoriasis, ichthyosis vulgaris, etc (Fuchs and Raghavan, 2002; Bernard *et al.*, 2012; Sen *et al.*, 2012).

2. Psoriasis

2.1. Etiology and pathogenesis

Psoriasis is a common inflammatory and autoimmune skin disease, which implies impaired barrier function of the skin due to hyperproliferation and abnormal differentiation of epidermal keratinocytes and massive infiltration of leukocytes (Kim and Krueger, 2017). Psoriasis has a complex etiology and is distributed globally, affecting 2-3% worldwide (Kanemaru *et al.*, 2015).

Psoriasis onset is common between the ages of 18 and 39 (Greb, *et al*., 2016), but it can appear at any age. Many of the individuals suffering from psoriasis have also associated co-morbidities, including metabolic syndrome, hypertension, diabetes, obesity, depression,

inflammatory bowel disease and arthritis impairing quality of life and work productivity significantly (Johnson-Huang *et al.*, 2012).

Although etiology of psoriasis is still not well established, psoriasis has been shown to be caused by genetic and environmental factors. Among the genetic factors we can find genes that are up-regulated in psoriasis and encode S100A8 and A9 expressed by keratinocytes from the granular layer and genes associated with adaptive and innate immunity such as β-defensins, TNF-α signaling pathway, the IL-23/Th17–related genes, STAT3 and C-JUN/JUNB (Johnson-Huang *et al.*, 2012; Wagner *et al.*, 2012).

Environmental factors can trigger the onset or exacerbate the psoriasis. These factors include smoking, alcohol consumption, obesity, medications (imiquimod (IMQ), beta blockers), infections, as well as stress (Kanemaru *et al.*, 2015; **Figure 3**).

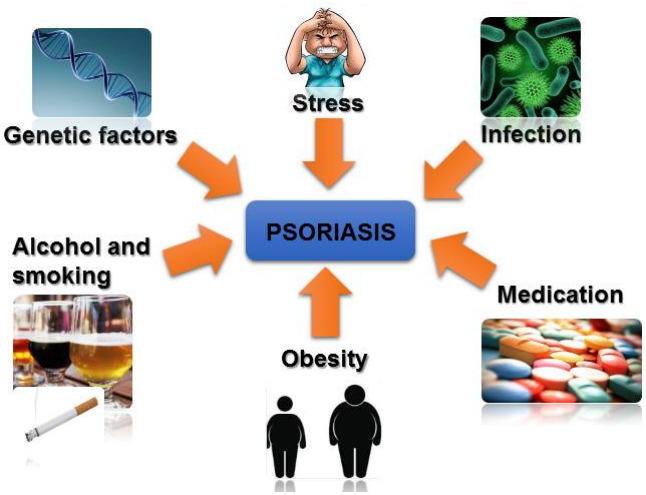

Figure 3. Risk factors associated with the development of psoriasis. Genetic and environmental factors are involved in the onset or exacerbation of psoriasis.

There are different types of psoriasis, termed as psoriasis vulgaris, guttate psoriasis, among others (Boehncke and Schön, 2015). In fact, up to 30% of individuals suffering from psoriasis may develop psoriatic arthritis (Johnson-Huang *et al.*, 2012). The most common clinical variant is psoriasis vulgaris, characterized by variable width of erythematous lesions covered by silvery-white scales over the whole body, which can cause pain and itch to the patient.

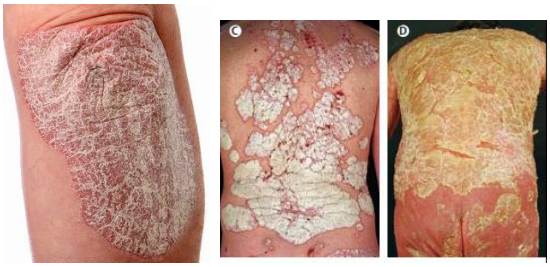

Figure 4. Clinical features of psoriasis vulgaris disease. Typical flaky white scale can appear in the whole body. These images show scales in legs and trunk. From Boehncke and Schön, 2015.

Psoriasis is characterized by the following features (Wagner *et al.*, 2010; **Figure 5**):

- Epidermal hyperplasia driven by hyperproliferation of keratinocytes, thickening of the *stratum corneum* (hyperkeratosis) and elongated epidermal invaginations termed as rete-ridges.
- Impaired keratinocyte differentiation and parakeratosis.
- Absence or reduction of granular layer.
- Dermal infiltration of inflammatory immune cells.
- Increased dermal vascularity

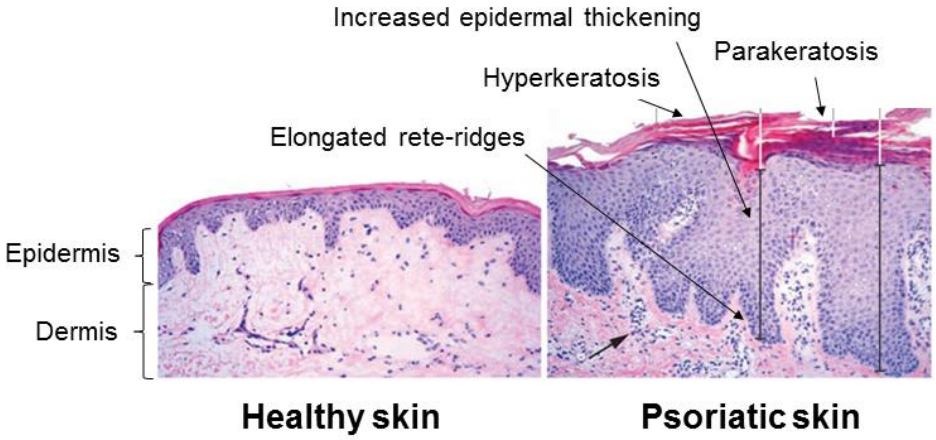

Figure 5. Structure of human healthy skin compared to psoriatic skin. The image shows all the microscopic features of healthy and psoriatic human skin. Adapted from Wagner *et al.*, 2010.

2.2. Immunopathogenesis: pathways implicated in psoriasis

Although pathogenesis is still not fully understood, certain immune cells from both the innate and adaptive immune system (neutrophils, dendritic cells, T cells), as well as epithelial cells (epidermal keratinocytes) have been found to be involved in the development and maintenance of psoriasis by producing cytokines (IL-6, IL-17A, IL-17F, IL-22, IL-23 and TNF-α) (Johnson-Huang *et al.*, 2012).

Toll-like receptors (TLRs) are part of the pattern recognition receptors and belong to the IL-1 Receptor/TLR superfamily, which is composed of 9 members (TLR1-TLR9), each recognizing different pathogens.There are transmembrane TLR in the cell membrane or endosomal compartments. TLR7 and 8 are the only TLRs expressed on the X chromosome and they can detect both self- and non-self-nucleic acids. Several autoimmune disorders (psoriasis, systemic lupus

erythematosus, rheumatoid arthritis, or systemic sclerosis) are associated with abnormal sensing of self-nucleic acids by TLR7, 8, or 9. TLR recognize bacteria and virus after they have crossed the barriers of the innate immune system, being very important in the initiation of the inflammatory response and in the development of adaptive immune responses, including the stimulation of naïve T cells (Flutter and Nestle, 2013).

In psoriasis, upon external stimuli, dendritic cells expressing the TLR 7/8/9, mature and migrate to the draining lymph nodes where they present the processed peptides (antigens) to naïve T cells and release cytokines such as IL-23, IL-6, IL-12, TNF-α and Interferon (IFN)-γ, which induce the T cell expansion and differentiation into different subsets of T cells. Then, these cells migrate back to the epidermis and dermis and interact with other immune cells (dendritic cells, mast cells, macrophages, and neutrophils), leading to a continuous proliferation of keratinocytes and T cells recruitment (Kim and Krueger, 2017).

Among the immune cells, T cell population have been shown to play a primary role in psoriasis since their reduction was associated with an improvement of psoriasis symptoms (Kim and Krueger, 2017). There are several types of T cells in lesional psoriatic skin, which are termed depending on the cytokines they produce: Th1, Th17, Th22 and Treg. The Th17 cells are driven by IL-1β, IL-6, transforming growth factor-β (TGF-β), and IL-23 and produce IL-22 and IL-17, a potent inducer of neutrophil activation and recruitment, in response to bacterial and fungal pathogens.

2.2.1. IL-23/Th17 axis

The IL-23/Th17 axis is involved in the pathogenesis of various inflammatory diseases, including rheumatoid arthritis, inflammatory

bowel disease and psoriasis (Han *et al.*, 2012). The main components that constitute this axis, IL-23, IL-22, IL-17, are up-regulated in psoriasis patients (Wolk *et al.*, 2006; Johnson-Huang *et al*., 2012). Skin dendritic cells secrete IL-23, which stimulates Th17 cells to produce pro-inflammatory mediators, including IL-17A, IL-17F, and IL-22. Then, these mediators activate keratinocytes and induce their hyperproliferation, subsequently producing pro-inflammatory cytokines, chemokines, and antimicrobial peptides, leading to further recruitment and activation of immune cells in the inflamed skin, finally amplificating the immune response. Although IL-1β, IL-6 and TGF-β produce the differentiation of Th17 cells, IL-23 is necessary for stabilization, survival and proliferation of the Th17 cell type (Johnson-Huang *et al*., 2012).

IL-22 is the strongest activator of keratinocytes and induces epidermal proliferation contributing to epidermis thickening. IL-22 can be produced by different sources, including natural killer, innate lymphoid cells, and adaptive $CD4^+$ or $CD8^+$T cells. The main targets of IL-22 are intestinal epithelial cells and skin since they express the IL-22R. IL-22 signaling results in the activation of pro-inflammatory signaling pathways, such as STAT3 and antimicrobial peptides β-defensin 2, β-defensin 3, and psoriasin (S100A7) in human keratinocytes, among others (Wolk *et al.*, 2006).

Among the different subtypes that constitutes the IL-17 family, IL-17A and IL-17F have been found up-regulated in psoriasis and are involved in the pathogenesis of inflammation. IL-17F is the most closely related to IL-17A with approximately 44% aa sequence homology. IL-17 is involved in the microabscess formation in the IMQ-induced psoriasis model and induces keratinocyte proliferation while inhibits

their differentiation, contributing to the epidermal hyperplasia (Ha *et al*., 2014).

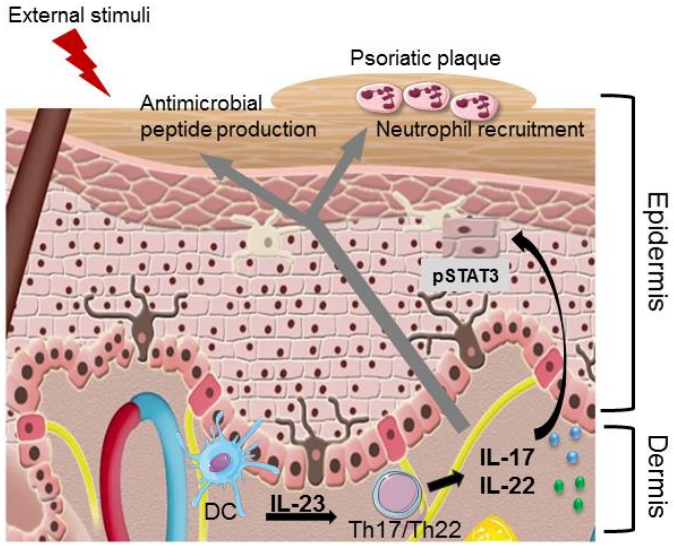

Figure 6. Scheme of pathways implicated in psoriasis. Immune cells are stimulated and secrete cytokines (IL-23), which activates the T cell subsets which consequently activate keratinocytes through IL-17 and IL-22 production. This cascade results in activation of STAT3 pathway and favours the recruitment of neutrophils and the production of antimicrobial peptides.

2.3. Therapy

Although no definitive cure for psoriasis has been discovered, some treatments alleviate the symptoms of this disease and improve life conditions for the psoriasis patients.

2.3.1. Topical treatment

Depending on the degree of psoriasis severity, different treatments are recommended. The main therapies are psoralen and ultraviolet A

(PUVA) photochemotherapy, topical treatment with corticosteroids, retinoids, immunosuppressants, vitamin D analogs, and biological therapies.

Both corticosteroids and vitamin D analogs act by binding and activating hormone receptors that belong to the nuclear hormone receptor superfamily. In fact, these intracellular receptors act as ligand-dependent TFs and are the most frequently targets in the treatment of inflammatory pathologies, including skin diseases (Boehncke and Schön, 2015).

Corticosteroids are the most and commonly used as topical treatment for psoriasis and for all the grades of this disease, either as monotherapy or in combination with systemic treatment. Their therapeutic response is mediated by vasoconstriction, anti-inflammatory and immunosuppressive effects; however, continuous treatments and/or high doses often cause severe systemic side effects, including hypertension, osteoporosis, cataracts, glaucoma, and diabetes, among others (Menter *et al.*, 2009). Regarding vitamin D analogs, they regulate genes involved in epidermal proliferation, inflammation, and keratinization. However, this treatment is also accompanied by side effects, as they can produce skin irritation and photosensitivity (Menter *et al.*, 2009).

2.3.2. Systemic treatment

Systemic treatments involve the administration of drugs either orally or by injection. Specific biologic compounds were designed after the observation of improvement of psoriasis patients under immunosuppressive agents. General anti-psoriatic therapies target pro-

inflammatory pathways, which involve the use of antibodies, soluble cytokine receptors, and fusion proteins.

The first biological drugs for the treatment of psoriasis vulgaris were developed to target TNF-α, an important inflammatory cytokine belonging to the Th1-derived cytokines, which exerts pleiotropic effects and regulates inflammation and immune system (Raychaudhuri and Raychaudhuri, 2009). However, as TNF-α is a major cytokine for the host defense, blocking this cytokine may cause side effects such as persistent fatigue and more severity of infections, among others.

The IL-23 and IL-17 cytokines are important mediators of psoriasis and play a major role in the immunopathogenesis of psoriasis (Johnson-Huang *et al.*, 2012). For this reason, the members of this axis have been considered as a potential target for the psoriasis treatment (Han *et al.*, 2012). Several inhibitors of IL-23 and IL-17 have been recently tested in psoriasis patients. For instance, Ustekinumab, a monoclonal antibody that targets both IL-12 and IL-23 is used to treat moderate-to-severe psoriasis and results in the inhibition of the following downstream signaling pathway in T cells. Similarly, secukinumab and ixekizumab are also monoclonal antibodies that are approved for the treatment of the psoriasis, that specifically bind to the IL-17. Additionally, monoclonal antibodies that are able to target IL-17 receptors were also developed.

2.4. Experimental models of psoriasis

Psoriasis is a complex immunopathological response. To understand the molecular events underlying this disease several *in vitro* and *in vivo* models have been generated. Most of the models

recapitulate critical events that take place in psoriasis patients. *In vitro* models include cultured psoriatic keratinocytes, whereas *in vivo* models include mice and humanized mice. Also, chemical induced models, including the IMQ-induced psoriasis mouse model are widely used to study psoriasis phenotypes in mice.

2.4.1. *In vitro* models of psoriasis

In vitro models of psoriasis can be either simple (culture of psoriatic keratinocytes alone or including additional cell types) or complex (reconstituted human epidermis). In this model that resembles a 3D structure, epidermal keratinocytes are obtained from individuals, and grown at the air-liquid interface to differentiate and stratify simulating the morphology of normal stratified epidermis. Under a mix of IL-22, TNF-α, and IL-17 conditions, displays histological features and up-regulation of the characteristic molecules of psoriasis, including S100a7 and *β*-defensin2 (Bernard *et al.*, 2012).

2.4.2. *In vivo* models of psoriasis

In 1996, Wrone-Smith and colleagues designed a mouse model for psoriasis consisting of the humanized xenotransplantation onto immunosuppressed mice (Wrone-Smith and Nickoloff, 1996) where keratome skin samples from healthy volunteers and psoriasis patients were grafted onto severe combined immunodeficient (SCID) mice. Mice carrying the human psoriatic skin displayed all the psoriasis histological abnormalities. This model showed that injecting the autologous psoriatic T cells into xenotransplanted normal skin from the same patient could induce psoriasis.

To study psoriasis *in vivo*, several knockout (KO) and transgenic mouse models have been generated. Among them, K5 (latent) TGF-β1 mice, which express TGF-β1 in the epidermis using a keratin 5 promoter. TGF-β1 is a potent keratinocyte growth inhibitor whose overexpression was reported to display unexpected features resembling psoriasis, including the histological parameters, as well as the immune increased infiltrates in the skin (Li *et al.*, 2004).

Another example of a transgenic mouse model for psoriasis is K5-STAT3C mice (Sano *et al.*, 2005), where keratinocytes expressed a constitutively (C) active form of STAT3. STAT3 is known to be up-regulated in human psoriatic lesions. By the 2 weeks of age, K5-STAT3C transgenic mice developed features found in psoriasis, including loss of granular layer, keratinocyte hyperproliferation, alteration in differentiation (parakeratosis), and leukocyte infiltrates, among others.

Also, mice with inducible, conditional deletion of both JUNB and c-JUN in basal keratinocytes (K5-JUNB/c-JUN) displayed the hallmarks of psoriasis at the 2 months of age despite single conditional KO mice for JUNB or c-JUN did not display any features of psoriasis (Zenz *et al.*, 2005). Both c-JUN and JUNB are components of the Activator Protein (AP)-1 family. It is important to note that K5-JUNB/c-JUN mice also developed arthritis, constituting a good model for psoriatic arthritis.

2.4.2.1. Imiquimod-induced psoriasis mouse model

IMQ is a known drug prescribed under a cream formulation called Aldara® and widely used to treat condyloma acuminata, solar keratosis and basal cell carcinoma by topical application on skin. In the past years

the application of Aldara in human patients for the treatment of the aforementioned skin alterations was shown to trigger lesions on skin that resembled psoriasis plaques (Fanti *et al.*, 2006). Based on this fact, in 2009, van der Fits and colleagues tested the daily topical application of Aldara cream on the shaved back mouse dorsal skin and revealed its power to induce psoriasis-like features. These alterations included all the clinical and histopathological features of human psoriasis in respect to erythema, scaling and induration and epidermal thickening, parakeratosis, neoangiogenesis and infiltration of immune cells in the dermis (Van der Fits *et al.*, 2009). The major biologic effects of IMQ are mediated through agonistic activity towards TLR7.

Aldara can also induce psoriasis-like skin inflammation through the IL-23/Th17 axis, which is a pivotal signaling in human psoriasis (Han *et al.*, 2012; Van der Fits *et al.*, 2009). Taken all together, this mouse model fulfils many of the necessary criteria to establish an ideal psoriasis mouse model (Van der Fits *et al.*, 2009). Furthermore, drugs to ameliorate features of IMQ-induced psoriasis can be tested, which explains that this is one of the best mouse models nowadays for studying the mechanisms of this disease (Van der Fits *et al.*, 2009).

3. Glucocorticoids

Glucocorticoids (GCs) are endogenous steroid hormones responsible for the regulation of many physiological functions (metabolism, embryonic development, stress response, inflammation, immune response, and cell proliferation, differentiation) (Sacta *et al.*, 2016). GCs are released in response to physical injury or psychological stress. The anti-inflammatory and immunomodulatory activities of GCs were discovered in the late 1940s and since then GCs have been used

for the treatment of various diseases, including asthma, hematological diseases, multiple sclerosis, rheumatoid arthritis, as well as psoriasis and atopic dermatitis, to name a few (Sacta *et al.*, 2016).

Besides the therapeutic effects of GCs, long-term use or high concentrations of GCs may cause adverse effects, such as hypertension, diabetes, muscle atrophy, and osteoporosis and specifically in the skin, atrophy and retarded wound healing (Sacta *et al.*, 2016).

3.1. Systemic GC production. The hypothalamic-pituitary-adrenal (HPA) axis

Systemic GCs are produced and controlled by the hypothalamic-pituitary-adrenal (HPA) axis. Upon an environmental (flight/fight, abrupt temperature changes, etc.) or physiological stressors, the hypothalamus secretes corticotropin-releasing hormone (CRH), which stimulates the pituitary to release adrenocorticotropic hormone (ACTH), which subsequently induces the production of mineralocorticoids and glucocorticoids by the adrenal cortex (in the glomerulosa and fasciculate of the adrenal gland, respectively). This hormone cascade results in an adaptive response to deal with stress generated by the environmental or physiological stressor. Once the stress has finished levels of GCs decrease rapidly (Oakley and Cidlowski, 2013). The levels of GCs are regulated by a negative feedback since elevated concentration of GCs inhibits their production (Sacta *et al*., 2016; **Figure 7**).

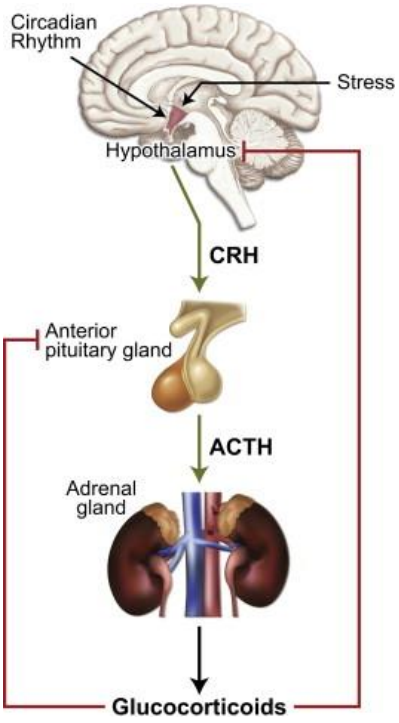

Figure 7. Representation of the function of the HPA axis upon stress. From Oakley and Cidlowski, 2013. CRH: corticotropin-releasing hormone; ACTH: adrenocorticotropic hormone.

Cortisol is the most predominant GC in humans, while corticosterone is the most predominant in rodents.

Besides external stressors, the release of GCs is under control of the circadian clock, which is maintained by the HPA axis, reaching a daily peak time in the morning for humans and evening for rodents, correlating with their respective highest activity. Continuous or repeated exposition to the stress develops constant high GC levels and deregulation of the negative feedback mediated by the HPA axis, what can lead to stress-induced pathologies.

Further studies discovered that GCs were synthesized not only in the adrenals, but also in other peripheral tissues, including lungs, skin, etc. Particularly, the skin expresses all elements of the HPA axis including CRH, ACTH, and GCs, as well as steroidogenic enzymes required for GC synthesis (Slominski *et al.*, 2013).

Keratinocytes and fibroblasts also express the enzymes 11β-hydroxysteroid dehydrogenase (11βHSD)1 and 11βHSD2, which transform inactive cortisone/11-dehydrocorticosterone to active cortisol/corticosterone and vice versa. 11βHSD1 expression is lower in psoriatic lesions relative to unlesioned skin (Slominski *et al.*, 2013).

4. Glucocorticoid receptor (GR)

GC effects are mediated by the protein named GC receptor (GR), encoded by the gene *NR3C1*, which is an important TF that belongs to the NR superfamily and is virtually expressed in all vertebrate tissues.

GR, formed by 9 exons and located on chromosome 5, exists in various splicing variants, among which GRα and GRβ are the most important and are generated from the alternative splicing at exon 9 of primary GR transcript. Importantly, only GRα can bind ligand although alternative roles have proposed for GRβ in different tissues, including a dominant negative function upon GRα (Weikum *et al.*, 2017).

4.1. Structure of GR

GR is constituted by three main domains (Weikum *et al.*, 2017; **Figure 8**):

In human GR, the N-terminal domain (NTD), constituted by 421 amino acids, comprises the ligand-independent activation function 1 (AF-1). This part is important for maximal transcriptional activation of the receptor since it interacts with coactivators, chromatin modulators, and the basal transcriptional machinery and activates target genes independently of ligand. It is the main site for the posttranslational modifications. This domain is the least conserved among all the members of the NR superfamily.

The central DNA binding domain (DBD) (residues 422 to 486) is the most conserved among the NRs and is composed of two highly conserved zinc fingers that mediate the binding of the receptor to DNA sequences named GC response elements (GREs), as well as protein-protein interactions. The first zinc finger contains the amino acids implicated in the GR binding to GRE, termed P box, whereas the second zinc finger contains the D box that drives the GR binding stabilization and homodimerization (Weikum *et al.*, 2017).

The DBD is connected to the C-terminally located **ligand binding domain** (LBD) by the hinge region (residues 487 to 526), which provides flexibility/elasticity to GR dimers, promoting GR DNA binding.

The **LBD** (residues 527 to 777) binds to GCs. It consists of the hydrophobic ligand-dependent activation function 2 (AF-2), which is formed by 12 α-helices and 4 β-sheets and facilitates the interaction, in

a ligand-dependent fashion, with cochaperone proteins, coregulators, and other transcriptional machinery. Nuclear localization signals in both the DBD and LBD mediate GR nuclear translocation (Oakley and Cidlowski, 2013).

Post-translational modifications (such as ubiquitination, acetylation, and phosphorylation) can regulate GR functions and influence the binding of GR to the DNA. In fact, GR phosphorylation may lead to a selective occupation of promoters on GR target genes and also regulate turnover, cofactor interaction, receptor stability, etc, ultimately influencing the role of GR in pathophysiology (Oakley and Cidlowski, 2013). GR can be phosphorylated by mitogen-activated protein kinase (MAPKs), cyclin-dependent kinases, c-Jun N-terminal kinases (JNK), etc, on 7 residues located in the NTD, which can alter the GR transcriptional activity. Specifically, the phosphorylation on serine 211 increases the GR transcriptional activity (Oakley and Cidlowski, 2013).

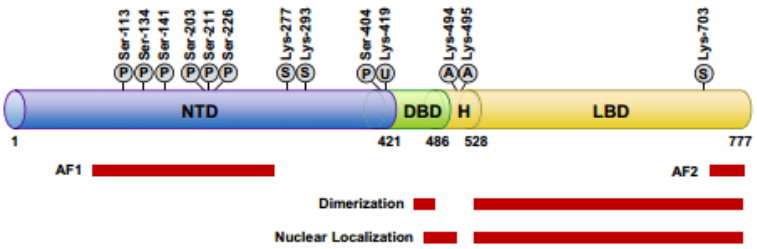

Figure 8. Structure of GR protein and post-translational modifications. The different domains of the structure of GR are depicted. The figure shows the sites of post-translational modification: phosphorylation (P), sumoylation (S), ubiquitination (U), and acetylation (A). From Oakley and Cidlowski, 2013).

4.2. Mechanisms of GR action

GCs binding to the GR can lead to the biological response through genomic or non-genomic actions.

The **genomic actions** are mediated through both DNA-binding-dependent and DNA-binding-independent mechanisms of GR. The first mechanism requires ligand-induced dimerization of GR and binding to specific DNA sequences to induce or repress gene expression, while the latter consists in the interaction with other TFs, such as nuclear factor kappa-light-chain-enhancer of activated B cells (NF-κB) and AP-1 (Weikum *et al.*, 2017).

In the absence of ligand, monomeric GR is normally localized in the cytoplasm of the cell in a complex with chaperone proteins containing heat shock protein (HSP) 90, HSP70, and other factors, so this interaction promotes high-affinity hormone binding and inactivates nuclear localization and DNA binding. Upon ligand binding to the receptor, GR is phosphorylated, changes its conformation, translocates to the nucleus, where it binds to the DNA and forms complexes with other transcription and co-regulatory factors to regulate gene expression (Weikum *et al.*, 2017).

GR can bind to different DNA regulatory sequences: **a)** specific DNA sequences called GREs, consisting in a palindromic sequence comprised of 2 half sites (the canonical DNA sequence AGAACA*nnn*TGTTCT, where *n* is any nucleotide). GR binds to GREs as an homodimer often resulting in gene induction (Weikum *et al.*, 2017); **b)** simple GREs (CTCC*nn*GGAGA), where GR binding often results in the suppression of gene expression (CRH, Proopiomelanocortin); **c)** inverted repeated IRnGRE, which results in

gene repression as reported for numerous genes including thymic stromal lymphopoietin (*Tslp*), which is repressed through binding of GC-activated GR in a mouse model of atopic dermatitis (Surjit *et al.*, 2011).

The GR binding sites (GBSs) are widely distributed in the genome, many of them being far from proximal promoters (Weikum *et al.*, 2017). Also, specific GBSs vary between tissues, where binding of additional cell-type specific TFs at adjacent or overlapping DNA regulatory elements modulates an effective GC-dependent transcriptional response.

As described above, GR can also interact with **other DNA-bound TFs** to activate or repress gene expression and it does not require the binding of GR to DNA sequences, a mechanism known as tethering (Weikum *et al.*, 2017). These DNA-bound TFs and their upstream signaling pathways are involved in inflammation and include NF-κB, AP-1, MAPK, among others.

NF-κB is a pro-inflammatory TF involved in many biological processes, such as cell growth, proliferation, development, and inflammatory and immune responses. It is constituted by five subunits: p50, p52, p65 (RelA), RelB, c-Rel. Inactive NF-κB remains in the cytosol bound to its inhibitor IκB, which avoids the NF-κB nuclear translocation. In response to external stimuli, IκB is phosphorylated and degraded through ubiquitination–proteasome pathway, releasing NF-κB and, thus, promoting translocation to the nucleus where it binds to DNA and regulates gene expression (DiDonato *et al.*, 2012).

GR is known to inhibit NF-κB activation through different mechanisms, including the inhibition of kinases responsible for the phosphorylation of IκB, its interaction with p65 subunit leading to its

cytoplasmic sequestration and *IκBα* up-regulation, in a cell-type dependent manner (De Bosscher and Haegeman, 2009).

MAPK family members regulate cellular processes including proliferation, differentiation, and inflammation. In mammals, MAPKs include extracellular signal-regulated kinases (ERK), JNK, and p38. They are activated by phosphorylation and subsequent phosphorylation of their downstream targets.

In keratinocytes, MAPKs regulate proliferation and differentiation. Several studies have shown GR to negatively regulate MAPKs function in keratinocytes (Herrlich, 2001).

AP-1 is a TF involved in various cellular events including proliferation, differentiation, survival and apoptosis, which demonstrates a relevant role in skin as AP-1 is involved in epithelial development, cancer and skin inflammation (Angel *et al.*, 2001). AP-1 is constituted by two main components including JUN and FOS subunits. JUN and FOS can dimerize and JUN is phosphorylated by JNK.

AP-1 and GR are described as mutual antagonists (DiDonato *et al.*, 2012). However, AP-1 has been also shown as a regulator of the accessibility of GR to the chromatin (Biddie *et al.*, 2011). GR can also inhibit AP-1 through a non-genomic mechanism resulting in the inhibition of JNK.

Non-genomic actions occur rapidly (within minutes) and independently of gene expression. GR can regulate signaling pathways, including phosphatidylinositol 3-kinase (PI3K) pathway or interacting with G protein-coupled receptors and membranous GR.

4.3. GR target genes in skin: Anti-inflammatory genes regulated by GCs

Zinc Finger Protein 36/Tristetraprolin* (*Zfp36/Ttp*) and *GC-induced leucine zipper (Gilz/Tsc22d3) are two genes typically induced by GR homodimers upon GC treatment in many cell types (Brahma *et al*., 2012; Smoak and Cidlowski, 2006; Ayroldi and Riccardi, 2009), including keratinocytes (Stojadinovic *et al.*, 2007).

4.3.1. Zinc Finger Protein 36/Tristetraprolin (ZFP36/TTP)

Most mammals express three family members, with rodents expressing a fourth member. The official gene names are *Zfp36*, encoding tristetraprolin (TTP, also known as ZFP36); *Zfp36l1*, encoding ZFP36L1 (also known as TIS11b); *Zfp36l2*, encoding ZFP36L2 (also known as TIS11D); and *Zfp36l3*, encoding ZFP36L3 (Brooks and Blackshear, 2013). All of these isoforms are found also in humans, except *Zfp36l3*, which is specific for rodents (Fu and Blackshear, 2017).

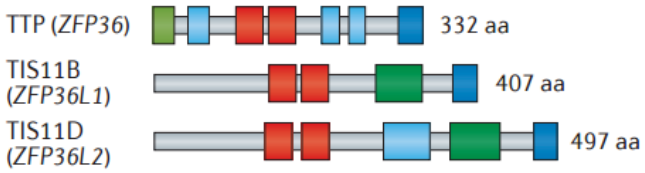

Figure 9. Schematic structure of human ZFP36 protein isoforms. From Fu and Blackshear, 2017.

ZFP36 is a member of a small family of CCCH tandem zinc finger proteins involved in the regulation of gene expression by binding to adenosine and uridine (AU)-rich elements (ARE) (heptameric sequence UAUUUAU), located in the 3′ untranslated region (3′UTR). Once they bind they accelerate rates of degradation of target mRNA by recruiting

the components of the mRNA degradation machinery (Brooks and Blackshear, 2013).

Studies of gain and loss of ZFP36 have been useful to reach a better understanding of the functions of ZFP36. In the case of ZFP36 KO mouse, the deficiency of this protein leads to a severe syndrome of growth retardation, cachexia, arthritis, inflammation and autoimmunity, demonstrating the anti-inflammatory role of this endogenous protein. However, the treatment with TNF-α antibodies avoid the characteristics of the aforementioned syndrome (Fu and Blackshear, 2017), demonstrating that TNF-α is a target mRNA of ZFP36. In contrast, the increment of the endogenous expression of ZFP36 in mice by enhancing its stability leads to the protection against immune and inflammatory diseases, including rheumatoid arthritis, psoriasis and multiple sclerosis (Patial *et al.*, 2016).

IL-22 and IL-23 are increased in ZFP36-deficient mice (Härdle *et al*., 2015; Molle *et al*., 2013), thus linking ZFP36 with autoimmune diseases such as psoriasis, as these cytokines were up-regulated in this disease (Wolk *et al.*, 2006; Johnson-Huang *et al*., 2012). ZFP36 also regulates other inflammatory pathways as ZFP36 physically interacts with the p65 subunit of NF-κB leading to decreased nuclear translocation (Fu and Blackshear, 2017). However, ZFP36 also regulates the expression of anti-inflammatory cytokines, such as IL-10 (Fu and Blackshear, 2017). In fact, ZFP36 has been shown to autoregulate its expression by direct binding to its own ARE, thus promoting its own degradation (Fu and Blackshear, 2017).

4.3.2. Glucocorticoid-induced Leucine Zipper (GILZ)

GILZ, encoded by *Gilz/Tsc22d3 (Transforming growth factor-β-stimulated clone-22/Glucocorticoid-induced leucine zipper)* located on the X chromosome (Pinheiro *et al.*, 2013), is a member of the transforming growth factor β-stimulated clone 22 domain (TSC22D) family of TFs. GILZ was first identified by D'Adamio and Riccardi in 1997, as a protein highly induced by the synthetic GC dexamethasone (Dex) in mouse thymocytes and protected T lymphocytes from apoptosis (D'Adamio *et al.*, 1997). Later GILZ was reported to be also induced in other cell types, including epithelial cells, lung, liver, brain and kidney (De Bosscher and Haegeman, 2009; Shi *et al*., 2007).

GILZ expression can be transcriptionally induced by glucocorticoids, TGF-β and the anti-inflammatory cytokine IL-10 (Ayroldi and Riccardi, 2009), to name a few. On the other hand, GILZ expression can be repressed by inflammatory cytokines (Ayroldi and Riccardi, 2009) and by lipopolysaccharide (LPS) through activation of TLR4 (Hoppstädter *et al.*, 2012).

4.3.2.1. Molecular structure and function of GILZ

GILZ family members contain three distinct domains: an N-terminus TSC (tuberous sclerosis complex) box, a middle leucine zipper domain, and a C-terminus polyproline-rich domain (Beaulieu and Morand, 2011; **Figure 10**).

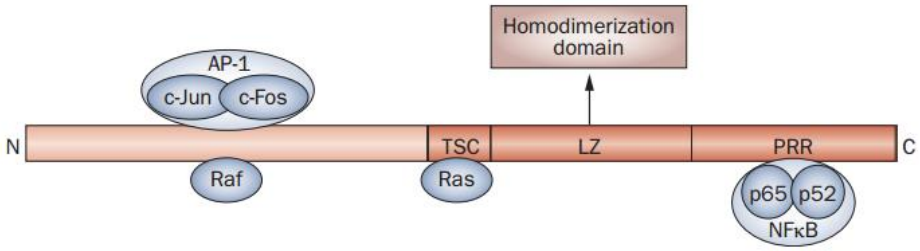

Figure 10. GILZ protein structure showing binding domains of TFs. AP-1, activator protein 1; GILZ, glucocorticoid-induced leucine zipper protein; LZ, leucine zipper; NF-κB, nuclear factor κB; PRR, proline-rich region; TSC box where ras binds . From Beaulieu and Morand, 2011.

Human *GILZ* mRNA presents a high similarity (89%) in nucleotide sequence with mouse *GILZ* and 97% in the coding region (Cannarile *et al*., 2001).

GILZ has been implicated in many processes, including immunosuppression, apoptosis (D'Adamio *et al.*, 1997), cell proliferation, control of tumorigenesis (Ayroldi and Riccardi, 2009), renal sodium transport (Rashmi *et al.*, 2017), adipogenesis (Shi *et al.*, 2007) and modulation of homeostasis of T cells (Ronchetti *et al.*, 2015). The regulation by GILZ of certain cellular functions has been found to be cell-type specific and also specific of agent stimulus.

In some cell types, GILZ has been shown to mediate most of the effects of GCs, including the inhibition of AP-1 and NF-κB transcriptional activity (Srinivasan and Janardhanam, 2011), as well as inhibition of Ras-driven cell proliferation (Ayroldi and Riccardi, 2009) through interaction with these TFs. This has led to the proposal that in many organs GILZ acts as an anti-inflammatory mediator of the GCs without producing GC-associated side effects (Ronchetti *et al.*, 2015).

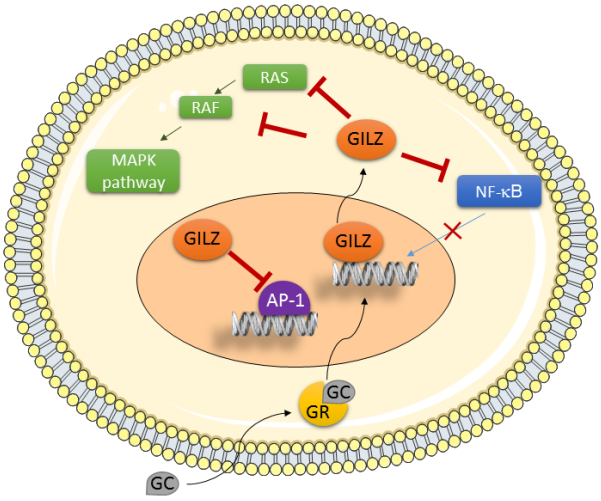

Figure 11. GILZ interaction with signaling pathways. GCs induce GILZ expression, which can inhibit the activity of TFs NF-κB and AP-1 and also the MAPK pathway through interaction with the upstream RAS and RAF.

Four isoforms have been characterized as splice variants of the *Tsc22d3* gene, known as GILZ1, GILZ2, GILZ3 and GILZ4 (Hoppstädter *et al.*, 2012). GILZ isoforms have also separated functions and can be expressed in different organs. For example, GILZ1, the canonical isoform with 137 aa, is normally present in thymus, spleen, and lung, whereas GILZ2 is detected in testis, liver, skin, and brain (Suarez *et al.*, 2012). Among all the GILZ isoforms, GILZ1 is the most studied. GILZ1 expression has been reported to be induced by aldosterone in the kidney. In addition, GILZ1 inhibits RAF-1 signaling pathway through protein-protein interaction leading to ENaC (Epithelial Na(+) channel) activation and also with other components of ENaC regulatory complex, in particular, serum and glucocorticoid-regulated kinase 1 (SGK1). Physical interaction of GILZ1 with RAF-1 results in inhibition of ERK1 and 2 and subsequently, along with SGK1, in the synergistic stimulation of ENaC expression through different mechanisms.

GILZ has been studied in animal models of inflammation and in many instances has been shown as an important mediator of inflammatory responses in both innate and adaptive immune systems (Cheng *et al.*, 2014).

Although GILZ KO male mice are sterile due to impaired spermatogenesis (Suarez *et al*., 2012; Ngo *et al*., 2013b), GILZ KO mice are viable and have been reported to have electrolyte alterations and display features resembling familial hyperkalemic hypertension (Rashmi *et al.*, 2017). The lack of GILZ did not alter the immune response in several diseases and neither decreased the anti-inflammatory effects of GCs in arthritis (Ngo *et al*., 2013a). Additionally, GILZ-deficient macrophages did not alter their response to LPS (Suarez *et al*., 2012). However, the overexpression of GILZ has been reported to be protective in inflammation. For example, transgenic mice overexpressing GILZ in T lymphocytes are less susceptible to a spinal cord injury mouse model (Esposito *et al.*, 2012). Furthermore, the use of GILZ peptide has demonstrated to suppress the inflammation in a rat model of experimental autoimmune encephalomyelitis (Srinivasan and Janardhanam, 2011). In addition, the injection of GILZ-adeno-associated virus into the joints in a mouse model of rheumatoid arthritis (Ngo *et al.*, 2013a) inhibited the development of the disease similar to GC treatment. Consistently, downregulation of GILZ by systemic administration of GILZ siRNA had the contrary effect (Beaulieu and Morand, 2011). Furthermore, the increased expression of GILZ has been shown to be the cause of the resistance to endotoxemia induced by LPS of a wild-derived inbred SPRET/Ei mouse strain (Pinheiro *et al*., 2013).

As it has been previously described, the phenotypes described for GILZ KO or GILZ overexpression in inflammatory models are not

always specular images, which likely reflects different roles for the endogenous GILZ (KO) *versus* the therapeutic GILZ (overexpression or GILZ peptide injection) (Ngo *et al.*, 2013a).

4.4. GR epidermal knockout (GR^{EKO}) mouse model

Previous studies in our laboratory using transgenic mice with gain and loss of GR function have shown the strong impact of this TF in skin homeostasis, demonstrating that GR is a potent anti-inflammatory, anti-proliferative, and anti-tumor mediator in this tissue (Pérez, 2011). On one hand, GR specific overexpression in epidermal keratinocytes, as well as generalized loss of GR resulted in major defects in mouse skin development (Pérez *et al*., 2001; Bayo *et al*., 2008). On the other hand, epidermal keratinocyte ablation of GR (GR epidermal KO or GR^{EKO} mouse) led to skin barrier defects and cutaneous inflammation at the perinatal age (Sevilla *et al.*, 2013). Adult GR^{EKO} skin was more susceptible to perturbation of skin homeostasis with detergent or phorbol ester and also to skin carcinogenesis (Sevilla *et al.*, 2013; Latorre *et al.*, 2013).

4.5. Interaction of GR with other transcription factors (TFs)

4.5.1. Krüppel-like factor (KLF) family

Krüppel-like factor (KLF) subfamily is formed by 17 mammalian zinc finger-containing TFs (evolutionarily conserved) homologs of *Drosophila Krüppel* gene (Pearson *et al.*, 2008). KLF proteins have been studied because of their involvement in cardiovascular, bone and skin development, as well as in erythrogenesis, neurogenesis and adipogenesis, and maintenance of pluripotency and cell proliferation (Pearson *et al.*, 2008). KLFs are also relevant in homeostasis of several

organs and are involved in several aspects of tumorigenesis (Rowland and Peeper, 2006). The functional domains of the KLFs involved in gene activation are at the N-terminus and vary between family members. For this reason, some KLF members activate and others repress gene expression, whereas some can do both functions. KLF4 is one of the KLF family members that can act either as an activator or repressor on gene expression.

4.5.1.1. KLF4

KLF4, Krüppel-like factor 4, formerly known as gut-enriched Krüppel-like factor or epithelial zinc finger, is a TF with three carboxyl C_2H_2 (Cys2-His2) zinc-fingers, which binds the DNA sequence 5-CACCC-3 (Pearson *et al*., 2008) regulating gene expression and thus, coordinating a variety of processes, such as proliferation and differentiation (Ghaleb and Yang, 2007).

KLF4 is a nuclear protein, which plays an important role for the development of the epithelia, such as cornea, lung and epidermal barrier formation (Segre *et al.*, 1999). In fact, KLF4 was first found to be highly expressed in the epithelia of intestine (postmitotic cells) and skin (suprabasal layer of the epidermis) (Ghaleb and Yang, 2017; Segre *et al.*, 1999) being important for the commitment to terminal differentiation of the epidermal keratinocytes and goblet cells in colon (Segre *et al.*, 1999; Katz *et al.*, 2002). The expression of KLF4 has also been found in other non-epithelial tissues, including the lung and cardiac myocytes (Ghaleb and Yang, 2017). KLF4 can act as an inductor or repressor of gene expression, depending on the cellular context and its association with co-activators (p300 and CREB-binding protein) or co-repressors (HDAC3) (Ghaleb and Yang, 2017).

Furthermore, the overexpression of KLF4, in cooperation with other TFs such as OCT3/4, SOX2, and c-MYC induce reprogramming of somatic cells by generating the cells termed as induced pluripotent stem cells (Takahashi *et al.*, 2007).

4.5.1.2. KLF4 in epithelial organs

The importance of KLF4 in skin has been determined in experiments of gain and loss of function. *Klf4* null mice die shortly (within 15 h) after birth because of dehydration due to defects in skin differentiation, (Segre *et al.*, 1999), as well as a reduced number of secretory goblet cells in the colon (Katz *et al.*, 2002). In contrast, the overexpression of KLF4 accelerates the skin barrier formation (Jaubert *et al.*, 2003). In addition, the antenatal injection of corticosteroids synergizes with the ectopic expression of KLF4 in accelerating the formation of the epidermal barrier, likely due to overlapping functions of KLF4 and GR (Patel *et al.* 2006). During epidermal differentiation, KLF4 is regulated by factors, such as ZNF750 and p63, among others (Ghaleb and Yang, 2017). Additionally, KLF4 overexpression results in inflammation in esophageal keratinocytes in a short period of time, whereas longer periods can produce carcinogenesis in mice (Ghaleb and Yang, 2017). Unexpectedly, deficiency of KLF4 has been also shown to promote an increase of cell proliferation and skin carcinogenesis in mice (Ghaleb and Yang, 2017).

4.5.2. Trp63/p63

Trp63 encodes p63, a relevant TF belonging to the p53/ p63/p73 family. It regulates a large number of cellular processes, such as the stem cell renewal, balance between proliferation and differentiation, as

well as morphogenesis during development, especially in the skin (Yang *et al*., 1999). In fact, p63 is considered one of the master regulators of epithelial development (Romano *et al.*, 2012). p63-null mice die after birth and show strong defects in the epithelia, limb, orofacial region, and external genitalia (Yang *et al.*, 1999). This is coincident with the alterations in ectodermal dysplasia found in humans caused by p63 mutations (Rizzo *et al*., 2016). Altered expression of p63 can be found in several diseases, for example, many squamous tumors including those of the head and neck, lung and skin show overexpression of p63. Also, p63 expression is altered in psoriasis (Rizzo *et al*., 2016).

p63 has several isoforms derived from distinct transcripts known as TAp63 and N-terminal deleted ΔNp63 arising from two different transcription initiation sites (Romano *et al.*, 2012). Additionally, alternative splicing can result in α, β, and γ isoforms, which differ in the C-terminus. All p63 isoforms bind to the same DNA sequences. However, ΔNp63, especially ΔNp63α is the predominant isoform present in most epithelial cells including skin keratinocytes and regulates the change from simple to stratified epithelium during development (Rizzo *et al.*, 2016; Romano *et al.*, 2012). p63 controls not only proliferation of keratinocytes, but also keratinocyte differentiation via its effect on the ZNF750-KLF4 regulatory axis (Sen *et al.*, 2012). Mice overexpressing ΔNp63 in their epidermis display characteristic features of atopic dermatitis, such as pruritus, epidermal hyperplasia, Th2 cells, elevated levels of cytokines, etc (Rizzo *et al.*, 2016). This is consistent with the high expression of ΔNp63 found in human atopic dermatitis lesional skin (Rizzo *et al.*, 2016).

Chapter II

Aims of the study

Significance of the study

Since GR mediates the therapeutic GC effects for the treatment of autoimmune and skin inflammatory diseases, it is important to understand the underlying transcriptional mechanisms. This includes analyzing how other TFs contribute to GR-mediated gene regulation in a given cell type. Also, the fact that chronic treatments with GCs are accompanied by side effects has pushed researchers to find other molecules with an improved therapeutic index (increased benefits/reduced risk).

The **objectives** of our work have been divided into two:

Part I:

Analysis of the functional cooperation of the glucocorticoid (GC) receptor (GR) and Krüppel-like factor (KLF) 4 in the regulation of gene expression in epidermal keratinocytes.

To identify GR direct transcriptional targets in epidermal keratinocytes, we recently performed GR chromatin immunoprecipitation followed by global analysis of the whole genome (ChIP-seq). Our results showed that most of the GR binding sites (GBSs) corresponded to GREs, but interestingly we also detected overrepresentation of binding sites for the TF Krüppel-like factor or KLF. Given the relevance of GR and the family member KLF4 in skin homeostasis (Pérez, 2011; Ghaleb and Yang, 2017), we focused our attention on the possible functional interactions among GR and KLF4. Since KLF4 overexpression and GC treatment have been shown to regulate a similar set of genes in the skin (Patel *et al.*, 2006), we

assessed whether both TFs may regulate coordinately the transcription of GC-target genes in keratinocytes.

Using an immortalized adult mouse keratinocyte cell line (Latorre et al., 2013), we focused our attention on two GC-regulated genes that are involved in inflammation in other cell types, *Glucocorticoid-induced leucine zipper (Gilz/Tsc22d3*) and *Tristetraprolin* (*Zfp36/Ttp)*. We also explored the functional relevance of GR and KLF4 in gene expression of these GC-targets using calcium-induced differentiated keratinocytes.

Part II:

Functional analysis of GILZ in transgenic mice with generalized overexpression: implications in psoriasis.

Psoriasis is a chronic autoimmune and inflammatory skin disease, for which there is no cure and seriously reduce the quality of life of patients. Often, GCs are commonly used to repress the hyperactivated immune state in the psoriatic skin.

Gilz/Tsc22d3 is a classical GR transcriptional target gene induced by GCs that has been shown to act as an anti-inflammatory mediator in different tissues producing therapeutic effects similar to the GCs without exerting their side effects (Ayroldi and Riccardi, 2009). Therefore, GILZ has been considered as a potential therapeutic tool for certain inflammatory diseases (Ronchetti *et al.*, 2015), although very little is known regarding its possible role in skin pathophysiology.

Using transgenic mice model with generalized overexpression of GILZ (GILZ-Tg) generated by the group of Prof. Claude Libert, we have investigated the role of GILZ in the imiquimod (IMQ) mouse model of

psoriasis. This model consists in topical repetitive application of IMQ, an agonist of the TLR7, which induces histopathological features and molecular alterations including up-regulation of the IL23/IL17 signaling pathways, which closely resembles human psoriasis. We have assessed the systemic and skin histopathological changes as well as the alterations in cytokines and signaling pathways typically up-regulated in psoriasis in GILZ-Tg relative to control mice. Additionally, we used cultured mouse keratinocytes to study the possible effects of GILZ overexpression in this cell type.

Chapter III

Material and methods

1.1. Isolation and culture of Mouse primary keratinocytes (MPKs)

Newborn mice (P0-P3) were sacrificed and tail sample collected for genotype analysis. Mice were immersed first in betadine, then in sterile distilled water, followed 70% ethanol and finally in PBS. Skin was incubated in 0.25% trypsin at 4°C overnight, then, the epidermis was separated from the dermis, minced, and homogenized in complete Eagle's medium essential medium (EMEM) with 0.05 mM $CaCl_2$ (low calcium). The homogenate was filtered, and the solution containing MPKs was collected by centrifugation (1200 rpm at 4°C for 5 min). 10^6 cells were plated into collagen I-coated on 35-mm diameter tissue culture dish (BD Biosciences) and cultured at 37°C in EMEM. After 24 h, the medium was replaced with growth medium (complete EMEM supplemented with 4% FCS (Biowest) previously treated with Chelex 100, 100 U/ml penicillin/100 µg/ml streptomycin (Biowest), 2.5 µg/ml amphotericin B (Biowest), 10 ng/ml EGF (Peprotech) and 0.05 mM CaCl2), and cells were grown until subconfluency using standard tissue culture conditions (5% CO_2 enriched atmosphere at 37°C).

1.2. Culture of immortalized adult mouse keratinocytes

The GR epidermal KO (GR^{EKO}) and control keratinocyte cell lines were generated from 8-week-old female mouse dorsal skin as previously described (Latorre *et al*., 2013) and cultured on mitomycin C treated 3T3-J2 feeders in collagen I-coated flasks in DMEM-Ham's F12 (3:1) medium (Gibco) supplemented with 1.8×10^{-4} mol/L adenine, 0.35 mM calcium, 7.5% Fetal Bovine Serum, 100 U/ml penicillin/100 µg/ml streptomycin (Biowest), 2 mM glutamine (Biowest), 0.25 µg/ml amphotericin B (Biowest), 5 µg/ml insulin, 10^{-10} M cholera toxin and 10 ng/ml EGF (Peprotech). Cells were maintained at standard tissue

culture conditions (5% CO_2 enriched atmosphere at 32°C) and media was changed every 48 h. Once keratinocytes reached subconfluency they were split as described below: First, culture medium was removed and keratinocytes adhered to the plate were washed with 0.02% EDTA to remove fibroblasts (feeders). Next, keratinocytes were collected after incubation with 0.25% trypsin for 5 min at 37°C. After trypsinization cells were centrifuged to remove the trypsin and resuspended in medium (as mentioned above). Keratinocytes were counted using a hemocytometer and cultured on mitomycin C treated confluent 3T3-J2 feeders.

For maintenance of 3T3-J2 feeders cells were grown in DMEM medium supplemented with 100 U/ml penicillin/100 µg/ml streptomycin, 0.25 µg/mL amphotericin B and 10% bovine serum in collagen I-coated 75 cm^2 flasks. Once feeders reached confluency cells were detached using 0.02% EDTA and subcultured by splitting them in 1:4 ratio.

1.3. Cell treatments

Prior to treatment with Dex (100 nM), cells were grown for 18–24 h in respective medium containing charcoal-stripped serum to deplete steroid hormones.

To induce terminal differentiation, keratinocytes were incubated with medium containing 1.2 mM $CaCl_2$. When indicated, cells were pretreated for 6 h with the GR antagonist RU486 (1 µM) or vehicle prior to addition of 1.2 mM $CaCl_2$.

1.4. Immunofluorescence staining

Cells were grown on collagen I-coated coverslips. After Dex treatment (100 nM, 2 h), cells were fixed with 4% paraformaldehyde

(PFA) for 10 min, then permeabilized with 0.2% Triton X-100 and washed three times with PBS. After blocking in PBS containing 5% donkey serum and 0.5% bovine serum albumin for 1 h at room temperature, cells were incubated with specific antibodies overnight at 4 °C. The following day, primary antibody was removed and cells were washed three times with PBS. Next, cells were incubated with the secondary antibody (Alexa fluor 555 Rabbit, dilution 1/1000; Life Technologies) and DAPI (4'-6-Diamidino-2-phenylindole) (Life Technologies) at room temperature for 1 h in darkness. After washes, samples were mounted using Mowiol (Calbiochem) and analyzed using a Leica DM 1000 microscope. Images were processed using Adobe Photoshop CS5 software.

1.5. Chromatin immunoprecipitation (ChIP) assays

ChIP experiments were performed as previously described (Sevilla *et al*., 2010), using MPKs or adult keratinocyte cell lines grown to confluency in 100 mm culture dishes (Thermo Scientific). Keratinocytes were incubated with freshly prepared 1% formaldehyde 8 min at room temperature to cross-link the protein-DNA. Next, 1 M Glycine was added for 5 min at room temperature to quench unreacted formaldehyde. After fixation, cells were washed with cold PBS and were collected in a solution containing PBS and protease inhibitors. After centrifugation (2000 rpm for 5 min at 4°C), supernatant was discarded and 200 µl of SDS Lysis Buffer containing protease inhibitors were added to the pellet and incubated on ice for 10 min. Cells were sonicated using the Bioruptor (Diagenode) to fragment chromatin (<500 bp fragments) set to high intensity for 30 min with 30 sec on/off cycles. Then samples were centrifuged at 13000 rpm at 6°C for 10 min to remove insoluble material and supernatant was collected to a new tube.

For the immunoprecipitation of cross-linked Protein/DNA 1.8 ml of dilution buffer containing protease inhibitors and 15 µl of Dynabeads Protein A (Life Technologies) was added and incubated for 2 h at 4°C with rotation to remove proteins or DNA that may bind non-specifically to the beads or protein A. Supernatant was recovered by using a magnet (DynaMag™-2, Invitrogen) to remove the magnetic beads and 40 µl of the supernatant was kept appart as Input. Sonicated chromatin was immunoprecipitated by adding 3 µg of either rabbit IgG (Sigma) (for negative control) or rabbit anti-GR (sc-1004; Santa Cruz Biotechnology) or anti-KLF4 to the supernatant fraction and incubated overnight at 4°C with rotation. The following day 20 µl of magnetic beads were added and incubated for 2 h at 4°C with rotation to collect the antibody/antigen/DNA complex. Using the magnet, supernatant was discarded and beads were washed with 1 ml of the following cold buffers: Low Salt, High Salt, LiCl and TE. Afterwards, protein/DNA complexes were eluted by incubation with 500 µl of elution buffer (1% SDS and 0.1 M $NaHCO_3$) at 25°C shaking at 300 rpm for 15 min. After ChIP, reversion of DNA-protein cross-linking was performed by adding 20 µl of 5M NaCl and incubating overnight at 65°C. Afterwards, samples were treated with 1 µl of 30 mg/mL of RNase A (Sigma) (30 min at 37°C) to remove contaminant RNA. To remove proteins, samples were incubated with a solution constituted by 0.5 M EDTA, 1 M Tris-HCl and proteinase K (10 mg/ml) at 55°C for 2 h.

The DNA was purified by phenol-chloroform extraction: after addition of the phenol-chloroform-isoamyl alcohol (500 µl), samples were mixed and centrifuged 13000 rpm at 4°C for 15 min. Upper aqueous phase was transferred to a fresh tube and 500 µl of chloroform was added, mixed and centrifuged again. Next, upper aqueous phase was transfer to a fresh tube and Glycogen (Roche) was added to

visualize pellet, as well as 18.8 µl of 5 M NaCl. Then samples were incubated overnight at -20°C after addition of 1 ml of absolute ethanol. Next day, samples were centrifuged 13000 rpm for 30 min at 4°C. Supernatant was removed and pellet was washed with 70% ethanol and centrifuged again at 13000 rpm for 10 min. Finally, supernatant was removed and pellet was air-dried before resuspending in nuclease-free water. DNA was quantified in Nanodrop measuring absorbance at 260 nm.

Low Salt	High Salt	LiCl	TE
0.1% SDS	0.1% SDS	0.25 M LiCl	1 mM EDTA
1% Triton X-100	1% Triton X-100	1% IGEPAL-CA630	10 mM Tris-HCl pH 8.0
2 mM EDTA	2 mM EDTA	1% deoxycholic acid	
20 mM Tris-HCl pH 8.1	20 mM Tris-HCl pH 8.1	1 mM EDTA	
150 mM NaCl	500 mM NaCl	10 mM Tris-HCl pH 8.1	

Table 1. Components of the buffers used for the beads washes in the ChIP assay.

QPCR was performed to assess the relative amplification of specified genomic sites in Dex *versus* mock-treated ChIPs, which were normalized to the amplification values of respective inputs.

Gene	Forward pimer 5'-3'	Reverse pimer 5'-3'
Axin 2	AGCTCTAGCTGGAGGCTGAT	ACAGGACCTGGCATGGATTG
Hipk2	GGGTTCCTGCAGGGGAATATCTGT	ATGTGCCATGCTGGGCTTGAGA
Per1	TACAGGACCGCTGTCGTTGGGT	CGTCAAAGCGGAGGCAGGAGG
Ror1	ATGCTCACATTCCGACTGGT	AAGCAGGCTTTAGCTTGGGA
Tsc22d3/Gilz2	GGAGGGAATGCAACTGGGAG	CCCCTCCCTTGAATGCTGAA
Zbtb16	GCCGCCAGAACAATGCGTACAGA	AGCTAGGGAGAGCCAAAGCGGG
Zfp36	TCCTCTATCAAGTCCGCCCA	AGGAACGGGATGTTTCCGTC

Table 2. Sequences of primers used in the ChIP-QPCR.

1.6. RNA isolation

Total RNA was isolated either from mouse dorsal skin, immortal keratinocyte cell lines or mouse primary keratinocytes, using TRIzol (Life Technologies). A small section of mouse dorsal skin was

immersed in 1 ml TRIzol and homogenized with the aid of a Polytron homogenizer to maximum speed for 1 min. Homogenates were centrifuged 8700 rpm at 4°C for 10 min to remove debris and insoluble material. Supernatant was incubated at room temperature for 5 min. Next, 200 µl chloroform was added to the supernatant and tubes were shaken vigorously for 15 seconds and subsequently kept at room temperature for 10 min. After centrifugation (11400 rpm at 4°C for 15 min), colorless upper aqueous phase was collected and transferred to a fresh tube. Isopropyl alcohol (500 µl) was added and samples were agitated and were incubated at room temperature for 10 min. After centrifugation (11400 rpm at 4°C for 10 min) supernatant was discarded and pellet was washed with 1 ml of 75% ethanol and centrifuged (11400 rpm at 4°C for 5 min). Ethanol was discarded and air-dried pellet was dissolved in nuclease-free water and incubated at 55°C for 10 min. Finally, RNA was quantified using NanoDrop measuring the absorbance at 260 nm and the absorbance ratio 260/280 to determine the RNA purity. Samples were stored at -80°C until use.

After RNA isolation, DNase treatment of the samples was performed according to the manufacturer's instructions (Thermo Scientific).

1.7. Synthesis of cDNA (reverse transcription)

RNA samples (1 µg) were reverse transcribed to make cDNA using RevertAid H Minus Reverse Transcriptase and using oligo dT primers.

For each reaction, oligo dT primers (Thermo Scientific) were added to 1 µg of RNA. Next, nuclease-free water was added to a final volume of 12.5 µl and mixed was incubated at 65°C for 5 min. Then, 8 µl of the

mix was added, containing 5x buffer, mix of nucleotides (10 mM), 20 units of RNase inhibitor (Thermo Scientific) and 200 units of reverse transcriptase (Revertaid, Thermo Scientific). Next, samples were incubated at 42°C for 1 h. Subsequently, the enzyme was inactivated by heating at 70°C for 10 min and was kept at 4°C (on ice). Finally, cDNA was further diluted 1:10 for quantitative RT-PCR.

1.8. Quantitative RT-PCR

Quantitative real-time PCR was performed using 8 µl of the diluted (1:10) cDNA, specific primers (10 µM) and 10 µl of FastStart Universal SYBR Green Master ROX (Roche) to a final volume of 20 µl and analyzed on Applied Biosystems 7500 Fast real time PCR machine. The following QPCR conditions were used: samples were incubated for 20 seconds at 50°C followed by a second incubation for 10 min at 95°C to activate the polymerase. Afterwards, they were amplified for 40 cycles, consisting of denaturation for 15 seconds at 95°C followed by annealing and extension at 60°C for 1 min.

Hprt1, *Ubc* and *Rpl* were used as housekeeping genes. At least four to five biological replicates were used per genotype and treatment. Technical triplicates were assessed to calculate the mean value ± SD. The sequences of primers used are represented in the table below:

Gene	Forward pimer 5'-3'	Reverse pimer 5'-3'
Axin 2	AGCGCCAACGACAGCGAGTT	CTTGGGCAGGCGGTGGGTTC
Hipk2	ACACACCTGCTTGACTTCCCCCA	TGGATGCCGCTGAGGGCTGGTT
Klf4	GTGCCCCGACTAACCGTTG	GTCGTTGAACTCCTCGGTCT
Nr3c1	AAAGAGCTAGGAAAAGCCATTGTC	TCAGCTAACATCTCTGGGAATTCA
Per1	GGGAGACAAGAAGCCCCCGGA	GTGTCGGCGACCAGGGGGAA
Ror1	CCGCAACCCTGGCAACCAGA	AGCCAGGGGAATGGCCACACT
Sprr2d	TGGTACTCAAGGCCGAGA	TTTGTCCTGATGACTGCTGAAGAC
Tsc22d3/Gilz2	CTGTTGGCCTCGACTGCTG	GCCGAAAGTTGCTCACGAAG
Zbtb16	CCCAGTTCTCAAAGGAGGATG	TTCCCACACAGCAGACAGAAG
Zfp36	CCACCTCCTCTCGATACAAGA	GCTTGGCGAAGTTCACCCA
Hprt1	AGTGTTGGATACAGGCCAGAC	CGTGATTCAAATCCCTGAAGT
Ubc	AGGTCAAACAGGAAGACAGACGTA	TCACACCCAAGAACAAGCACA
Rpl	CCTGCTGCTCTCAAGGTT	TGGTTGTCACTGCCTCGTACTT
S100a8	AAATCACCATGCCCTCTACAAG	CCCACTTTTATCACCATCGCAA
S100a9	ATACTCTAGGAAGGAAGGACACC	TCCATGATGTCATTTATGAGGGC
Il-17f	CCCAGGGCTGTTCTAATTCCTT	GACACAGGTGCAGCCACCTTT
Stat3	AGCTGGACACACGCTACCT	AGGAATCGGCTATATTGCTGGT
Il-22	TCAGTGCTAAGGATCAGTGCT	TGATTGCTGAGTTTGGTCAGG
Il-23a	AAAATAATGTGCCCCGTATCCAG	GCTCCCCTTTGAAGATGTCAG
Il-6	TAGTCCTTCCTACCCCAATTTCC	TTGGTCCTTAGCCACTCCTTC
Tsc22d3/Gilz1	CGGTCTATCAGCTGCACAATTT	ACATCCCCTCCAAGCAGAGA

Table 3. Sequences of primers used in the RT-QPCR.

1.9. *Klf4* knockdown

Keratinocytes were plated in collagen I-coated 35 mm dish. Then they were transfected with 25 nM *Klf4* specific (L04001010005) or Control (D0018101005) On-Target plus siRNA Smartpool (Thermo Scientific) using Lipofectamine 2000 (Life Technologies) and Optimem medium (Life Technologies). Transfection was performed in DMEM-Ham's 12 medium without antibiotics or antimycotic. Medium was changed 5 h after addition of siRNA–Lipofectamine 2000 complexes. Experiments were conducted 48 h following transfection.

1.10. Western blotting

1.10.1. Protein isolation

Whole-cell protein extracts from mouse dorsal skin and cultured keratinocytes were isolated and prepared for posterior analysis. Collected frozen sample (skin, spleen, gut) were ground in liquid nitrogen using a mortar and a pestle. Next, protein was extracted from tissue (Buffer C: 20 mM HEPES pH 7.9, 0.4 M NaCl, 1 mM EDTA, 1 mM EGTA and 25% glycerol) or cells (RIPA buffer: 50 mM Tris–HCl pH 8, 150 mM NaCl,1% NP-40, 0.5% sodium deoxycholate, 0.1% SDS) using protease (complete Mini EDTA-free; Roche) and phosphatase inhibitors (PhosStop; Roche) by three freezing (liquid nitrogen) and thawing (37°C) cycles. Afterwards, 10% Igepal CA-630 was added to the lysed samples and they were incubated on ice for 15 min. Subsequently, samples were centrifuged 10000 rpm at 4°C for 20 min. Protein concentration of collected supernatants was measured by Bradford reaction (Bio-Rad) using *Wallac Victor 1420 multilabel counter.* Bovine serum albumin was used for the preparation of the standard curve. 25-30 µg of protein were used for the western blots.

1.10.2. Gel electrophoresis and protein transfer

Protein samples (25-30 µg protein) were boiled in Laemmli buffer (containing 6% SDS and 1% β-Mercaptoethanol) at 95°C for 10 min for protein denaturation. Denaturated protein extracts and molecular-weight size marker (Spectra™ Multicolor Broad Range Protein Ladder; Thermo Scientific) to identify the approximate size of the proteins were loaded onto 8-15% SDS-polyacrylamide (SDS-PAGE) gel constituted by the following components:

		Separating gel		
Stacking gel 5%			**8%**	**10%**
40% polyacrylamide	750 µL	40% polyacrylamide	2.4 mL	3 mL
1 M Tris-HCl pH 6.8	750 µL	1.5 M Tris-HCl pH 8.8	3 mL	3 mL
10% amonium persulfate	60 µL	10% amonium persulfate	120 µL	120 µL
10% SDS	60 µL	10% SDS	120 µL	120 µL
TEMED	6 µL	TEMED	7.2 µL	4.8 µL
H_2O	4.4 mL	H_2O	6.36 mL	5.76 mL

Table 4. Components of the polyacrylamide gels.

Samples were run at 100 V for 2 h and transferred to a nitrocellulose membrane (Hybond ECL, Amersham) at 80 mA for 75 min using transfer buffer (25 mM Tris, 192 mM glycine and 20% methanol) and semi-dry blotting system (Trans Blot SD Semi-dry Transfer Cell, Bio-Rad). Gel loading control was done by Ponceau S staining on the membranes after transfer.

1.10.3. Blocking, incubation and band detection

Blocking buffer (5% non-fat dry milk in 0.1% Tween 20 (Sigma) in PBS buffer) was used to block the membrane for 1 h at room temperature and then incubated overnight at 4°C in primary antibody diluted in the blocking buffer followed by the three washes with PBS-0.1% Tween 20 buffer. Next, peroxidase-conjugated secondary antibodies were diluted in the same blocking buffer solution and incubated for 1 h at room temperature. After the incubation, membranes were washed three times with PBS-0.1% Tween 20 buffer. The immunoreactive bands were detected using ECL2 (Thermo Scientific) with the ImageQuant 4000 Biomolecular Imager (GE Healthcare). Quantification of the protein band density was determined using Image J software. Experiments were performed with a minimum of three biological replicates. Tubulin or actin was used as protein loading control. Peroxidase-conjugated secondary antibodies were purchased from GE HealthCare.

The primary and secondary antibodies are listed below:

Antibody	Dilution	Company	Species
GR (sc-1004)	1/1000	Santa Cruz Biotechnology	Rabbit
Klf4 (sc-20691)	1/1000	Santa Cruz Biotechnology	Rabbit
p63 (sc-8431)	1/1000	Santa Cruz Biotechnology	Rabbit
p-GR Ser 211 (4161S)	1/1000	Cell Signaling Technology	Rabbit
GILZ (14-4033)	1/1000	eBioscience	Rat
pSMAD2/3 Ser 465/467 (3108P)	1/1000	Cell Signaling Technology	Rabbit
SMAD2 (5339P)	1/1000	Cell Signaling Technology	Rabbit
SMAD3 (9523P)	1/1000	Cell Signaling Technology	Rabbit
Tubulin (T6199)	1/4000	Sigma-Aldrich	Mouse
Actin (A2066)	1/1000	Sigma-Aldrich	Rabbit

Table 5. List of the antibodies used in the western blot analysis.

2. Immunoprecipitation

Keratinocytes were lysed using a buffer containing 50 mM Tris pH 7.6, 150 mM NaCl, 5 mM EDTA, 0.5% Igepal CA-630 with protease and phosphatase inhibitors (Roche). Proteins were immunoprecipitated using 2 µg of KLF4 specific antibody or rabbit IgG as a negative control and Dynabeads Protein A (Life Technologies). After washing with buffer containing 0.2% Igepal CA-630, proteins were eluted from beads by boiling in Laemmli buffer for analysis by immunoblotting.

HRP-conjugated Clean-blot IP Detection Reagent (Thermo Scientific) was used for immunoblotting of immunoprecipitation experiments.

3. Mice

Female mice were maintained at 12 light/12 dark cycles, caged in groups (4–6 per cage) under SPF conditions, and having access to *ad*

libitum food and water. All the animal protocols were approved by the ethical committee of the Faculty of Sciences at Ghent University.

3.1. Generation of GILZ transgenic mice

Mice were generated in the laboratory of Prof. Claude Libert (Inflammation Research Center, Ghent) as follows:

Conditional GILZ-Tg overexpressing mice were generated using a Gateway-compatible ROSA26 locus targeting vector (Nyabi et al., 2009), knocking in the construct containing the mouse *Tsc22d3/Gilz-1* cDNA preceded by a loxP flanked stop cassette under control of the ROSA26 promoter, and followed by an IRES-EGFP (Enhanced Green Fluorescent Protein) cDNA. Chimeric mice that transmitted the transgene to their offspring were generated, once the targeted embryonic stem cell clones were identified correctly by Southern blot analysis. GILZ-Tg mice that were used for experimentation were generated by intercrosses of one transgenic line homozygous for the GILZ-loxP construct and mice carrying one allele of Nestin-cre, which express Cre in all cell types (Betz *et al*., 1996).

Due to some degree of leakiness of the loxP flanked stop cassette, control mice with exactly the same genetic background (C57BL/6) as the GILZ-Tg mice, but without the cassette (GILZ-Wt) were used.

For genotyping, the following primers and conditions were used: PCR cycling for the stop cassette consisted of denaturation at 94°C for 5 min, 35 cycles of 94°C for 1 min, annealing at 57°C for 1 min and extension at 72°C for 2 min, followed by 10 min at 72°C. Primer sequences were used as followed: forward primer 5’ GTGATCTGCAACTCCAGTCTTTC 3’; reverse primer 5’ CCATCTGCACGAGACTAGTG 3’.

3.2. Imiquimod-induced psoriasis mouse model

For the IMQ experiment female GILZ-Wt and GILZ-Tg mice of 8-12 weeks of age were used. Either Aldara® (containing 5% IMQ, 3 M Pharmaceuticals; 62.5 mg) or control cream (Ava, Fagron NV) was applied topically on mouse dorsal shaved skin daily for 7 days. Skin erythema and scaling were daily scored independently on a scale from 0 to 4: 0, none; 1, slight; 2, moderate; 3, marked; 4, very marked. Gut, spleen and a section of dorsal skin were collected, snap-frozen in liquid nitrogen and stored at -80°C until use or fixed in 70% ethanol for two days and embedded in paraffin for immunohistochemical analysis. Spleens were collected and weight was expressed relative to mouse body weight. In total 31 animals were used in two independent experiments (15 GILZ-Wt, 16 GILZ-Tg).

3.3. Tissue collection

After sacrificing mice, skin samples from adult and newborn (P0) mice were dissected and immediately fixed in 70% ethanol for 48 h at room temperature.

3.4. Histological procedures

After fixation, skin samples were mounted in cassettes and introduced in the tissue processor (Spin Tissue Processor STP 120, Myr) where samples were dehydrated by immersion in a series of ethanol solutions of increasing concentration, followed by xylene (Merck) and finally in paraffin (Panreac). Subsequently, tissues were embedded in paraffin blocks in a Modular Tissue Embedding Center 350, Myr. Then paraffin-embedded tissue blocks were sectioned 4 µm using a microtome (Rotary microtome HM 340 E, Microm) and sections were placed on the polylysine-coated microscope slides and air dried

(Menzel Glässer). Tissue processor protocol was followed as shown in the table below:

Reactive	Time (hours)
70% Ethanol	1
95% Ethanol	3
95% Ethanol II	1.5
100% Ethanol I	2
100% Ethanol II	6
Xylene I	1.5
Xylene II	2.5
Paraffin I	2.5
Paraffin II	2

Table 6. Steps followed in the tissue processor.

3.5. Hematoxylin-eosin staining

Mouse dorsal skin sections (n=15 GILZ-Wt and 16 GILZ-Tg) were first deparaffinized by heating at 60°C for 30 min and posterior incubation twice in xylene for 10 min. Next, sample sections were hydrated by immersion in a series of ethanol solutions of decreasing concentration (100%, 90%, 70% y 50%), followed by water. After hydration, sample sections were immersed in hematoxylin Harris (Panreac), Bluing Reagent (Thermo Scientific) and yellow eosin (Panreac). Afterwards, sample sections were dehydrated by immersion in a series of ethanol solutions of increasing concentration (50%, 70%, 90% and 100%) and xylene. Finally, sample sections were mounted with a synthetic resin which is a xylene-based mounting medium like *DPX* (Merck). Samples were observed using the optical microscope *Leica DM 1000* and images were acquired using the digital camera Leica EC3.

3.6. Immunohistochemical analysis

Mouse dorsal skin sections (n=15 GILZ-Wt and 16 GILZ-Tg) were first deparaffinized by heating at 60°C for 30 min and posterior incubation twice in xylene for 10 min and twice in 100% EtOH for 10 min. Subsequently, to block the endogenous peroxidase activity, sample sections were immersed in a solution of methanol: H_2O_2 (29:1) for 20 min at room temperature in the dark. Next, sections were blocked with 5% fetal bovine serum in PBS for 20 min, followed by incubation with the primary antibody diluted in a solution of 1% bovine serum albumin (in PBS) overnight at 4°C. Next, samples were washed with PBS to remove the excess of primary antibody, and secondary biotin-conjugated antibody (diluted in a solution of 1% bovine serum albumin (in PBS) (Jackson ImmunoResearch, West Grove, PA) was added and incubated at room temperature for 1 h. After washes with PBS, sample sections were incubated with the avidin-biotin-peroxidase complex (ABC, Vectastain; PK-6100; Vector Laboratories). Then sections were visualized using a kit of diaminobenzidine (DAB; Vector Laboratories), a chromogen for immunohistochemical staining as it is a peroxidase substrate and reaction was stopped by immersion in water. Next, sections were counterstained with hematoxylin. Samples were dehydrated and mounted as described in the "hematoxylin-eosin staining" section.

Antibody	Dilution	Company	Species
K6 (PRB-169P)	1/2000	Covance	Rabbit
loricrin (PRB-145P)	1/1000	Covance	Rabbit
Caspase-14 (sc-5628)	1/1000	Santa Cruz	Rabbit
p-SMAD2/3 (sc-11769-R)	1/1000	Santa Cruz	Rabbit

Table 7. Antibodies used in the immunohistochemistry of the mouse skin.

4. Keratinocyte transfection and dual luciferase assay

4.1. Keratinocyte transfection

For transfection experiments, keratinocytes were seeded on a collagen I-coated 24-well plate to a confluence of about 80% 24h prior transfection. Then, transient transfections were performed with the indicated plasmids using Lipofectamine 2000 Reagent (Invitrogen) according to the manufacturer's protocol. Renilla was used as a co-reporter for normalization of experimental variations such as differences in transfection efficiencies. After 5 h, transfection medium was replaced by growth medium (low calcium medium) and transfected keratinocytes were incubated with 1 ng/µl TGF-β1 for 20 h. The empty expression vector cassette pCDNA4 was provided by Invitrogen.

The pEGFP-C1-Gilz plasmid was kindly provided by Prof. Claude Libert (Inflammation Research Center, Ghent).

The SMAD-Luc/reporter plasmid containing SMAD Binding Regions (Alonso-Merino *et al.*, 2016) was kindly provided by Dr. Ana Aranda (Instituto de Investigaciones biomédicas "Alberto Sols", CSIC-UAM, Madrid).

4.2. Dual luciferase reporter assay

To examine the transcription activity, dual luciferase reporter assays were performed using the dual luciferase assay system (Promega). After removing the cell supernatant of the transfection assay (24-well plate), 100 µl diluted Passive Lysis Buffer (Promega Corp., Madison, WI) was added and shaken at 1000 rpm for 15 min at 25 °C (in a thermomixer comfort from Eppendorf®). Then 25 µL from

each cell homogenate was added to a 96-well plate and the luciferase activity was measured using a Wallac Victor^2 1420 multilabel counter according to the manufacturer's protocol. Firefly-luciferase activity of each well was corrected using the corresponding Renilla-luciferase activity.

5. Keratinocyte transfection and treatment with IL-17A

Keratinocytes were seeded in a 6-well plate to a confluence of about 80% 24 h prior to transfection. 5 h after transfection, medium was replaced and cells were treated with recombinant human IL-17A (100 ng/ml for 24 h, R&D Systems). After 24 h, keratinocytes were collected and lysed for posterior RNA isolation and determination of *S100a8* expression by RT-QPCR.

6. Determination of serum cytokine levels

This protocol was performed in the laboratory of Prof. Claude Libert. IL-17A, IL-17F, and TNF-α were analyzed in the serum samples using Luminex technology (BioPlex, Bio-Rad) following the manufacturer's protocol.

7. Isolation of lymph nodes, treatments, and determination of IL-17A levels

This protocol was performed in the laboratory of Prof. Claude Libert. At day 7 ear-draining (brachial) lymph nodes were isolated from GILZ-Tg and GILZ-Wt mice treated with Aldara or control cream. After mincing the lymph nodes through a 70 µm cell strainer (BD Falcon) to obtain single cell suspensions, cells were cultured in RPMI-1640L medium supplemented with Glutamax, 10% fetal calf serum,

gentamycin and β-mercaptoethanol (Gibco; Life Technologies). Then cells were re-stimulated with 10 μg/ml Aldara or control cream for 3 d. The levels of IL-17A cytokine production was measured in the supernatant of cultured cells using Luminex technology (BioPlex; Bio-Rad) in accordance with the manufacturer's protocol.

8. Statistical Analysis

Experimental data were analyzed using Microsoft Excel and IBM SPSS Statistics 23 software. In all graphs, data are expressed as the mean value ± SD. Prior to parametric testing, the Levene's test was used to determine whether samples within groups had equal variance. For comparisons between two experimental groups, we used the Student's unpaired two-tailed t-test. For comparisons multiple experimental groups, we used the one-way ANOVA which if statistically significant was followed by a post hoc Tukey multiple comparison test. P values less than 0.05 were considered statistically significant.

Chapter IV

Results and discussion

Part I

Analysis of the functional cooperation of the glucocorticoid (GC) receptor (GR) and Krüppel-like factor (KLF) 4 in the regulation of gene expression in epidermal keratinocytes

It is well known that the synthetic GC dexamethasone (Dex) induces the translocation of GR to the nucleus in many cell types, where it binds to specific sequences in the DNA and regulates the expression of genes associated with homeostasis and differentiation (Ramamoorthy and Cidlowski, 2016). In mouse primary keratinocytes (MPKs), Dex also induced GR translocation to the nucleus, as shown by immunofluorescence (**Figure 12**; and Sevilla *et al*., 2010).

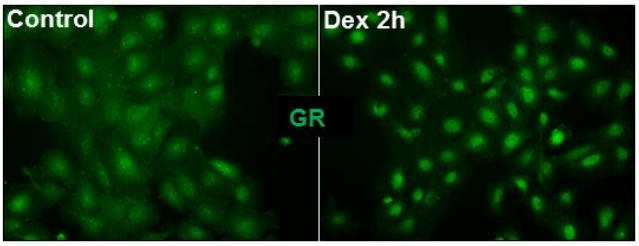

Figure 12. Dex induces GR nuclear translocation in mouse primary keratinocytes (MPKs). Representative confocal microscopy image of GR translocation to the nucleus induced after Dex (2h, 100 nM) treatment on MPKs.

Previous studies in our laboratory have identified genes directly regulated by Dex-activated GR in MPKs by GR ChIP followed by global analysis of the whole genome (ChIP-seq). These data have permitted us to identify 104 peaks with GR binding in keratinocytes after Dex treatment. The identified associated genes included *Tsc22d3/Gilz*, *Per1* (Period circadian clock 1), *Ror1* (receptor tyrosine kinase-like orphan receptor) and *Zfp36*, already described in literature as directly regulated by GR in several cell types including keratinocytes (Newton, 2014; Stojadinovic *et al*., 2007). We also identified novel GR-target genes in keratinocytes such as *Axin2*, an inhibitor of Wnt signaling also known to be induced by Dex in other tissues (Naito *et al.*, 2015); *Hipk2* (homeodomain-interacting protein kinase 2), which encodes a nuclear serine-threonine kinase that regulates gene expression by

phosphorylating TFs and can act as an oncogene or tumor suppressor (Imberg-Kazdan *et al.*, 2013); and *Zbtb16* (*zinc finger and BTB domain containing 16*), which encodes the protein Zbtb16 and also known as PLZF (promyelocytic leukemia zinc finger).

However, the exact DNA binding sites of GR and mechanism of regulation of these genes in keratinocytes were not previously investigated.

1. 1. Validation of GR direct transcriptional targets identified in mouse keratinocytes by GR ChIP-seq

In order to validate the results obtained from ChIP-seq analysis, we performed an independent experiment of GR ChIP using cultured MPKs that were either left untreated or treated with Dex for 2 h followed by qRT-PCR using specific sequence primers. As shown, Dex treatment led to the GR recruitment to the regulatory sequences of the selected genes (**Figure 13**). The extent of GR recruitment was found to be 2.5-fold for *Axin2* and ~20-25-fold for *Ror1, Tsc22d3* and *Zfp36*.

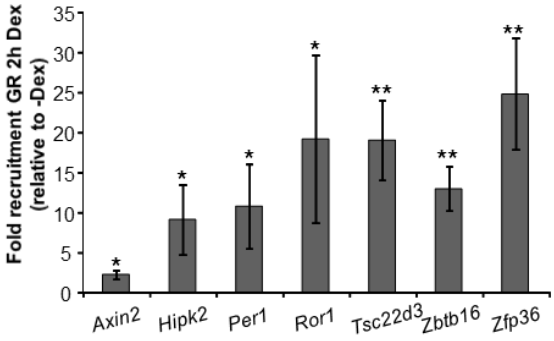

Figure 13. Validation of GR transcriptional targets in MPKs. Primary epidermal keratinocytes from newborn mice were cultured and treated either with Dex (100 nM, 2 h) or vehicle followed by GR ChIP and qRT-PCR using specific sequence primers for the indicated genes. Mean values ± SD show fold GR recruitment in Dex- *versus* mock-treated MPKs. Asterisks indicate

statistically significant differences between groups (Student's t-test, n = 3; *p < 0.05, **p < 0.01).

Subsequently, we evaluated the expression of these genes after Dex treatment and found significant up-regulation in all cases (**Figure 14**). Dex induced the mRNA levels of *Axin2, Hipk2*, *Ror1* and *Zfp36* by approximately 2-fold while *Tscd22d3* and *Per1* expression were induced around 6-fold (**Figure 14**). Remarkably, Dex induced the expression of the TF *Zbtb16*, a general transcriptional repressor, by more than 250-fold. Although its expression has been reported to be induced in response to GCs in lymphoid cells in acute lymphoblastic leukemia protecting cells from apoptosis acting as a repressor on Bim-transcription (Wasim *et al.*, 2010), there is no mention of the GR recruitment to its regulatory sequences. ZBTB16 has been implicated in tumor suppression in melanoma (Shiraishi *et al.*, 2007).

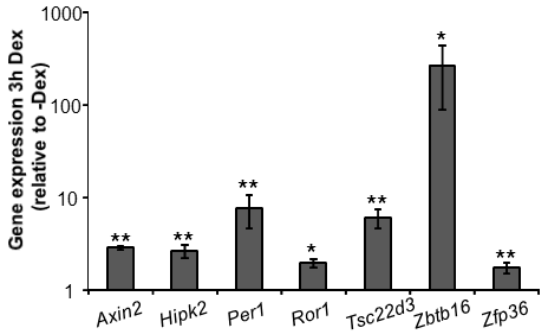

Figure 14. Evaluation of gene expression in MPKs in response to Dex. Gene expression of the indicated genes was assessed in cultured MPKs after Dex treatment (100 nM, 3 h) by RT-QPCR. Mean values ± SD show the relative gene expression in Dex- *versus* mock-treated. Asterisks indicate statistically significant differences between groups (Student's t-test; n = 3; *p < 0.05, **p < 0.01).

However, no clear correlation between the level of transcriptional activity (induced by Dex) and GR recruitment was observed. This fact has also been reported by other authors (Schöne *et al.*, 2016). For example, the *Zbtb16* GBS, which showed one of the highest transcriptional activities among the validated genes showed lower occupancy (**Figures 13 and 14**).

1.2. Analysis of TF binding motifs in GR ChIP-Seq peak regions

We wondered whether the genomic DNA sequences associated with GR ChIP-seq peaks correlated with the overrepresentation of one or several TF binding motifs. For this, we used MEME (http://meme.nbcr.net/meme/), a web-based tool for analyzing motifs in DNA. Our survey showed that most of the 104 regulatory sequences contained canonical binding motifs for GR (GREs: AGAACAnnnTGTTCT, (64%), AP-1 (TGAGTAAT, 28%) and KLF (Krüppel like factor) (CACCC; 43%) (**supplementary table 1**). This overrepresentation of binding sites demonstrates the importance of these TFs in the early response to GCs of epidermal keratinocytes. It also suggests that GR, in combination with these TFs coordinately regulates gene expression in this cell type.

Overrepresentation of GRE binding motifs was expected and the GR/AP-1 interference has been also widely described (Newton, 2014). It is known that GR inhibits AP-1 through protein-protein interaction (tethering) resulting in inhibition of the AP-1 activity (DiDonato *et al*., 2012), and thus repression of numerous pro-inflammatory genes, such as IL-6, IL-1β y TNF-α (De Bosscher and Haegeman, 2009; Newton, 2014). Alternatively, GR can bind to composite regulatory elements that contain both the GRE and AP-1 motifs (Newton, 2014). Additionally, it has been reported that AP-1 colocalizes in the DNA with GR and

promote its accessibility to regulatory elements in the DNA (Biddie *et al*., 2011). This mechanism has been also shown for other TFs belonging to the NR family, such as estrogen receptor (Miranda *et al.*, 2013).

However, the examples of functional interactions between GR and KLFs have been less studied and depend on the expression patterns of various KLF members (Chinenov *et al*., 2014; Knoedler *et al.*, 2014). As mentioned in the introduction section, KLF is a family of TFs that mediate many relevant biological processes. All the family members act as TFs binding to specific DNA sequences (CACCC or related GC-rich elements) in the promoter and enhancer regions. One of the members of the family, KLF4, is highly expressed in the differentiated and post-mitotic cells in gut and skin. Among the different KLF members, we focused on KLF4 given the crucial role of this TF in epidermal development and homeostasis (Segre *et al.*, 1999; Jaubert *et al.*, 2003)**.**

Both GR and KLF4 play important roles in epidermal development and homeostasis, which is demonstrated by either inhibiting or overexpressing these TFs individually (Pérez, 2011; Ghaleb and Yang, 2017).

Absence of KLF4 in mice led to abnormal epidermal barrier formation due to alterations in the expression of the late-differentiation structures from the cornified envelope (Segre *et al.*, 1999) and increased tumorigenesis when chemically induced (Ghaleb and Yang, 2017). On the other side, ectopic expression of KLF4 *in vivo* in basal keratinocytes accelerated the barrier acquisition in mouse (Jaubert *et al.*, 2003). However, inducible activation of KLF4 in the epidermal basal layer led to an unexpected epithelial dysplasia (Foster *et al*., 2005). The KLF4 acts as a tumoral suppressor or oncogene depending on the cellular context (Rowland and Peeper, 2006).

Mice overexpressing GR in epidermis and other stratified epithelia showed defects in the cutaneous development as well as in ocular, tooth epithelia, and secretory glands, and delay in cutaneous wound healing. Also, mice with epithelial GR overexpression showed protection against epidermal inflammation and skin tumorigenesis (Pérez *et al*., 2001; Cascallana *et al*., 2005; Budunova *et al*., 2003; Pérez, 2011; Sanchis *et al*., 2012).

On the other side, mouse models with total or epidermis-specific GR inactivation (GRnull and GR epidermal KO/GR^{EKO} mice, respectively) displayed impaired epidermal barrier formation (Bayo *et al.*, 2008; Sevilla *et al.*, 2013). Also, GR^{EKO} adult mice were more susceptible to inflammatory stimuli and more prone to development and conversion of skin tumors (Sevilla *et al.*, 2013; Latorre *et al*., 2013).

Furthermore, both antenatal GC treatment and the ectopic expression of KLF4 accelerated the formation of the skin barrier (Segre, 2003; Jaubert *et al.*, 2003) and there was overlapping between target genes regulated during the epidermal development by antenatal corticosteroids and KLF4 (Patel *et al*., 2006; Sevilla *et al*., 2010; Sevilla *et al*., 2013). Altogether, these antecedents made plausible that both TFs collaborate to regulate expression of common genes in epidermal development.

Among the genes identified as GR transcriptional targets in cultured keratinocytes, we focused our study on two genes that contained both GR and KLF binding sites, and that are involved in inflammation in other tissues, *Tsc22d3/Gilz* and *Zfp36/Ttp* (**supplementary Table 1 and Figure 15**).

Tsc22d3/Gilz encodes a protein named GILZ, which has been reported to be an anti-inflammatory mediator in several cell types. The

mechanisms of action of GILZ to block inflammatory gene transcription include its interaction with NF-κB, AP-1 and Raf-1, thus inhibiting the downstream MAPK pathway (Srinivasan and Janardhanam, 2011; Ayroldi and Riccardi, 2009). GILZ is known to have several isoforms. The GBSs identified in this study map 13251 bp downstream of transcriptional start site (TSS) of isoforms *Gilz1* and *Gilz*3, and 71645 bp downstream of TSS of *Gilz2*; these GBSs are separated by 6 bp of the KLF binding site (**Figure 15**).

Zfp36 gene codes for the protein Tristetraproline (TTP), which regulates the expression of many pro-inflammatory cytokines, including IL-22 and IL-23, which are important in autoimmune and inflammatory diseases (Härdle *et al.*, 2015; Molle *et al.*, 2013). TTP exerts its anti-inflammatory role by binding to RNAs that contain AU-rich elements and recruits enzymes that degrade RNA or avoids translation of mRNAs of pro-inflammatory genes, including *Tnf-α* (Brooks and Blackshear, 2013). TTP activity is regulated by phosphorylation (Patial *et al.*, 2016). Furthermore, TTP overexpression has been shown to have protective effects in immune inflammatory diseases (Patial *et al.*, 2016). The GBSs identified in this study map 2732 bp downstream of TSS and are separated by 1 and 98 bp of the two KLF binding sites (**Figure 15**).

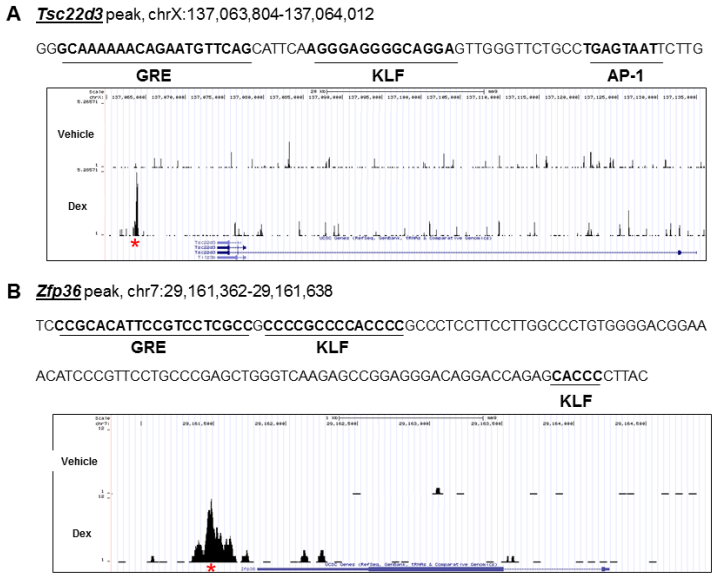

Figure 15. GREs and KLF sites present in *Tsc22d3* (A) and *Zfp36* (B) genomic sequences bound by GR. Genomic sequences near *Tsc22d3* and Zfp36 where GR was bound in ChIP-seq. GREs and adjacent KLF and AP-1 sites are underlined. GR-bound peaks are denoted by asterisks in *Tsc22d3* (A) or *Zfp36* (B). Genome build: NCBI37/mm9.

1.3. GR and KLF4 bound on *Tsc22d3* and *Zfp36* after Dex induction in immortal adult mouse keratinocytes

Like any other primary cells, MPKs also have some restrictions, such as limited lifespan and low transfection efficiency. Hence, we decided to use an immortalized keratinocyte cell line from adult mouse epidermis, which was previously established and characterized in our group (Latorre *et al*., 2013). We first confirmed that there were no differences between the primary and immortalized keratinocytes due to the variability and differences that may be present in the basic biology of keratinocytes according to their stage of development and their status (primary or immortalized) (Yano and Okochi, 2005).

For this purpose, we first compared the GR recruitment and subsequent gene expression changes elicited by Dex treatment in both primary and immortal keratinocyte cell lines.

Our data confirmed that GR was recruited to the regulatory sequences of *Tsc22d3* and *Zfp36* in the established keratinocyte cell line (**Figure 16**). Accordingly, *Tsc22d3* and *Zfp36* mRNA levels were significantly induced after Dex treatment (5.2-fold, and 1.6-fold, respectively) in this cell line (**Figure 17).** No significant differences were observed between the primary and immortalized cells regarding GR recruitment and expression of *Tsc22d3* and *Zfp36* after Dex treatment (**Figure 16 *versus* Figure 13 and Figure 17 *versus* Figure 14**), This indicates that the developmental stage and status of epidermal keratinocytes (primary or immortalized) did not influence the relative expression levels of the genes *Tsc22d3* and *Zfp36* or their induction by GCs.

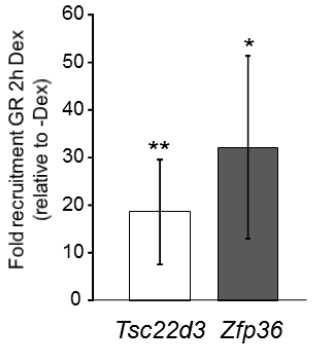

Figure 16. Dex induces similar GR binding to *Tsc22d3* and *Zfp36* in an immortal adult mouse keratinocyte cell line. Dex (100 nM) treatment for 2 h in an immortal adult mouse keratinocyte cell line induced recruitment of GR to putative regulatory sequences of *Tsc22d3* and *Zfp36* after ChIP-QPCR. Mean values ± SD show fold GR recruitment in Dex- *versus* mock-treated cells. Statistically significant differences between groups are indicated by asterisks (Student's t-test, n = 4; *p < 0.05, **p < 0.01).

To evaluate whether the induction of *Tsc22d3* and *Zfp36* by Dex is strictly dependent on GR, we used an immortalized adult keratinocyte cell line deficient in GR, or GR^{EKO} cells (Latorre *et al*., 2013).

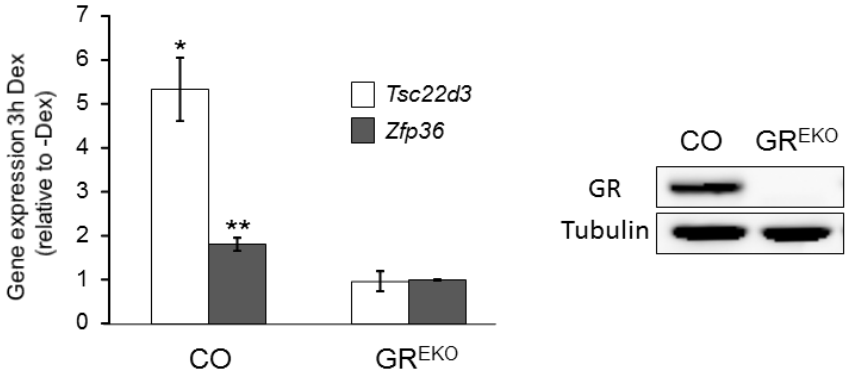

Figure 17. *Tsc22d3* and *Zfp36* expression is not regulated by Dex in an adult mouse keratinocyte cell line deficient for GR (GR^{EKO}). *Tsc22d3* and *Zfp36* mRNA levels after Dex treatment (100 nM, 3 h) were assessed in GR^{EKO} and control (CO) cell lines by RT-QPCR. Mean values ± SD show relative gene expression in Dex- *versus* mock-treated samples. Statistically significant differences between groups are indicated by asterisks (Student's t-test; n = 3; *p < 0.05; **p < 0.01). Representative immunoblotting showing lack of GR in GR^{EKO} relative to CO keratinocytes. Tubulin was used as a loading control.

We analyzed the expression of *Tsc22d3* and *Zfp36* mRNA levels in control (CO) and GR^{EKO} cells treated with either vehicle or Dex for 3 h (**Figure 17).** The lack of induction of both *Tsc22d3* and *Zfp36* in the GR^{EKO} cells indicates that the GR function is indispensable for the induction of both genes by Dex (**Figure 6**). Similar to GR^{EKO} keratinocytes, it was reported that specific deletion of GR in cardiomyocytes led to a lack of *Zfp36* and *Lipocalin2* induction (Sacta *et al.*, 2016) in response to Dex (6 h).

Next, we evaluated whether KLF4 was recruited to the identified *Tsc22d3* and *Zfp36* regulatory regions by ChIP-QPCR in the control

keratinocyte cell line. ChIP-QPCR using an anti-KLF4 antibody showed that Dex treatment induced significant KLF4 binding to both sequences (4.7-fold and 2.9-fold, respectively) (**Figure 18, CO**).

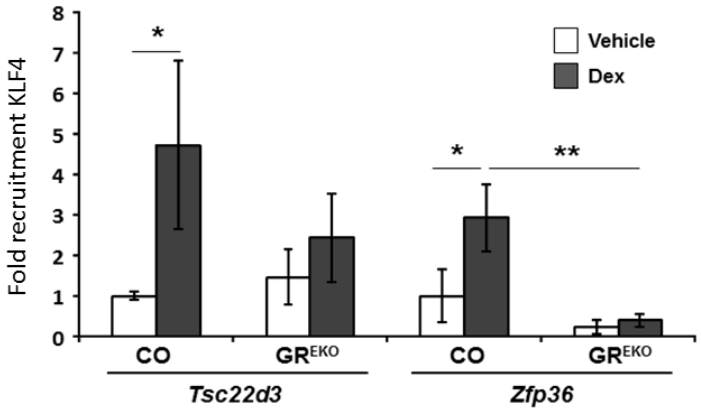

Figure 18. Dex induces binding of KLF4 to *Tsc22d3* and *Zfp36* in immortal adult mouse keratinocytes. KLF4 was recruited to regions near *Tsc22d3* and *Zfp36* and increased upon Dex treatment (100 nM, 2 h) in CO but not in GR^{EKO} cells. Mean values ± SD show fold GR recruitment in Dex- *versus* mock-treated CO and GR^{EKO} cells. Statistically significant differences between groups are indicated by asterisks (Student's t-test; n = 4; *p < 0.05; **p < 0.01). For *Tsc22d3,* there was a decrease between Dex-treated CO and GR^{EKO}, although it did not reach statistical significance (p=0.09).

However, in GR^{EKO} keratinocytes, the Dex-induced recruitment of KLF4 to *Tsc22d3* decreased by 2-fold compared to CO cells although it did not reach statistical significance (p=0.09). In the case of *Zfp36*, the recruitment of KLF4 in the absence (0.22-fold) and presence (0.39-fold) of Dex was greatly and significantly reduced in the GR-deficient cell line relative to CO cells (**Figure 18**). Therefore the recruitment of KLF4 to *Tsc22d3* and *Zfp36* genomic regions containing both GR and KLF binding sites after Dex treatment suggests cooperation between these TFs in regulating these anti-inflammatory genes.

1.4. Evaluation of the response to Dex of *Tsc22d3* and *Zfp36* after *Klf4* knockdown

To further evaluate the contribution of KLF4 to the expression of *Tsc22d3* and *Zfp36* and their regulation by GCs, we performed *Klf4* knockdown assays in keratinocytes. KLF4 expression was decreased by approximately 70% at the RNA and protein level after transfection of the keratinocyte CO cell line with siRNA specific for *Klf4* (**Figure 19**). Interestingly, GR protein levels were not affected by the *Klf4* knockdown (**Figure 19A**), suggesting that KLF4 is not required for constitutive expression of GR. The induction of *Tsc22d3* by Dex was decreased by approximately 2-fold in cells expressing the *Klf4* siRNA relative to control siRNA (**Figure 19B**) demonstrating that both GR and KLF4 are required for proper transcriptional responses to GCs.

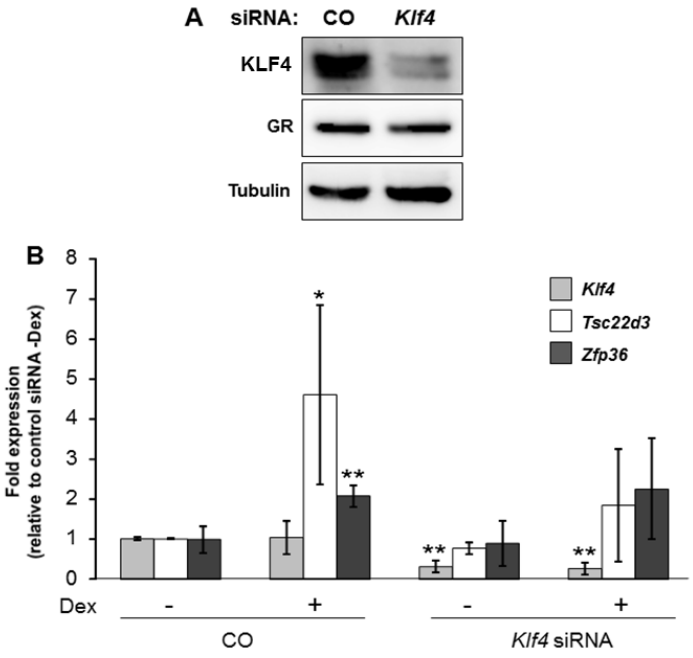

Figure 19. Knockdown of *Klf4* interferes with Dex-induction of *Tsc22d3*. A) Representative immunoblotting showing the expression of KLF4 in

keratinocytes transfected with control and *Klf4* siRNA. *Klf4* knockdown did not alter the GR expression. Tubulin was used as a loading control. **B)** Dex (100 nM, 3 h) induced a significant increase in *Tsc22d3* and *Zfp36* in cells transfected with control but not *Klf4* siRNAs as shown by RT-QPCR. Mean values ± SD show fold change in expression relative to mock-treated control siRNA transfectants. Statistically significant differences between groups are indicated by asterisks (Student's t-test; n = 4; *p < 0.05; **p < 0.01).

In contrast, *Zfp36* was still induced in the *Klf4* knockdown cells (**Figure 19B**). This could be due to the fact that *Zfp36* would require a complete *Klf4* knockdown or that KLF4 regulates this gene differently. Furthermore, KLF4 is required for *Zfp36* induction as we observe recruitment of KLF4 in presence of Dex to *Zpf36*, and this recruitment is decreased in the absence of GR (**Figure 18**).

1.5. Assessment of direct functional associations between GR and KLF4

Whether or not GCs regulate the *Klf4* gene expression in epidermal keratinocytes is still a controversy. According to a published microarray in cultured human keratinocytes, Dex induced *Klf4* expression 2-fold after 4 h, but not at 1 or 24 h (Stojadinovic *et al*., 2007). However, no up-regulation was observed after an antenatal GC treatment in developing mouse skin (Patel *et al*., 2006).

We evaluated the basal levels of *Klf4* gene expression in immortalized cultured keratinocytes by RT-QPCR. Although *Klf4* mRNA expression levels decreased in GR^{EKO} *versus* CO cells (**Figure 20**), no *Klf4* induction was observed in CO keratinocytes treated with Dex for 3 h (**Figure 19B**).

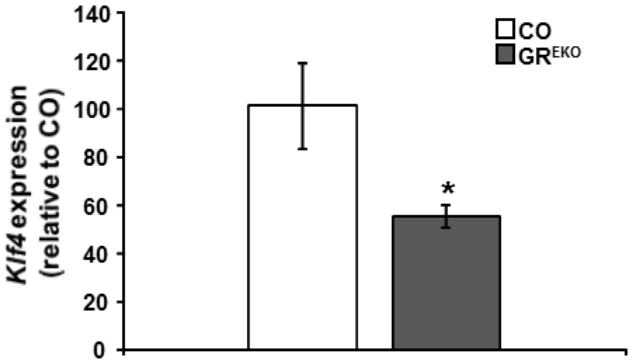

Figure 20. Reduced expression of *Klf4* in GR^{EKO} relative to CO keratinocytes. *Klf4* mRNA expression was determined by RT-QPCR. Mean values ± SD are shown, with asterisks denoting statistically significant differences in GR^{EKO} relative to CO (Student's t-test; n = 3; *p<0.05).

We evaluated the levels of *Klf4* mRNA in adult immortalized mouse keratinocytes after Dex treatment at additional time points (30 min, 1 h and 3 h).

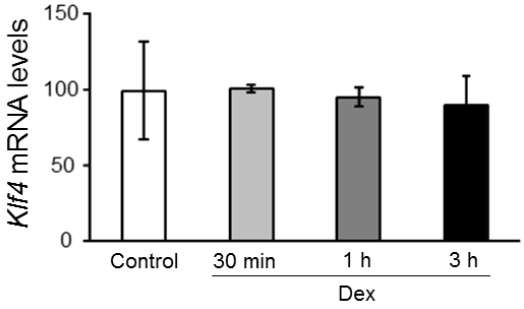

Figure 21. No changes of *Klf4* mRNA levels in response to Dex at different time points. Adult immortalized mouse keratinocytes were treated with Dex 100 nM at different time points (30 min, 1 h and 3 h) and *Klf4* was determined by RT-QPCR. Mean values ± SD are shown. n=3.

We did not observe changes in the regulation of *Klf4* by Dex (**figure 21**), consistent with the results observed by Patel (Patel *et al.*, 2006). However, recent experiments in macrophages and also in

human cultured keratinocytes showed an induction of *Klf4* in response to Dex (Chinenov *et al.*, 2014; Stojadinovic *et al.*, 2007). This suggests that the induction of *Klf4* by Dex may be cell-type specific, as it is induced in macrophages (cells of the immune system) but not in mouse keratinocytes or *in vivo*.

1.5.1. GR ChIP to assess binding at putative *Klf4* regulatory regions

While these experiments were ongoing, Chinenov reported that in macrophages Dex induced GR recruitment to GBSs near *Klf4* sites in *Klf4* gene. These authors identified two putative GREs located at −3830 bp and +5896 bp relative to the *Klf4* TSS (Chinenov *et al*., 2014). In order to evaluate whether recruitment to this genomic region near *Klf4* also occurred in keratinocytes, we performed GR ChIP-QPCR using the reported primers flanking this region. Primers specific for a GBS near *Tsc22d3* were used as a positive control.

We did not observe GR recruitment to the aforementioned genomic regions in *Klf4* in the presence of Dex, suggesting cell-type specific events likely due to expression of distinct co-regulators (**Figure 22**).

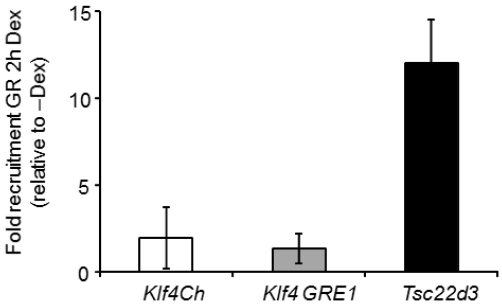

Figure 22. Dex does not induce GR recruitment to the genomic regions of *Klf4* in MPKs. After GR ChIP was carried out in MPKs treated with vehicle or Dex for 2 h.Then QPCR was performed using primers specific for genomic binding regions identified in our ChIP-Seq near *Klf4* (*Klf4Ch*) or for a putative GRE near *Klf4* identified in experiments with mouse macrophages (*Klf4 GRE1*; Chinenov *et al.*, 2014). Primers specific for a GBS near *Tsc22d3* were used as a positive control.

We next assessed the direct interaction between GR and KLF4 after Dex treatment (**Figure 23**). To address this, CO keratinocytes were treated with Dex for 0, 30 or 60 min, then cells were lysed and immunoprecipitated with antibody specific for KLF4 or a nonspecific rabbit IgG (RIgG) (t0). Input controls and immunoprecipitates were analyzed by immunoblotting with GR, p-GR and KLF4 antibodies.

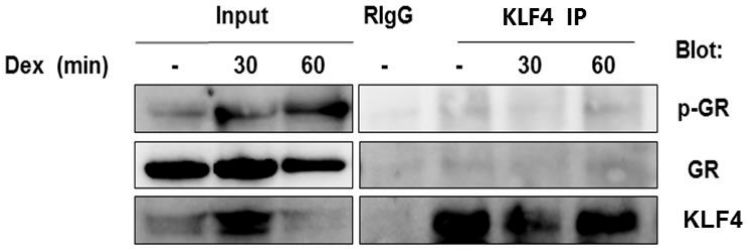

Figure 23. Dex treatment does not increase the direct interaction between GR and KLF4 in keratinocytes. Assessment of GR-KLF4 interaction via co-immunoprecipitation. Cells treated with Dex for 0, 30 or 60 min were lysed and immunoprecipitated with antibody specific for KLF4 or a nonspecific rabbit IgG (t0). Input controls and immunoprecipitates were analyzed by immunoblotting with GR, p-GR and KLF4 antibodies.

The amount of GR in KLF4 immunoprecipitates was almost undetectable either in the absence or presence of Dex treatment, suggesting that there was no direct protein-protein interaction between these TFs (**Figure 23**). Although we assayed different technical conditions, it is also feasible that optimized conditions are required to detect this interaction. It is also possible that KLF4 recruitment facilitates the GR recruitment to their regulatory sequences promoting the chromatin accessibility as described for TF C/EBPβ in liver (Grontved *et al*., 2013).

1.6. *Klf4*, *Zfp36*, and *Tsc22d3* up-regulation during *in vitro* keratinocyte differentiation depends on GR

As mentioned in the introduction, the keratinocytes of the epidermis undergo constant renewal and go from the more basal layers through the suprabasal layers following the terminal differentiation.

A proper keratinocyte terminal differentiation is important for a correct function of the skin and anomalies in this process correlate with several inflammatory skin diseases, including atopic dermatitis and psoriasis (Guttman-Yassky *et al.*, 2017). During terminal differentiation GR, *Klf4*, *Tsc22d3* and *Zfp36* are up-regulated (Sen *et al*., 2010; Yoon *et al*., 2014). Furthermore, both *Tsc22d3* and *Zfp36* are known to be induced by Dex in human keratinocytes (Stojadinovic *et al*., 2007). This suggests possible involvement of the *Tsc22d3* and *Zfp36* in keratinocyte differentiation process. However, the function and regulation of these genes in the epidermis has not been extensively studied.

We evaluated whether *Tsc22d3* and *Zfp36* required GR for their induction in keratinocyte differentiation. For this purpose we evaluated

the changes in the expression of *Zfp36* and *Tsc22d3* in wild type and GR-deficient keratinocytes under high calcium conditions (1.2 mM) for 0 and 72 h (**Figure 24)**, a well-known method to stimulate keratinocyte differentiation *in vitro* (Hennings *et al*., 1980). This method resembles the *in vivo* gradient of calcium in the epidermis with low levels in the basal layer and high levels in the suprabasal layers.

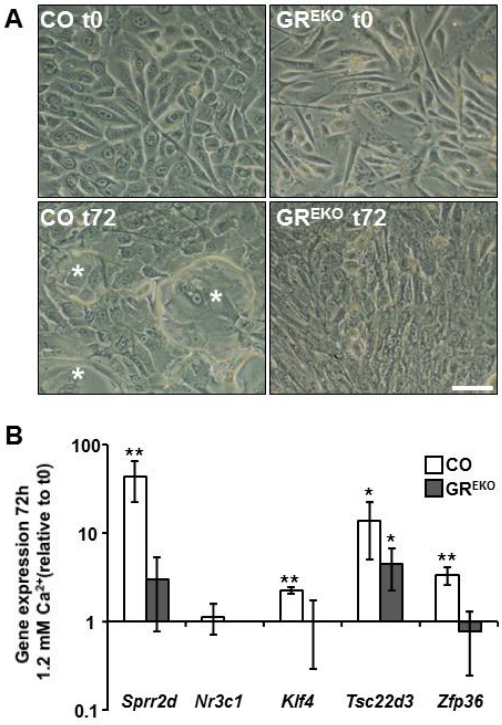

Figure 24. Absence of GR (GR^{EKO} cell line) provoked a deficient calcium-induced differentiation. A) Representative microphotographs showing differential features in morphology after differentiation induced by 1.2 mM calcium for 72 h in CO and GR^{EKO} cells. Cornified envelopes are present in CO cells as indicated by asterisks, but not in GR^{EKO} cells. Scale bar: 50 µm. **B)** Gene expression of *Sprr2d*, *Nr3c1*, *Klf4*, *Tsc22d3*, and *Zfp36* in CO or GR^{EKO} cells treated for 0 or 72 h with 1.2 mM calcium was assessed by RT-QPCR. Mean values ± SD show changes in gene expression relative to t0. Statistically

significant differences relative to untreated controls are indicated by asterisks (Student's t-test; n = 4; *p < 0.05; **p < 0.01). The graph has a logarithmic scale.

In the presence of high calcium (1.2 mM), CO keratinocytes underwent terminal differentiation as observed by the morphological changes. CO cells displayed flattening, extensive cell–cell contacts, stratification and formation of cornified envelopes (**Figure 24A**; asterisks). However, GR^{EKO} cells exhibit defective terminal differentiation as shown by an aberrant morphology featuring a spindle-like phenotype with decreased cell–cell contacts in normal calcium conditions (**Figure 24A**) and after high calcium, GR^{EKO} cells also lacked cornified envelopes (**Figure 24A**). In addition, in order to allow quantification of differentiation we evaluated the mRNA expression of the late differentiation marker *Sprr2d* (Small Proline Rich Protein 2D), which is an important constituent of the cornified envelope in the skin and known to be induced by calcium and regulated by GR (Jackson *et al.*, 2005; Pérez, 2011). *Sprr2d* was strongly induced in calcium-treated CO but not in GR^{EKO} cells, as shown by RT-QPCR (**Figure 24B**), confirming impaired cell differentiation in the absence of GR.

We next examined whether the mRNA levels of *Nr3c1*/GR and *Klf4* changed in high calcium conditions. Although *Nr3c1* mRNA levels were not increased in calcium-treated CO cells, (**Figure 24B**) GR protein levels increased moderately (**Figure 29**), which is in line with the results reported by Yoon and colleagues (Yoon *et al.*, 2014). As mentioned above and as expected, *Klf4* mRNA and protein were up-regulated in calcium-treated CO cells. However, in GR^{EKO} cells there was no significant expression of *Klf4* in terminal differentiation-induced conditions (**Figures 24B and 29**). Induction of *Klf4* is a requirement for keratinocyte terminal differentiation (Segre *et al*., 1999). Thus, the non-appropriate response to calcium-induced terminal differentiation in

GR^{EKO} cells may be a consequence of both the absence of GR and the partial lack of *Klf4*.

We also evaluated the levels of *Tsc22d3* and *Zfp36* under high calcium conditions. The mRNA levels expression of both genes increased during differentiation of CO cells (**Figure 24B**), which was consistent with published microarray data (Sen *et al*., 2012). On the other hand, high calcium medium in GR^{EKO} cells did not up-regulate *Zfp36*, whereas *Tsc22d3* decreased 3-fold in induction relative to the CO (**Figure 24B**).

The calcium-induced terminal differentiation experiments (**Figure 24**) were performed with medium supplemented with serum containing endogenous corticosteroids. So, in order to corroborate that GR is necessary for terminal differentiation in CO keratinocytes, we incubated cells with 1.2 mM calcium in the absence or presence of the GR antagonist RU486 (also known as mifepristone) for 72 h (**Figure 25**). Cells treated with RU486 failed to properly differentiate, not only by a reduced number of cornified envelopes relative to vehicle-treated cells (**Figure 25**; asterisks), but also by a significant decreased expression of *Sprr2d* and *Klf4* (**Figure 25B**).

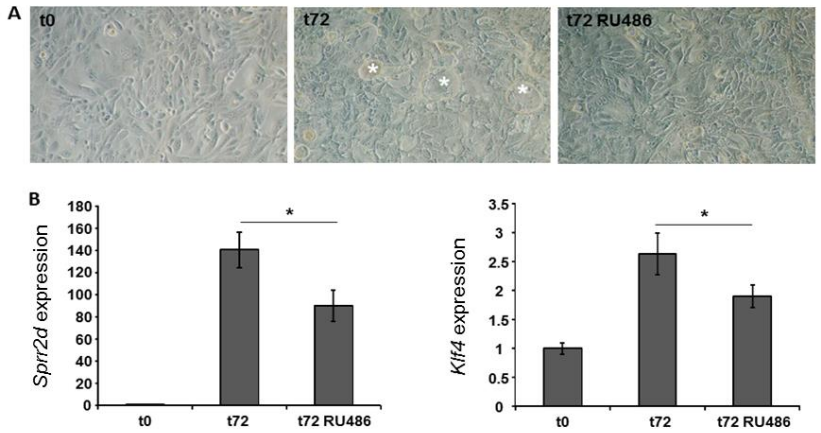

Figure 25. The GR antagonist RU486 decreases the terminal differentiation induced by calcium in mouse CO keratinocytes. A) Representative microphotographs showing differential features in morphology after differentiation induced by 1.2 mM calcium for 72 h in CO and in presence of RU486 (1 μM, 6 h pretreatment). Cornified envelopes are present in CO cells as indicated by asterisks, but not in presence of RU486. Scale bar: 50 μm. **B)** The mRNA expression of *Sprr2d* and *Klf4* in CO cell line treated with vehicle or RU486 under calcium-induced terminal differentiation was assessed by RT-QPCR. Statistically significant differences between groups are indicated by asterisks (Student's t-test; n = 4; *p < 0.05).

TSC22D3/GILZ is known to be involved in inflammatory signaling response through direct binding to RAS and RAF-1 thus inhibiting the ERK downstream signaling. This inhibition of MAPK signaling in keratinocytes is relevant for stopping the inflammation and favoring differentiation (Tarutani *et al*., 2003). On the other hand, ZFP36 is responsible for destabilizing *Tnf* mRNA (Brooks and Blackshear, 2013) thus acting as an anti-inflammatory molecule. Furthermore, ZFP36 can also regulate a variety of additional cytokines involved in skin immunity and keratinocyte differentiation, as well as factors that can affect the cell cycle control, including Cyclin D1 (Brooks and Blackshear, 2013). Therefore, we hypothesize that the lack of up-regulation of *Tsc22d3 and Zfp36* in the calcium-induced terminal differentiation in GR^{EKO}

keratinocytes could have an effect on both inflammatory signaling, as well as the process of differentiation.

1.7. GR downregulates mRNA levels of distinct *Trp63* isoforms in keratinocytes

Since Dex treatment did not alter *Klf4* expression in cultured mouse keratinocytes (**Figure 19B**), we considered other mechanisms for its dysregulation during calcium-induced differentiation of GR^{EKO} cells.

In our ChIP-seq datasets, we found also a genomic region peak near *Trp63* gene, which maps to chromosome 16. *Trp63* is an important master regulator of the epidermis since it encodes p63, a TF necessary for the development and homeostasis of the skin. (Yang *et al*., 1999).

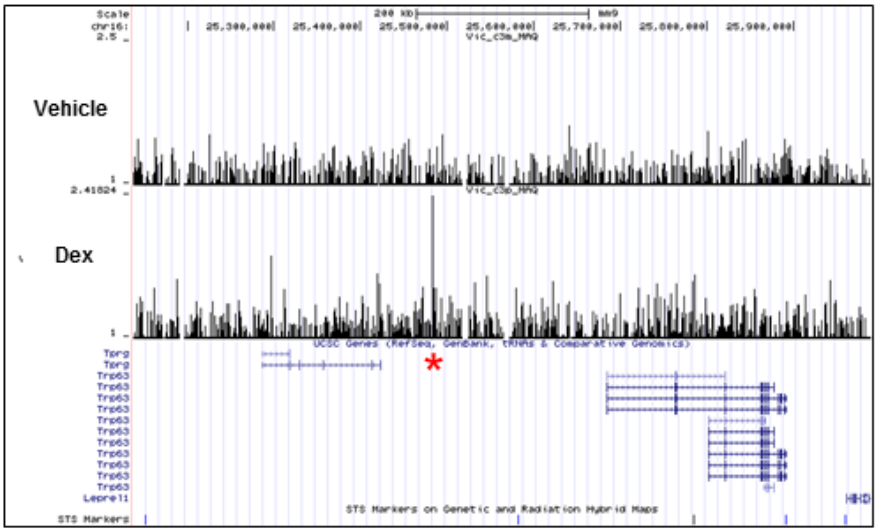

Figure 26. Genomic region peak near *Trp63*. Evaluation of GR binding to genomic regions near Trp63. A. Screenshot of peak (red asterisk) which lies in between *Trpg* and *Trp63* genes.

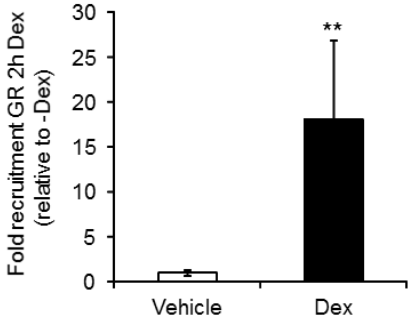

Figure 27. GR recruitment to genomic region near *Trp63*. MPKs were incubated with Dex 100 nM for 2 h. GR recruitment to the genomic region near *Trp63* was determined by ChIP followed by QPCR (n=4, Student's t-test, ** $p<0.01$).

We found a high GR recruitment (around 18-fold) to the genomic region near *Trp63* after Dex treatment (100 nM, 2 h).

Trp63 encodes for two isoforms either containing (TAp63) or lacking (ΔNp63) the N-terminal transactivation domain. The predominant isoform of *Trp63* in the epidermis is ΔNp63 (Melino, 2011). GR is a known repressor of ΔNp63, as mice overexpressing GR in epidermal keratinocytes present low levels of ΔNp63 (Cascallana *et al.*, 2005). Furthermore, it has been shown that ΔNp63 represses *Klf4* expression by directly binding to its promoter (Cordani *et al*., 2011), and both ΔNp63 and KLF4 have different patterns of expression in the epidermis, as ΔNp63 is detected in the basal layer, whereas KLF4 is expressed suprabasally.

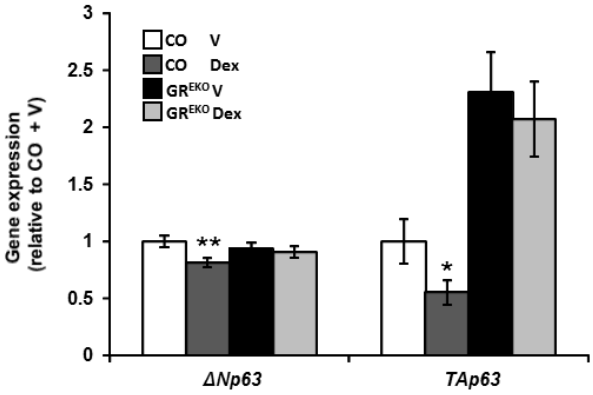

Figure 28. Dex repressed expression of *Trp63* isoforms *ΔNp63* and *TAp63* in CO but not in GR^{EKO} cells. The mRNA levels were assessed by RT-QPCR after Dex treatment (100 nM, 3h). Mean values ± SD are shown. Statistically significant differences relative to mock-treated (V) CO cells are denoted by asterisks (Student's t-test; n = 3; *p < 0.05; **p < 0.01).

We assessed whether Dex-activated GR could modulate *Klf4* expression through the control of *Trp63.* First, we assessed the mRNA levels of *Trp63* isoforms, *ΔNp63* and *TAp63*, in CO and GR^{EKO} cell lines (**Figure 28**). Dex treatment downregulated the mRNA levels of both genes in CO keratinocytes, however, no effect was observed in GR^{EKO} cells (**Figure 28**), suggesting that Dex-activated GR may inhibit their expression. It is noteworthy, that *TAp63* levels were increased by 2-fold in GR^{EKO} relative to CO keratinocytes (**Figure 28**). It has been reported the role of TAp63 as a tumor suppressor (Vanbokhoven *et al*., 2011), whereas inducible epidermal overexpression results in hyperproliferation and deficient terminal differentiation (Koster *et al*., 2006). This discrepancy may be due to different functions depending on cellular context.

1.8. Impaired regulation of p63 and KLF4 during calcium-induced terminal differentiation

Next, we evaluated the protein levels of GR, KLF4 and ΔNp63 by using immunoblotting. We assessed the levels of the isoform ΔNp63, as the predominant p63 protein isoform detected in keratinocytes by immunoblotting (Truong *et al*., 2006), whereas TAp63 is expressed at low levels in this tissue and is difficult to detect (Melino, 2011).

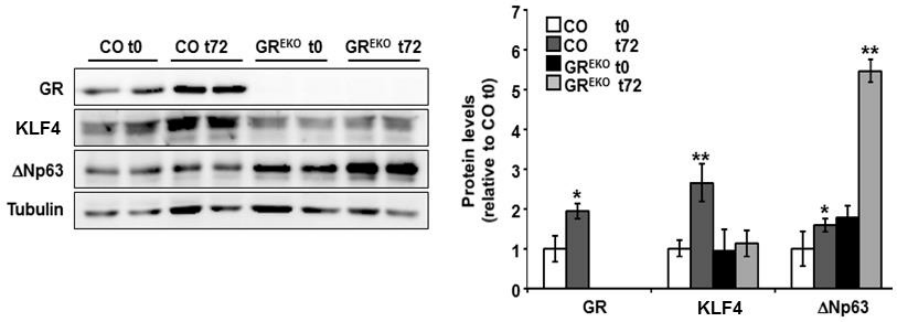

Figure 29. Impaired regulation of p63 and KLF4 during calcium-induced terminal differentiation. Representative immunoblotting (left panel). Tubulin was used as a loading control. Quantification of immunoblotting experiments. Mean values ± SD are shown, with asterisks denoting statistically significant differences relative to CO at t0 (Student's t-test; n = 4; *p < 0.05; **p < 0.01).

We observed a small increase of ΔNp63 in calcium-induced differentiated CO keratinocytes (**Figure 29,** 1.6-fold). In undifferentiated GR^{EKO} cells, ΔNp63 protein levels were up-regulated 1.8-fold relative to CO and these levels were further increased (5-fold) after high calcium treatment (**Figure 29**).

These results suggest that the presence of GR is necessary for the appropriate levels of KLF4 and results in inhibition of p63. Furthermore, the lack of induction of *Klf4* shown in **Figure 24** during calcium-induced

differentiation in GR^{EKO} cells is likely an indirect effect of the loss of GR expression, such as the proposed negative regulation by p63.

Although KLF4 was known to interfere with inflammatory signaling pathways in immune cells such as macrophages (Chinenov *et al*., 2014), the GR/KLF4 interaction was not previously studied in keratinocytes. Our results demonstrate a direct cooperation between GR and KLF4 in the regulation of the anti-inflammatory genes such as *Tsc22d3* and *Zfp36* expression in keratinocytes by binding at their genomic regulatory regions.

1.9. GR downregulates mRNA levels of distinct *Trp63* isoforms during keratinocyte differentiation

We next evaluated the expression of both *Trp63* isoforms in CO and GR^{EKO} keratinocytes during calcium-induced terminal differentiation (**Figure 30**).

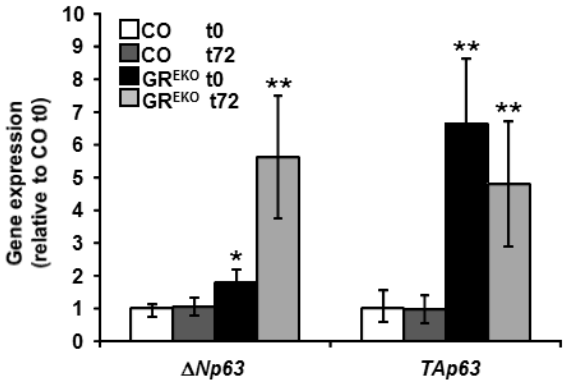

Figure 30. Increased expression of *ΔNp63* and *TAp63* isoforms during calcium-induced terminal differentiation in GR^{EKO} *versus* CO cells. Relative mRNA levels were assessed by RT-QPCR. Mean values ± SD are shown. Statistically significant differences relative to CO at t0 are represented by asterisks (Student's t-test; n = 3; *p < 0.05; **p < 0.01).

The mRNA expression of both *ΔNp63* and *TAp63* transcripts did not change after calcium-induced differentiation in CO cells, whereas the expression of both transcripts was up-regulated in GR^{EKO} cells relative to CO cells at t0 by 1.8- and 6.6-fold, respectively. Furthermore, in calcium-induced differentiation, *ΔNp63* expression was up-regulated 3-fold in GR^{EKO} cells, whereas *TAp63* expression did not change significantly in the GR^{EKO} cells treated with calcium (**Figure 30**).

Note that these basal levels differ from those shown in the previous experiment (**Figure 28**), which can be explained by the use of complete serum in the calcium experiments instead of charcoal-stripped serum used for the Dex treatments. This suggests that other lipophilic compounds present in the serum participate in the basal regulation of *Trp63* isoforms.

Finally, we present a model that summarizes the ideas obtained in the first part of the dissertation (**Figure 31**).

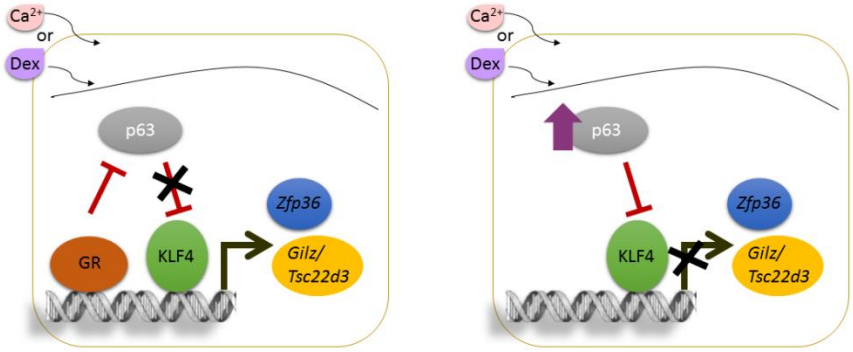

Figure 31. GR and KLF4 are necessary for proper expression and regulation of *Gilz/Tsc22d3* and *Zfp36* in epidermal keratinocytes. Left: In keratinocytes, GR and KLF4 bind to adjacent regulatory sequences of *Gilz/Tsc22d3* and *Zfp36* and coordinately induce gene expression in response to Dex or calcium. GR transcriptionally represses p63, an inhibitor of KLF4 expression, and thus indirectly modulates KLF4 under various conditions. **Right:** In the absence of GR, p63 expression increases while KLF4 expression is decreased. Altogether, lack of GR along with reduced KLF4 results in inappropriate *Gilz/Tsc22d3* and *Zfp36* gene expression in response to Dex or calcium.

Part II

Functional analysis of GILZ in transgenic mice with generalized overexpression: implications in psoriasis

Previous studies have shown the role of GILZ as an anti-inflammatory mediator in several mouse models of pathologies (Cannarile *et al.*, 2009, Pinheiro *et al.*, 2013, Esposito *et al.*, 2012, Srinivasan and Janardhanam, 2011). These studies postulate that GILZ can exert the same anti-inflammatory and immunosuppressive effects as the GCs, without having their associated side effects. Thus, it has been suggested that GILZ could be used as a potential therapeutic tool in various inflammatory diseases (Ronchetti *et al.*, 2015). However, the role of GILZ in the pathophysiology of the skin is poorly studied. We previously described that GCs induce *Gilz* mRNA expression in epidermal keratinocytes by direct recruitment of GR to *Gilz* regulatory sequences (Part I of this dissertation). As GILZ is an anti-inflammatory mediator in other cell types, we decided to study the effects of GILZ using transgenic mice with generalized overexpression of this protein (Prof. Libert, University of Ghent) and the imiquimod (IMQ) mouse model of psoriasis.

Tsc22d3/Gilz has 4 different isoforms, among them, *Gilz1* and *Gilz2* (Soundararajan *et al.*, 2007). In our experiments, we observed that both *Gilz1* and *Gilz2* are induced by Dex (100 nM for 3 h) in adult mouse immortal keratinocytes by 8.7- and 4.1-fold, respectively (**Figure 32**).

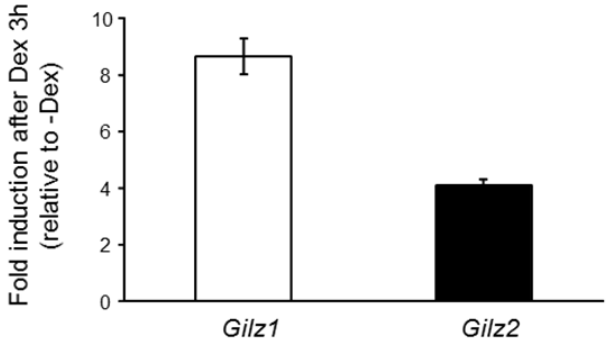

Figure 32. *Gilz1* and *Gilz2* isoforms are induced upon Dex treatment. Immortal mouse adult keratinocytes were treated with Dex 100 nM for 3 h and mRNA expression of *Gilz* isoforms (*Gilz1* and *Gilz2*) was assessed by RT-QPCR (n=3).

In contrast, *Gilz1* and *Gilz2* showed a different response to calcium-induced keratinocyte differentiation (1.2 mM calcium for 72 h). While *Gilz1* mRNA expression decreased weakly (1.3-fold) although significantly after calcium treatment, *Gilz2* was up-regulated by around 3-fold. Although some studies addressed the different functions of GILZ isoforms in the regulation of proliferation and ion transport (Soundararajan *et al.*, 2007), there is little knowledge regarding the differential regulation of distinct isoforms. Understanding the cell-type specific regulation of GILZ isoforms would require further research.

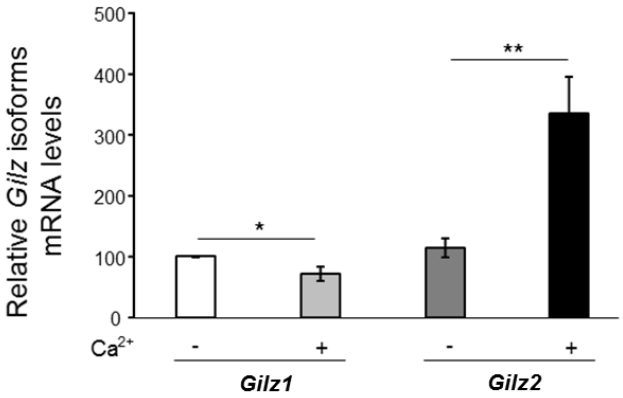

Figure 33. Regulation of *Gilz1/Gilz2* isoforms in keratinocytes in response to calcium-induced differentiation. Immortal mouse adult keratinocytes were treated with high calcium concentration (1.2 mM for 72 h) to induce terminal keratinocyte differentiation. The mRNA expression *of Gilz* isoforms (*Gilz1*/*Gilz 2*) was assessed by RT-QPCR (n=3; Post hoc Tukey test *p<0.05; **p<0.01).

2.1. Mice with generalized overexpression of GILZ (GILZ-Tg)

For the following *in vivo* experiments, we have used mice with generalized overexpression of the GILZ1 isoform (GILZ-Tg), the canonical and most widely studied. GILZ-Tg mice were generated as described in Material & Methods (**Figure 34**). Mice with the same genetic background as the GILZ-Tg mice were used as control mice (GILZ-Wt).

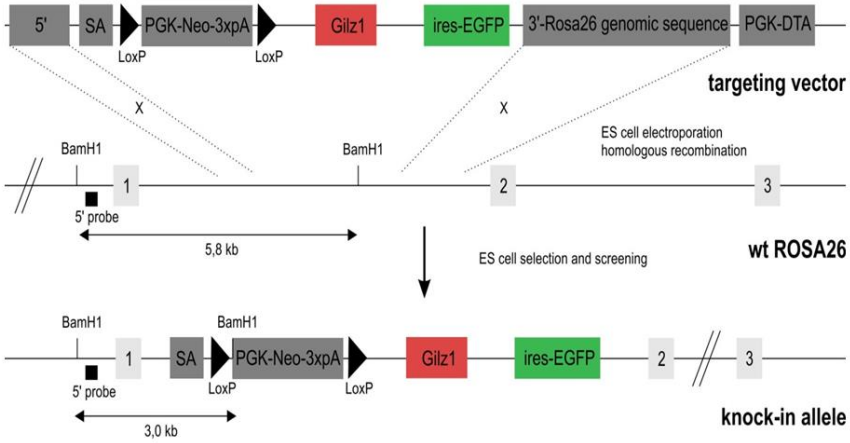

Figure 34. Generation of mice overexpressing GILZ (GILZ-Tg mice). Scheme of the transgene construct. Conditional GILZ-Tg overexpressing mice were generated by knocking in the mouse *Tsc22d3/Gilz-1* cDNA preceded by a loxP flanked stop cassette under control of the ROSA26 promoter, using a Gateway-compatible ROSA26 locus targeting vector. Mice homozygous for the loxP flanked stop cassette and one allele of Nestin-cre, expressing Cre in all cell types, were generated by crossing.

We first determined the relative expression of GILZ at the mRNA and protein level in several tissues of GILZ-Tg mice. The skin of GILZ-Tg mice showed a relative increase of expression both at the mRNA and protein levels ranging between 3- and 8-fold in comparison to GILZ-Wt (**Figure 35**). Significant increases of GILZ (mRNA and protein level) in spleen and bone marrow-derived macrophages of GILZ-Tg relative to GILZ-WT mice ranged between 3- and 6-fold (**Figure 35**), and confirmed the generalized overexpression of GILZ in this transgenic mouse model.

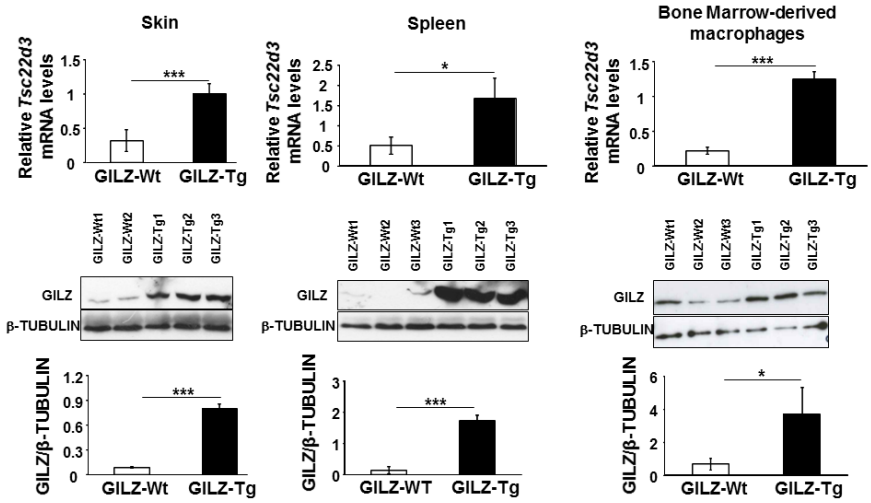

Figure 35. Relative *Tsc22d3/Gilz* mRNA and protein levels in GILZ-Tg *versus* GILZ-Wt mice. Relative mRNA levels of *Tsc22d3*/*Gilz* in skin, spleen and bone marrow-derived macrophages were determined by RT-QPCR and relative protein levels by Western blot. Tubulin was used as a loading control. Mean values ± SD are shown. Statistically significant differences relative to controls are denoted by asterisks (Student's *t* test; n = at least 3 per genotype; *p <0.05; ***p<0.001).

2.1.1. Phenotypic characterization of the skin in GILZ-Tg mice

To evaluate whether the overexpression of GILZ may affect the skin architecture, we examined skin sections of newborn (P0) and adult GILZ-Tg and GILZ-Wt mice by hematoxylin and eosin (H&E) staining. Newborn GILZ-Tg mice were viable and did not show any macroscopic abnormalities relative to control newborn mice. Skin sections from newborn and adult GILZ-Tg mice stained with H&E did not reflect any impairment in their architecture as compared to control mice (GILZ-Wt) (**Figures 36 and 37**).

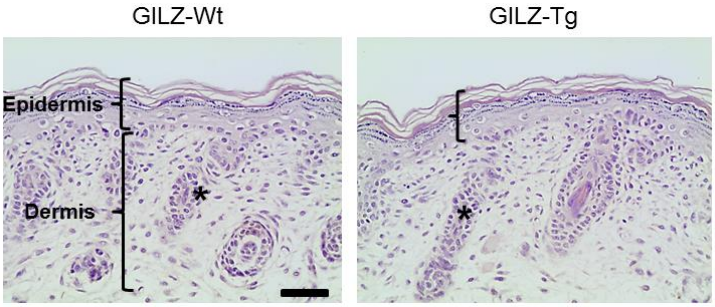

Figure 36. GILZ-Tg newborn mice show normal skin architecture. Representative H&E stained sections of newborn mouse skin of GILZ-Wt and GILZ-Tg mice (n=10 per genotype) at day of birth (P0). Brackets separate epidermis from dermis and hair follicle is denoted by asterisks. Scale bar: 50 µm.

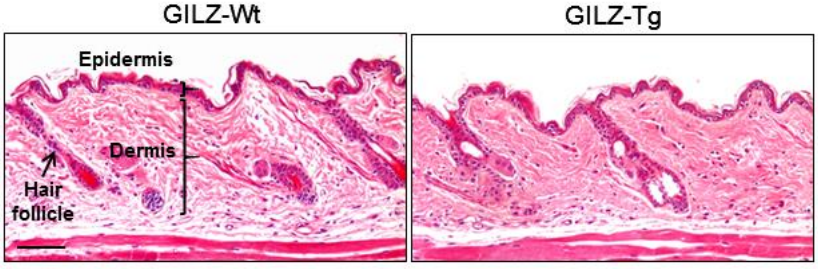

Figure 37. GILZ-Tg adult mice show normal skin architecture. Representative H&E stained sections of the adult mouse skin of GILZ-Wt and GILZ-Tg mice showing no major differences in tissue architecture (n=5 per genotype). Scale bar: 50 µm.

2.2. GILZ increases IMQ-induced psoriasis-like skin lesions in adult mice

To evaluate the implication of the overexpression of GILZ in psoriasis, GILZ-Tg mice were subjected to the IMQ-induced mouse model.

The IMQ-induced psoriasis-like mouse model was first described by Van der Fits and colleagues (Van der Fits *et al.*, 2009). IMQ is an agonist of the TLR 7/8 and is used topically in the formulation of a cream named Aldara®, which contains 5% of IMQ. We topically applied Aldara® on shaved mouse dorsal skin daily for 7 days, which led to a macroscopic phenotype resembling human psoriasis. The kinetics and severity of the IMQ response were assessed in both GILZ-Tg and GILZ-Wt mice, as described below.

Macroscopically, we daily scored erythema (redness) and scaling (desquamation) of both genotypes upon IMQ treatment for the whole duration of the experiment (**Figure 38)**. GILZ-Tg mice displayed a more pronounced response to IMQ treatment compared to GILZ-Wt mice consisting in increased skin erythema (**Figure 38**, asterisks) and more severe desquamation (**Figure 38**, arrows). These differences were more marked from day 4 onwards until the end point of the IMQ experiment (**Figure 38**).

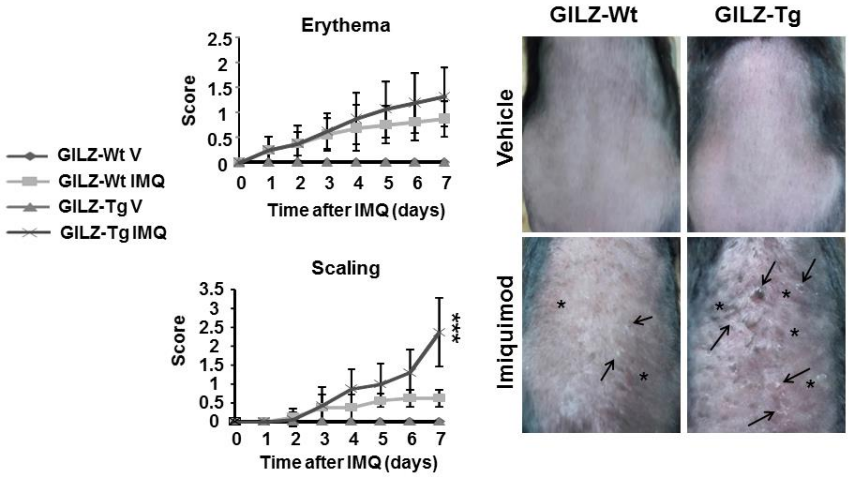

Figure 38. GILZ-Tg mice show increased psoriatic features in response to IMQ. Left panel: Score of the erythema and scaling in GILZ-Wt and GILZ-Tg for the duration of the experiment. **Right panel:** Macroscopic appearance of

GILZ-Wt and GILZ-Tg mice treated with IMQ at day 7. Mean values ± SD are shown. Post hoc Tukey test ***p<0.001, n=at least 5 per genotype and treatment.

Although GILZ has been reported to act as an anti-inflammatory therapeutic protein in various animal models of inflammatory diseases (Cannarile *et al.*, 2009; Ngo *et al*., 2013a), the overexpression of GILZ in other cells has been shown to be contrary to the expected results. For example, continuous GC treatment induces adipocyte differentiation by activating the adipogenic peroxisome-proliferator-activated receptor-γ2 (PPAR-γ2) promoter. In contrast, overexpression of GILZ inhibits PPAR-γ2 transcriptional activation, thus blocking adipocyte differentiation (Shi *et al.*, 2007). GILZ has also been reported to be associated with other GC-induced side effects, such as the inhibition of the repair of respiratory epithelial cells (Liu *et al.*, 2013). We may speculate that high levels of exogenous GILZ also cause side effects in skin, similar to those reported in chronic GC treatments. Further experiments assessing GILZ expression in skin after continuous GC exposure may help to understand this issue.

As we have studied the effects of the overexpression of the GILZ1 isoform, it could be possible that a misbalance between the isoforms, for example, GILZ1 and GILZ2 isoforms may also contribute to a pro-inflammatory phenotype.

2.2.1. Histopathological assessment of GILZ-Tg mouse skin after IMQ-induced psoriasiform lesions

To examine the morphological differences between the IMQ-treated GILZ-Wt and GILZ-Tg mice we initially performed a histopathological assessment of the skin samples at day 7 by H&E staining. The H&E-stained control skin sections displayed the

characteristic features of the IMQ treatment that included epidermal thickening (acanthosis) and thickening of the stratum corneum (hyperkeratosis) relative to vehicle-treated groups (**Figure 39, left**). However, IMQ-treated GILZ-Tg mice displayed even more pronounced features in terms of epidermal thickening, hyperkeratosis, as well as increased dermal cellularity in comparison to GILZ-Wt mice (**Figure 39, left**).

In GILZ-Tg mice, the more severe lesions also included increased epidermal protrusions (rete-ridges), abnormal keratinocyte differentiation with retention of the nuclei in the stratum corneum (incomplete cornification), the outermost layer of the epidermis (parakeratosis), and neutrophil infiltration (Munro-like abscess) (Wagner *et al*., 2010).

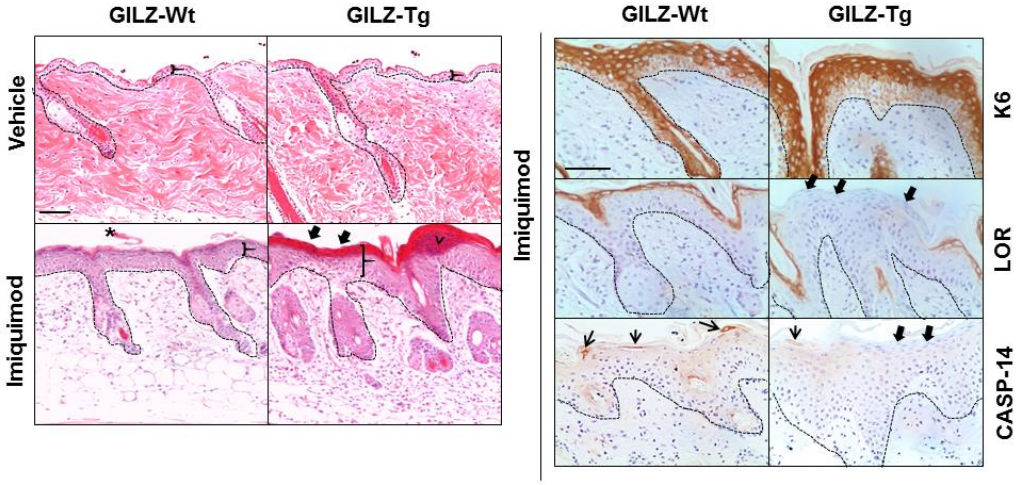

Figure 39. Histological characterization of adult GILZ-Wt and GILZ-Tg mouse skin sections after IMQ treatment. Left panel: H&E stained skin sections: Epidermal thickening is denoted by brackets; hyperkeratosis by asterisks; abnormal differentiation with parakeratosis by thick arrows, and epidermal infiltrate (Munro-like abscess) by thin arrowhead. **Right panel:**

immunostaining with keratin 6 (K6), Loricrin (LOR), and Caspase-14 (CASP-14) antibodies. Scale bar: 50 µm. Samples from two independent experiments were assessed (n= 15 GILZ-Wt, n= 16 GILZ-Tg).

Although mouse skin normally does not present rete-ridges, repeated treatment with IMQ can induce their formation (Lawlor and Kaur, 2015).

Next, we assessed the expression of keratin 6 (K6), an epithelial marker whose expression is normally restricted to hair follicles and absent in the interfollicular epidermis of adult mouse skin. However, K6 expression is up-regulated during pathophysiological skin conditions including hyperproliferative states (Haines and Lane, 2012). Immunostaining of skin sections showed that K6 was present in the upper layers of the epidermis of both IMQ-treated GILZ-Wt and GILZ-Tg mice, besides the hair follicles (**Figure 39**, K6). We also evaluated the expression of loricrin (LOR), a terminal differentiation marker that is present in the upper layers of the epidermis and constitutes the 80% of the cornified envelope (Segre, 2003). In IMQ-treated GILZ-Wt mice, loricrin was restricted to the upper differentiated layers of the epidermis, however, in GILZ-Tg mice, this marker was focally absent correlating with augmented parakeratosis (**Figure 39**, LOR; denoted by black arrows).

This parakeratosis or aberrant cornification resulting in the accumulation of nuclei in the outermost epidermal layer may be produced by several mechanisms (Denecker *et al.*, 2008). One mechanism includes impaired expression or function of Caspase-14 (CASP-14). CASP-14 is the only non-apoptotic epidermal-specific protease which is confined to the suprabasal layers of the epidermis. It plays a key role in the epidermal barrier function as it has been reported to be involved in the terminal keratinocyte differentiation. It is activated in cornification and it normally induces the formation of mature filaggrin

and its degradation into free amino acids, thus providing a competent stratum corneum (Denecker *et al*., 2008; Hoste *et al*., 2011). Caspase-14 expression levels are low in human lesional psoriatic skin likely due to the action of T-helper type 2 cytokines (Denecker *et al*., 2008; Hvid *et al*., 2011). It has been previously reported that CASP-14 deficient mice were more predisposed to develop parakeratosis after IMQ treatment (Hoste *et al*., 2013). In our study, we observed that CASP-14 was expressed in the suprabasal layers of the GILZ-Wt mice skin after IMQ treatment (**Figure 39**, CASP-14 expression denoted by thin arrows), whereas it was absent in GILZ-Tg skin. Although this absence of expression coincided with the presence of areas with parakeratosis (**Figure 39**, parakeratosis denoted by thick arrows), the lack of CASP-14 is more likely to be a result of a defective epidermal barrier, rather than the cause of it. Thus, CASP-14 knockout mice did not show spontaneous parakeratosis but IMQ treatment induced increased parakeratosis (Denecker *et al*., 2008). The link between GILZ and the modulation of CASP-14 is still unknown. However, it is possible that the reduced expression of CASP-14 in GILZ-Tg skin may be due to the fact that other TFs responsible for the regulation of epidermal differentiation are altered due to ectopic or augmented expression of GILZ (Denecker *et al*., 2008).

2.2.2. Molecular changes in the skin of GILZ-Tg mice after IMQ treatment

It has been reported that GILZ is down-regulated by several inflammatory stimuli such as inflammatory cytokines IL-1, TNF-α and IFN-γ in human airway epithelial cells further contributing to the inflammatory process (Ayroldi and Riccardi, 2009). We thus evaluated the relative mRNA levels of *Tsc22d3/Gilz* upon the IMQ treatment. In GILZ-Wt skin, IMQ down-regulated the expression of endogenous

Tsc22d3/Gilz mRNA around 60% while in GILZ-Tg skin, these levels remained high before and after the IMQ treatment (**Figure 40**).

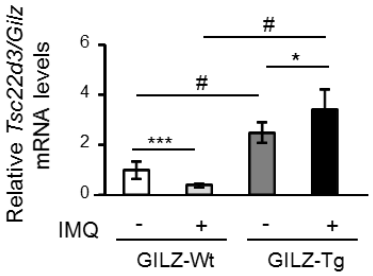

Figure 40. Determination of relative *Tsc22d3/Gilz* mRNA levels in skin from GILZ-Wt and GILZ-Tg treated with vehicle or IMQ at day 7 by RT-QPCR. Mean values ± SD are shown. Post hoc Tukey test *, # p<0.05; ***p<0.001, n=at least 5 per genotype and treatment. Asterisks: significance between treatments within each genotype; hashes: significance between genotypes in the same treatment group.

However, note that the higher constitutive mRNA levels of *Tsc22d3/Gilz* in GILZ-Tg mice were further up-regulated by IMQ treatment probably due to the lack of regulatory sequences in the transgene construct (**Figure 40).** Importantly, the observed decrease of *Tsc22d3/Gilz* mRNA levels in IMQ-treated control skin correlated with the reported low *Tsc22d3/Gilz* levels found in human psoriatic lesions (Jones *et al.*, 2015).

In addition, the down-regulation (2.6-fold) of *Tsc22d3/Gilz* was reported in psoriatic human lesions *vs* non-lesional matched biopsies (Suárez-Fariñas *et al.*, 2012). The *Tsc22d3/Gilz* down-regulation observed in IMQ-treated GILZ-Wt but not in GILZ-Tg skin (**Figure 40**) may suggest that GILZ down-regulation is necessary for the resolution of inflammation. However, the continuous expression of GILZ may produce effects different to the anti-inflammatory expected ones. It

would be possible that the constitutive GILZ overexpression may induce side effects, similar to the results of the continuous treatment with GC.

2.2.3. Determination of cytokines related with psoriasis in GILZ-Tg skin

Next, we assessed the mRNA expression of cytokines related to the IL-23/Th17 axis, as well as other inflammatory markers whose expression is found to be increased in human psoriasis and mouse psoriatic skin (Wagner *et al*., 2010; Flutter and Nestle, 2013). The expression of *Il-17f* and *Il-22* mRNA levels (2.5- and 4-fold, respectively) increased significantly in IMQ-treated GILZ-Wt compared to the untreated GILZ-Wt mice. This induction was higher in GILZ-Tg mice. IL-22 has been shown to be involved in epidermal hyperplasia and production of antimicrobial peptides by keratinocytes in humans and mice, inducing plaque formation and protective skin function (Van Belle *et al.*, 2012). Although *Il-23* presented a tendency to increase in IMQ-treated GILZ-Wt mice, it was up-regulated in IMQ-treated GILZ-Tg mice (**Figure 41**). After IMQ treatment, cytokines were highly induced in GILZ-Tg mice relative to the IMQ-treated GILZ-Wt mice (**Figure 41**).

Lesional psoriatic skin presents high levels of calcium-binding proteins S100A8/A9, which are expressed in keratinocytes and other immune cells such as neutrophils (Lee *et al*., 2012). Other inflammatory cytokines including IL-6 and STAT3 are also induced in human patients and mouse models of psoriasis (Johnson-Huang *et al*., 2012).

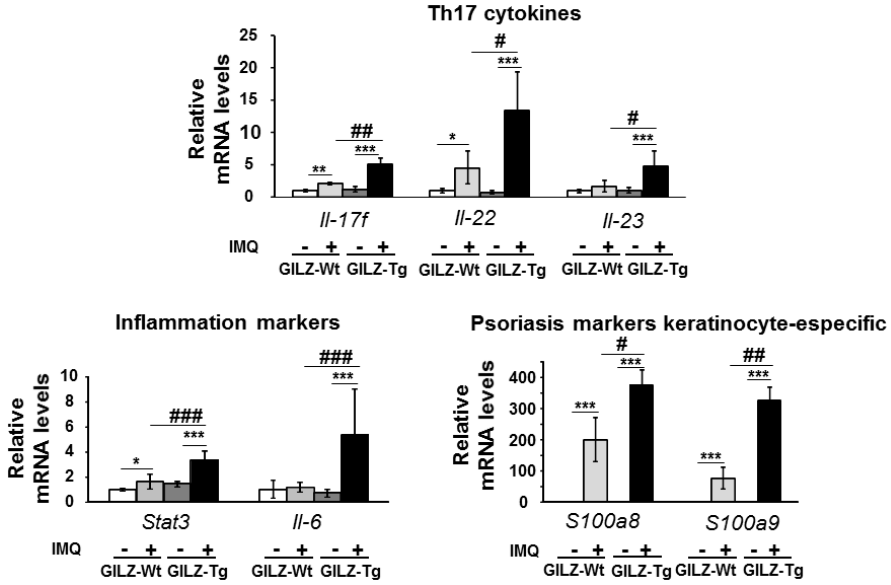

Figure 41. Up-regulation of inflammatory mediators in IMQ-treated GILZ-Tg relative to GILZ-Wt mouse skin. Relative mRNA levels of the indicated genes were assessed by RT-QPCR in skin collected from the same individuals after IMQ treatment (7d). Mean values ± SD are shown. Post hoc Tukey test *, $^{\#}p<0.05$; **, $^{\#\#}p<0.01$; ***, $^{\#\#\#}p<0.001$; n=at least 5 per genotype and treatment. Asterisks: significance between treatments within each genotype; hashes: significance between genotypes in the same treatment group.

STAT3 is a widely studied member of the Signal transducers and activators of transcription (STATs) family. Once STAT3 is activated through phosphorylation, form dimers and translocates to the nucleus transmitting extracellular signals to the nucleus. STAT3 has an important role in various biological activities, including cell proliferation, survival and cell migration. STAT3 activation in keratinocytes is essential for skin wound healing (Sano *et al.*, 2005). Furthermore, the overexpression of STAT3 directed to epidermal keratinocytes produces features resembling psoriasis.

S100a8, S100a9, and *Stat3* were significantly up-regulated in IMQ-treated GILZ-Wt mice (200, 70, and 1.6-fold, respectively) and these increases were even higher in IMQ-treated GILZ-Tg mice compared to IMQ-treated GILZ-Wt (**Figure 41**).

2.2.4. Serum cytokines and immune cells in IMQ-treated GILZ-Tg mice

Besides the epidermal alterations and elevated serum cytokines, psoriasis is characterized by pronounced inflammatory infiltrates mainly consisting of T cells and dendritic cells, as well as neutrophils, mastocytes, and macrophages.

We wondered whether the higher susceptibility observed in GILZ-Tg after IMQ treatment could be due to an increase in serum cytokines. To address this question we collected serum from IMQ-treated GILZ-Tg and GILZ-Wt mice at different time points (0, 2, 4 and 7 days) and assessed the levels of the cytokines IL-17A, IL-17F and TNF-α using Luminex technology (Bio-plex, Bio-Rad) (**Figure 42**).

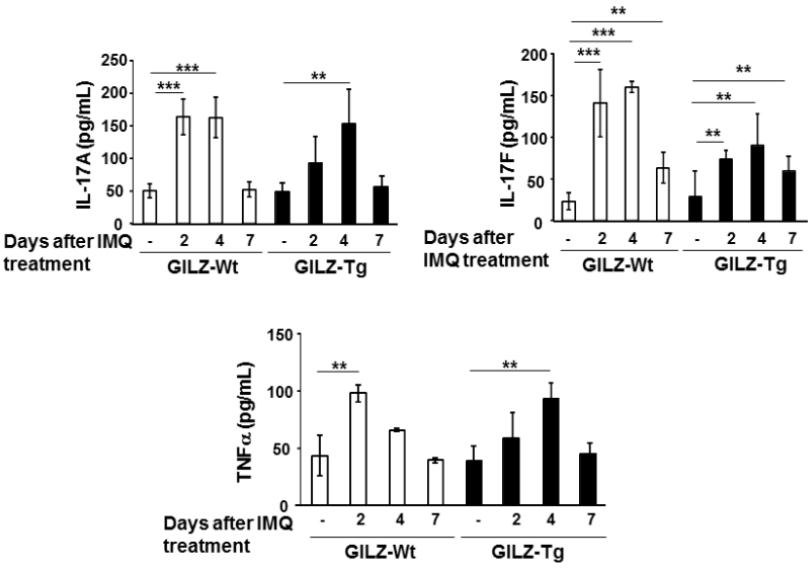

Figure 42. Serum cytokines IL-17A, IL-17F and TNF-α did not contribute to the further susceptibility of GILZ-Tg mice to IMQ. Cytokines IL-17A, IL-17F and TNF-α were collected at different time-points of the IMQ experiment and measured by using Luminex technology (Bio-plex, Bio-Rad). Post hoc Tukey test **p<0.01; ***p<0.001; n=at least 3 per genotype and treatment.

The indicated cytokines presented a peak of expression at days 2 and 4 after IMQ treatment but no significant differences were found among genotypes, suggesting that serum cytokines are not responsible for the more severe phenotype in IMQ-treated GILZ-Tg mice.

Also, GILZ-Tg IMQ-treated mice displayed increased dermal cellularity compared to GILZ-Wt mice, as observed in the H&E stained sections (**Figure 39**).

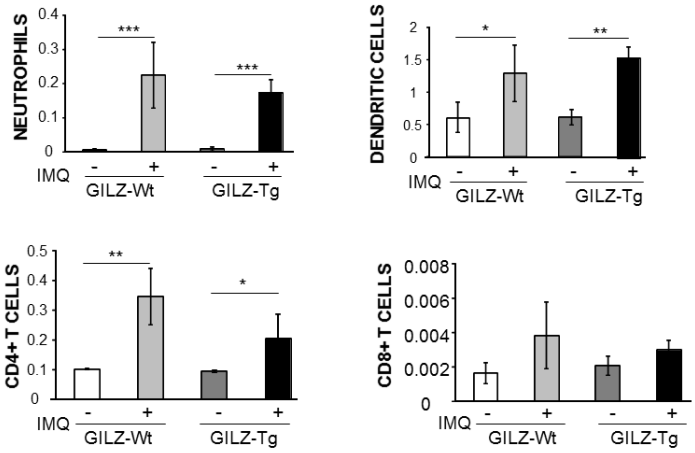

Figure 43. Distinct immune cell populations in skin did not contribute to the further susceptibility of GILZ-Tg mice to IMQ. Neutrophils, dendritic cells, CD4+ T cells and CD8+ T cells were isolated at day 7 of the IMQ experiment and measured by FACS. Post hoc Tukey test *p<0.05; **p<0.01; ***p<0.001, n= 4 per genotype and treatment. Asterisks: significance between treatments within each genotype.

In the IMQ mouse model of psoriasis, the number of immune cells is increased by the treatment and it contributes to the severity of the disease (Van der Fits *et al.*, 2009). For this reason, we assessed different subpopulations of immune cells in the skin of IMQ-treated GILZ-Tg *vs* GILZ-Wt mice. To answer this question, we treated mouse ears of both genotypes with IMQ daily for up to 7 days and analyzed the composition of the isolated immune cells using flow cytometry (FACS). Although neutrophils, dendritic cells, CD4+T cells and CD8+ T cells showed a significant increase after IMQ treatment in both genotypes, this increment was not higher in GILZ-Tg compared to GILZ-Wt (**Figure 43**). Since T cells are not the only producers of IL-22 and IL-17, we cannot rule out the contribution of other immune cells to the more impaired phenotype in the GILZ-Tg mice treated with IMQ and the increased levels of cytokines in the GILZ-Tg skin (**Figure 41**).

2.2.5. Systemic effects of topical imiquimod: impact in spleen and gut

It has been previously reported that topical application of IMQ also induced systemic effects through TLR7 and type I IFN (Grine *et al*., 2015). One of the systemic effects observed after the daily treatment with IMQ includes splenomegaly in control mice (van der Fits *et al*., 2009; Flutter and Nestle, 2013). Recently, it has been described that part of the psoriasis-like effects induced by IMQ are due to the oral uptake of this substance and are subsequently enhanced by the absorption in the intestine (Grine *et al*., 2016). Considering all this, we collected several tissues including spleen and gut at day 7 and examined the levels of cytokines that had been measured in the skin.

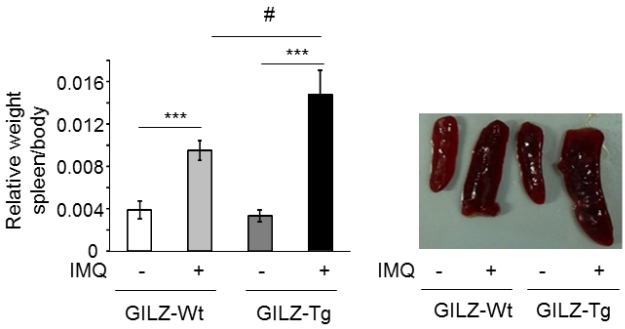

Figure 44. Relative weight spleen/body increased in both genotypes after IMQ treatment. Spleens were collected at day 7 of IMQ experiment and splenomegaly was determined by the weight ratio of spleen relative to body. Mean values ± SD are shown. Post hoc Tukey test $^{\#}p<0.05$; ***$p<0.001$, n=at least 5 per genotype and treatment. Asterisks: significance between treatments within each genotype; hashes: significance between genotypes in the same treatment group.

Splenomegaly was determined by the ratio of spleen relative to body weight. As expected IMQ induced an enlargement of the spleen

in control mice, however, splenomegaly was even more pronounced in GILZ-Tg mice (**Figure 44**).

We next assessed cytokines related with IL-23/Th17 axis in spleen and gut. We evaluated also whether the splenomegaly induced by the IMQ treatment correlated with changes in the mRNA expression of the cytokines up-regulated in skin, as well as possible differences between GILZ-Tg and GILZ-Wt mice. Spleen is a lymphoid organ where many cells of the immune system are present, which includes T cells (**Figure 44**).

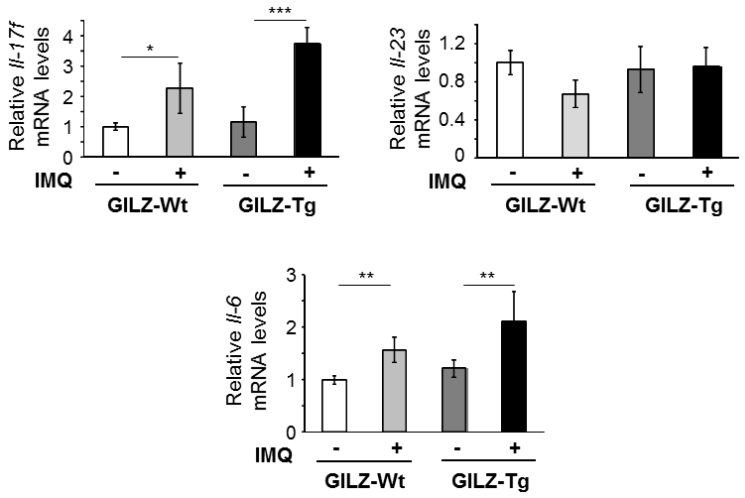

Figure 45. Cytokine regulation in spleen after IMQ treatment. Relative mRNA levels of the indicated genes were assessed by RT-QPCR in spleen collected after IMQ treatment (7d). Mean values ± SD are shown. Post hoc Tukey test *p<0.05; **p<0.01; ***p<0.001; n=at least 5 per genotype and treatment. Asterisks: significance between treatments within each genotype.

Il-17f and *Il-6* mRNA levels were up-regulated after IMQ treatment (**Figure 45**), whereas no major differences were observed in *Il-23* mRNA levels. *Il-17f* and *Il-6* are induced by IMQ in both GILZ-Wt and

GILZ-Tg, suggesting that the overexpression of GILZ in immune cells does not trigger an increased activation of the IL-23/Th17 axis. The augmented up-regulation of the pro-inflammatory cytokine *Il-6* in the spleen of IMQ-treated GILZ-Tg mice is consistent with the increased splenomegaly relative to GILZ-Wt animals.

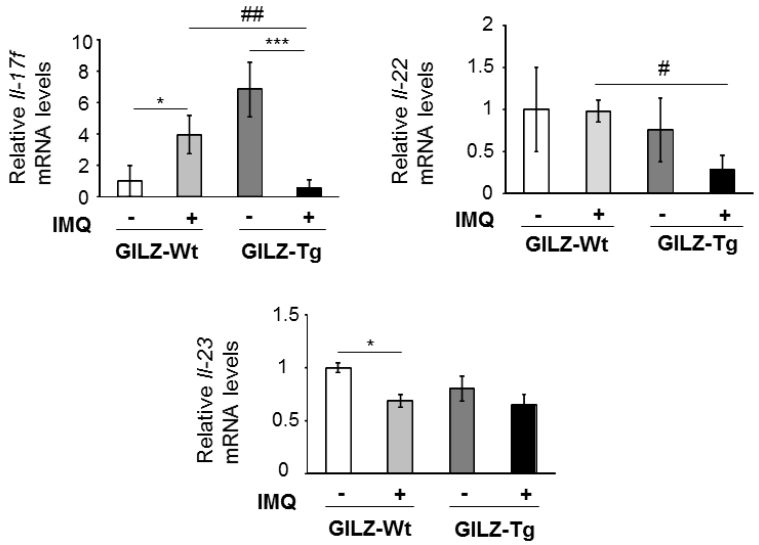

Figure 46. Cytokine regulation in gut after IMQ treatment. Relative mRNA levels of the indicated genes were assessed by RT-QPCR in gut collected after IMQ treatment (7d). Mean values ± SD are shown. Post hoc Tukey test *, # p<0.05; ##p<0.01; ***p<0.001; n=at least 5 per genotype and treatment. Asterisks: significance between treatments within each genotype; hashes: significance between genotypes in the same treatment group.

In gut, IMQ induced *Il-17f* mRNA levels in GILZ-Wt mice, whereas GILZ-Tg mice showed a significant reduction. Additionally, *Il-22* expression did not change in GILZ-Wt mice in response to IMQ. However, we observed a tendency to reduced levels in IMQ-treated GILZ-Tg mice. In the case of *Il-23*, there was a significant decrease in GILZ-Wt in response to IMQ, whereas no changes were presented in GILZ-Tg mice.

The fact that there are no major differences in the levels of cytokines between both mouse genotypes in gut and spleen suggests that, in these organs, the overexpression of GILZ did not play a major role in the more severe phenotype presented in GILZ-Tg after IMQ treatment and also that the alterations are skin specific.

Altogether, our data demonstrate that the cytokine profile in the skin of IMQ-treated GILZ-Tg mice was different to that of intestine or spleen and suggests that in this disease model, GILZ overexpression may have a pro-inflammatory role in the skin while playing a protective or neutral role in other organs. In addition, the increased levels of circulating cytokines in serum in response to IMQ, as reported by other groups (Grine *et al.*, 2016), showed no differences among genotypes, suggesting that the systemic response is not responsible for the severe phenotype observed in the skin of IMQ- treated GILZ-Tg mice.

While the experiments in GILZ-Tg mice were ongoing, it was reported that GILZ knockout mice were more susceptible to the IMQ model, developing histological psoriasis features, splenomegaly, and up-regulation of IL-17A and IL-23 levels (Jones *et al.*, 2015). The fact that both gain- and loss-of-function approaches lead to a similar skin phenotype and higher susceptibility to psoriasis is apparently contradictory. However, several issues must be considered. It is important to note that untreated GILZ-deficient mice already displayed increased levels of lymph node cells producing IL-17A and IL-22. Altogether they demonstrated the importance of GILZ for the regulation of Th17-dependent cytokines by T cells and dendritic cells. However, it is not clear whether this basal inflammation contributes (and to what extent) to the increased susceptibility of GILZ-deficient mice to IMQ. Our results, however, showed similar expression of the *Il-23*, *Il-22* and *Il-17* cytokines in the skin of both genotypes in the absence of

IMQ and displayed a significantly enhanced increase only after IMQ treatment (**Figure 41**).

Furthermore, the skin alterations in IMQ-treated GILZ-deficient mice were not characterized by histopathological assessment. This makes difficult to compare whether the excess or deficiency of this protein has a similar impact on epidermal proliferation, differentiation, etc. The contribution of GILZ-deficient keratinocytes to the reported cutaneous phenotype was neither examined.

The fact that the GILZ overexpressing mice and GILZ-deficient mice displayed similar phenotypic skin alterations in response to IMQ, suggests that GILZ levels must be tightly regulated to effectively reduce inflammation, as high or low doses may have pathological consequences. Therefore, GILZ levels should be controlled when used as an alternative treatment for psoriasis, as it may behave as a pro-inflammatory protein in certain tissues, such as the skin.

On the other hand, GILZ has been reported to show a compensatory balance with another GC-induced and pro-resolving inflammatory protein named Annexin A1 to resolve inflammation naturally (Vago *et al.*, 2015). Maybe the excess of GILZ provokes a decompensation in the balance with Annexin A1.

2.3. IMQ-induced psoriasis in GILZ-Tg mice involves cutaneous activation of TGF-β1/SMAD2/3

We next investigated other signaling pathways that may contribute to the pro-inflammatory action of GILZ in the IMQ model of psoriasis. It has been reported that GILZ enhances TGF-β1 signaling by binding to and promoting SMAD2/3 phosphorylation and activation of FoxP3 expression (Bereshchenko *et al.*, 2014). TGF-β1 is the most

predominant in several human tissues, including the skin (Han *et al.*, 2012).

Moreover, mice overexpressing TGF-β1 in keratinocytes developed phenotypes and molecular alterations similar to human psoriasis, via SMAD2/3-dependent mechanism (Li *et al*., 2004; Zhang *et al*., 2014). In order to evaluate whether GILZ overexpression correlated with an augmented TGF-β1-mediated signaling, we isolated the skin, gut and spleen from GILZ-Wt and GILZ-Tg untreated and IMQ-treated mice and determined the activation status of SMAD2/3 by using the relative ratio of phosphorylated (p)- vs total SMAD2/3 expression by western blotting.

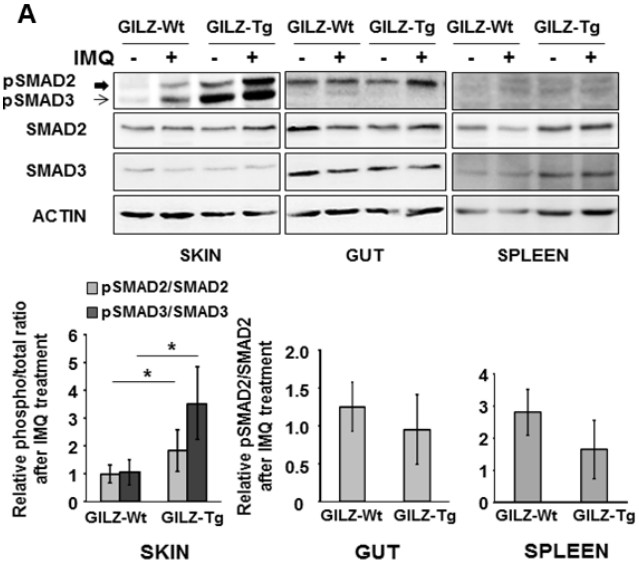

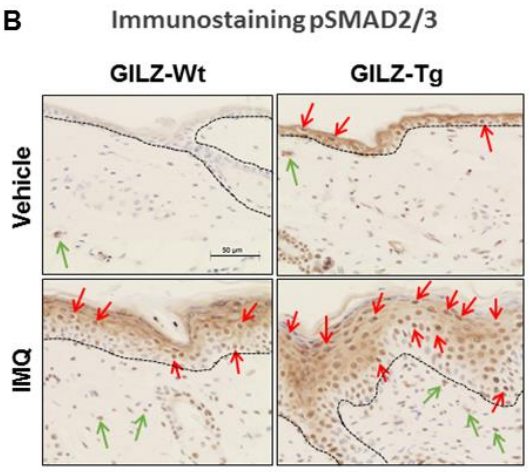

Figure 47. Skin-specific increased activation of SMAD2/SMAD3 by IMQ treatment in GILZ-Tg mice. (A) Representative immunoblotting images and quantification (below image) of total and phospho(p)-SMAD2/3 expression in skin, gut and spleen collected at day 7 of the IMQ experiment. Actin is shown as a loading control. The values shown are the mean ± SD; asterisks indicate statistically significant differences relative to controls, as assessed using Student's *t* test (n =31; *p < 0.05). **(B)** Immunohistochemistry using p-SMAD2/3 antibody demonstrates activation of TGF-β1 signaling mediators in the epidermis and dermis of IMQ-treated GILZ-Tg and GILZ-Wt mice. Bar: 50 μm.

Immunoblotting showed an increased constitutive activation of SMAD2/3 (**Figure 47A**) in GILZ-Tg mouse skin. In addition, IMQ induced SMAD2/3 activation in both genotypes, although the increase was much higher in GILZ-Tg mice (**Figure 47A**). However, SMAD2/3 activity was unchanged in gut and spleen of GILZ-Tg vs GILZ-Wt mice, suggesting a specific activation of this signaling pathway in skin. Furthermore, we localized p-SMAD2/3 in epidermis and dermis, but the expression was mostly found in the epidermal keratinocytes (**Figure 47B**).

To evaluate whether the observed activation of TGF-β1/SMAD signaling pathway was due to its transcriptional up-regulation, we measured *Tgfβ1* mRNA levels in the skin of untreated or IMQ-treated

GILZ-Wt and GILZ-Tg mice at day 7. However, we found no changes between both treated and untreated genotypes in skin and spleen.

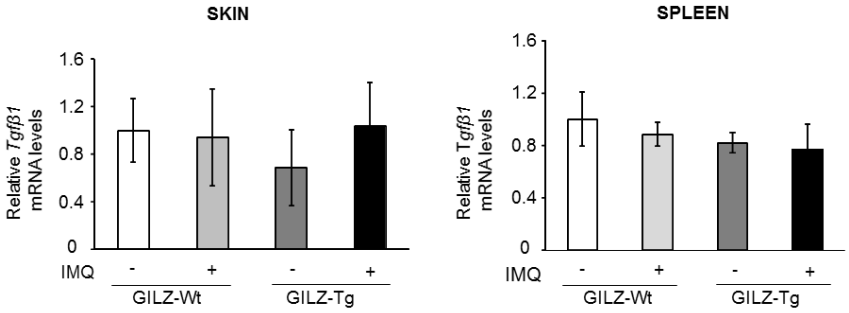

Figure 48. No changes in *Tgfβ1* mRNA levels in skin of GILZ-Tg *vs* GILZ-Wt mice. Relative mRNA levels of *Tgfβ1* were assessed by RT-QPCR in skin collected after IMQ treatment (7d). Mean values ± SD are shown. n= 6 per genotype and treatment.

Although we cannot rule out that *Tgfβ1* mRNA is induced in the skin by IMQ at earlier time-points, our data suggest that GILZ overexpression modulates TGF-β1 activity without altering its mRNA levels at day 7 of IMQ treatment.

TGF-β1 has been reported to impair the GC-induced transcriptional activation in human bronchial epithelial cells, reducing GILZ expression through ALK5-SMAD2/3 (Keenan *et al.*, 2014). This is consistent with our results in IMQ-treated GILZ-Wt skin, where *Gilz* mRNA levels are decreased maybe due to the activation of SMAD2/3. The fact that an increased activation of SMAD2/3 in IMQ-treated GILZ-Tg mice did not reduce the *Gilz* mRNA levels could be due to the lack of regulatory sequences in the *Gilz* transgene.

2.4. Contribution of immune cells and keratinocytes to psoriasis-like alterations in GILZ-Tg mice

IMQ stimulates dendritic cells to produce IL-23, which activates immune cells in the lymph nodes and induces the expression of IL-17A (Van der Fits *et al.*, 2009), thus activating signaling pathways in other cells (**Figure 49**).

We wondered whether immune cells in lymph nodes could contribute to the more severe skin phenotype in GILZ-Tg mice after IMQ treatment.

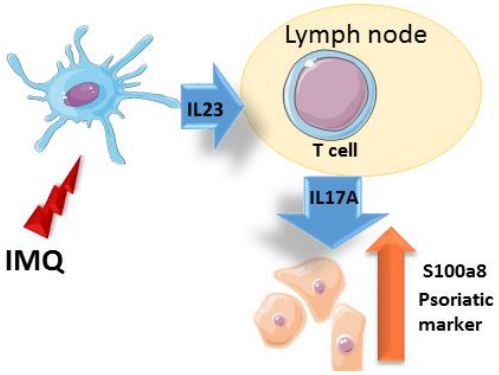

Figure 49. Scheme of relative contribution of immune cells and keratinocytes after IMQ treatment. IMQ induces the expression of IL-23 in dendritic cells, which stimulates T cells to secrete IL-17A, enhancing the subsequent activation of signaling pathways in several cell types and the up-regulation of the psoriasis marker *S100a8* in keratinocytes.

To address this question we topically applied IMQ on mouse ear and isolated the cells from brachial lymph nodes and cultured them. Subsequently, cultured cells were re-stimulated with Aldara (10 µg/ml) for 3 days and then IL-17A expression was measured in the

supernatant. We found that IMQ induced the expression of IL-17A in lymph node cells. However, this increase was not significantly different in GILZ-Tg compared to GILZ-Wt cells after IMQ treatment (**Figure 50**).

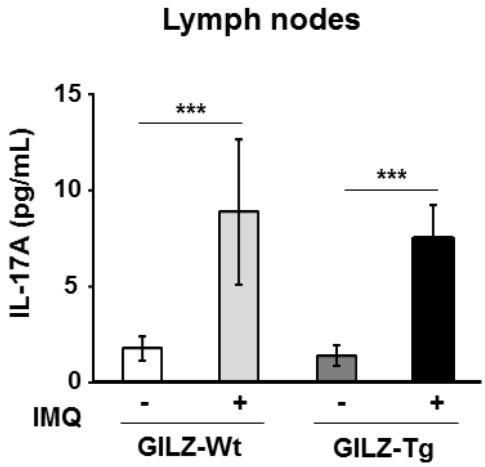

Figure 50. IL-17A is similarly up-regulated by IMQ in lymph node cells from GILZ-Tg and GILZ-WT mice. Immune cells were isolated from brachial lymph nodes of either vehicle- or IMQ-treated GILZ-Wt and GILZ-Tg mice after 7 d. Then lymph node cells were cultured and treated with Aldara 10 µg/ml. After 3 days, IL-17A was measured in the supernatant by Luminex technology. n = 3 mice per genotype and treatment. Mean values ± SD are shown. Post hoc Tukey test ***p<0.001.

The IL-17A is secreted by immune cells and activates other cells including keratinocytes and induces the expression of the psoriatic marker *S100a8* (Ha *et al.*, 2014; **Figure 49**). To assess the specific contribution of keratinocytes, we transfected an established mouse keratinocyte cell line with an empty vector or GILZ; then cells were treated with vehicle or IL-17A (**Figure 51**). IL-17A increased *S100a8* mRNA levels by 2-fold in the control keratinocytes. It is worth noting that in GILZ overexpressing keratinocytes *S100a8* expression was significantly up-regulated compared with the control keratinocytes (**Figure 51**).

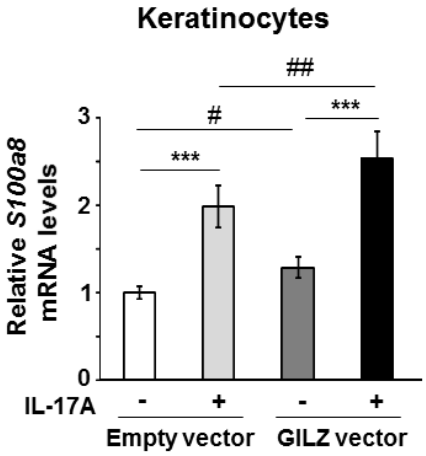

Figure 51. Increased up-regulation of *S100a8* mRNA levels in GILZ-transfected keratinocytes. Adult immortalized mouse keratinocytes were transfected with an empty vector or GILZ; then cells were treated with vehicle or IL-17A (100 ng/mL) for 24 h and relative mRNA levels of *S100a8* were assessed by RT-QPCR. Mean values ± SD are shown. n=at least 6 independent replicates per transfection and treatment. Post hoc Tukey test $^{\#}p<0.05$; $^{\#\#}p<0.01$; ***p<0.001. Asterisks: significance between treatments within each genotype; hashes: significance between genotypes in the same treatment group.

Next, we used cultured keratinocytes that were transfected with empty vector or GILZ and treated with vehicle or TGF-β1, and performed assays using a SMAD-luciferase reporter. In response to TGF-β1 (1 ng/μL, 20 h), we detected 26- to 31-fold activation of the SMAD-luc reporter (**Figure 52**, empty and GILZ vectors, respectively). Although GILZ overexpressing cells presented a tendency to increase activation of SMAD-luc activity after TGF-β1 treatment, it did not reach statistical significance compared with keratinocytes transfected with empty vector. The increased trend of SMAD activation observed *in vitro* in GILZ-transfected keratinocytes is consistent with our previous results in GILZ-Tg relative to GILZ-Wt skin.

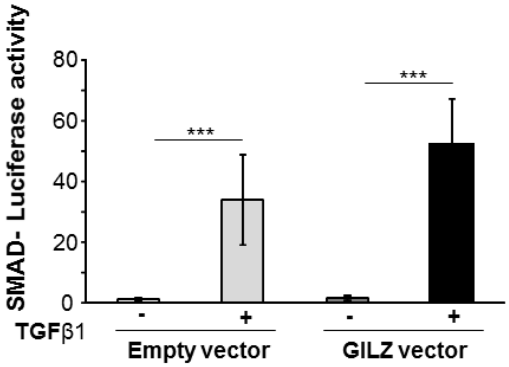

Figure 52. GILZ overexpression in cultured keratinocytes does not significantly increase the TGF-β1–induced SMAD activity. Cultured control or GILZ-overexpressing keratinocytes were treated with TGF-β1 (1 ng/μL, 20 h) and activation of a SMAD-luc reporter was determined. Mean values ± SD are shown. n=3 independent experiments.Post hoc Tukey test ***p<0.001.

Altogether our data demonstrated that the overexpression of GILZ exerted pro-inflammatory actions specifically in skin. Additionally, the *in vitro* data suggest that keratinocytes but not immune cells isolated from lymph nodes contributed to an altered skin phenotype in IMQ experiment in the presence of higher amounts of GILZ.

Finally, we propose a schematic model to summarize the effects of GILZ overexpression in IMQ-induced psoriasis mouse model (**Figure 53**).

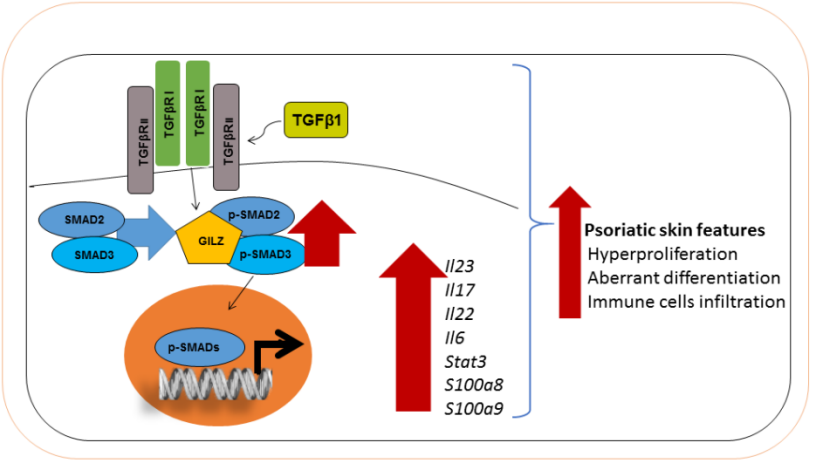

Figure 53. Consequences of generalized GILZ overexpression in the IMQ-induced mouse psoriasiform skin lesions. During the protocol of IMQ-induced mouse psoriasis, the generalized overexpression of GILZ led to the enhancement of pro-inflammatory cytokines (both systemically and in skin lesions), skin-specific overactivation of the TGF-β1/SMAD2/3 pathway, resulting in histopathological and molecular psoriasis-like alterations in GILZ-Tg mice.

Chapter V

Conclusions

Part I: Analysis of the functional cooperation of the glucocorticoid (GC) receptor (GR) and Krüppel-like factor (KLF) 4 in the regulation of gene expression in epidermal keratinocytes

1. GC primary transcriptional targets previously identified in ChIP-seq assays performed in cultured mouse keratinocytes contained overrepresented canonical binding motifs for GR (64%), AP-1 (28%) and KLF (43%), suggesting the importance of these TFs in the early response of epidermal keratinocytes to GCs.

2. GR and KLF4 cooperate to regulate the transcription of the anti-inflammatory genes *Gilz* and *Zfp36* by binding at adjacent genomic regulatory regions in response to GCs in epidermal keratinocytes, as well as during terminal differentiation, as demonstrated by gene expression and ChIP-QPCR analyses in cultured cells.

3. KLF4 is recruited to the genomic regulatory sequences of *Gilz* and *Zfp36* after GC treatment in keratinocytes in a GR-dependent manner. GR is also important for the induction of *Klf4*, *Gilz* and *Zfp36* during keratinocyte differentiation.

4. The presence of GR is necessary to terminal differentiation commitment in epidermal keratinocytes, which correlates with a downregulation of *Trp63* isoforms due to transcriptional regulation of both ΔNp63 and TAp63, which ultimately results in *Klf4* up-regulation.

Part II: Functional analysis of GILZ in transgenic mice with generalized overexpression: implications in psoriasis.

1. In the IMQ-induced psoriasis mouse model, GILZ overexpression promotes increased susceptibility to develop more severe psoriasiform skin lesions, as shown by the histopathological (epidermal thickening with immune infiltrates, abnormal differentiation) and molecular alterations (IL-23/Th17 axis).

2. Overexpression of GILZ correlates with skin-specific overactivation of TGF-β1/SMAD signaling, which contributes to the increased susceptibility to psoriasis.

3. Our data indicate that the pro-inflammatory actions of GILZ are specific to the skin as other organs such as the spleen did not show increased levels of Th17-dependent cytokines relative to controls and no significant difference in the circulating cytokines was observed.

4. Cultured keratinocytes overexpressing GILZ show significantly higher up-regulation of the psoriasis marker *S100a8* in response to IL-17 and an increased trend of TGF-β1-induced SMAD activation. Our results indicate that the overexpression of GILZ in keratinocytes *versus* immune cells contribute differently to the susceptibility to psoriasis.

Conclusiones

Parte I: Análisis de la cooperación funcional del receptor de glucocorticoides (GR) y Krüppel-like factor (KLF) 4 en la regulación de la expresión génica en queratinocitos epidérmicos

1. Las dianas transcripcionales primarias de glucocorticoides (GC) previamente idenificadas en experimentos de ChIP-seq realizados en queratinocitos en cultivo de ratón contenían una sobrerepresentación de motivos de unión canónicos para GR (64%), AP-1 (28%) y KLF (43%), lo que sugiere la importancia de estos factores de transcripción en la respuesta temprana a GCs en este tipo celular.

2. GR y KLF4 cooperan para regular la transcripción de los genes antiinflamatorios *Gilz* y *Zfp36* mediante la unión a las regiones reguladoras genómicas adyacentes en respuesta a GCs en queratinocitos epidérmicos, así como durante la diferenciación terminal, como se demuestra por la expresión génica y los análisis de ChIP-QPCR en células en cultivo.

3. KLF4 se recluta a las secuencias reguladoras genómicas de *Gilz* y *Zfp36* después del tratamiento con GC en queratinocitos de una manera dependiente de GR. Además, GR es importante para la inducción de *Klf4*, *Gilz* and *Zfp36* durante la diferenciación de queratinocitos.

4. La presencia de GR es necesaria para el compromiso de la diferenciación terminal en queratinocitos epidérmicos, lo que se correlaciona con una regulación negativa de las isoformas *Trp63* debido a la regulación transcripcional tanto de ΔNp63 como de TAp63, que finalmente da lugar a una regulación positiva de *Klf4*.

Parte II: Análisis funcional de GILZ en ratones transgénicos con sobreexpresión generalizada: implicaciones en psoriasis.

1. En el modelo de psoriasis en ratón inducido por IMQ, la sobreexpresión de GILZ promueve una mayor susceptibilidad a desarrollar lesiones cutáneas psoriasiformes más severas, como se demuestra por las alteraciones histopatológicas (engrosamiento epidérmico con infiltrados de células inmunes, diferenciación anormal) y alteraciones moleculares (eje IL-23/Th17).

2. La sobreexpresión de GILZ se correlaciona con la sobreactivación de la señalización de TGF-β1/SMAD específica de la piel, lo que contribuye a la susceptibilidad aumentada en la psoriasis.

3. Nuestros datos indican que las acciones pro-inflamatorias de GILZ son específicas de la piel, ya que otros órganos tales como el bazo no mostraron niveles aumentados de citocinas dependientes de Th17 en comparación con los controles y no se observó ninguna diferencia significativa en las citocinas circulantes.

4. Los queratinocitos en cultivo que sobreexpresan GILZ muestran una aumento significativamente mayor del marcador de psoriasis *S100a8* en respuesta a IL-17 y una tendencia aumentada de la activación de SMAD inducida por TGF-β1. Nuestros resultados indican que la sobreexpresión de GILZ en queratinocitos frente a células inmunitarias contribuyen de manera diferente a la susceptibilidad de la psoriasis.

References

Alonso-Merino E, Martín Orozco R, Ruíz-Llorente L, Martínez-Iglesias OA, Velasco-Martín JP, Montero-Pedrazuela A, Fanjul-Rodríguez L, Contreras-Jurado C, Regadera J, Aranda A. (2016). Thyroid hormones inhibit TGF-β signaling and attenuate fibrotic responses. *Proc Natl Acad Sci U S A*. 113(24):E3451-60.

Angel P, Szabowski A, Schorpp-Kistner M. (2011). Function and regulation of AP-1 subunits in skin physiology and pathology. *Oncogene.* 29(19):2413-23.

Ayroldi E, Riccardi C. (2009). Glucocorticoid-induced leucine zipper (GILZ): a new important mediator of glucocorticoid action. *FASEB J*. 23(11):3649-58.

Bayo P, Sanchis A, Bravo A, Cascallana JL, Buder K, Tuckermann J, Schütz G, Pérez P. (2008). Glucocorticoid receptor is required for skin barrier competence. Endocrinology. 149(3):1377-88.

Beaulieu E, Morand EF. (2011). Role of GILZ in immune regulation, glucocorticoid actions and rheumatoid arthritis. *Nat Rev Rheumatol*. 7(6):340-8.

Bereshchenko O, Coppo M, Bruscoli S, Biagioli M, Cimino M, Frammartino T, Sorcini D, Venanzi A, Di Sante M, Riccardi C. (2014). GILZ promotes production of peripherally induced Treg cells and mediates the crosstalk between glucocorticoids and TGF-β signaling. *Cell Rep*. 7(2):464-75.

Bernard FX, Morel F, Camus M, Pedretti N, Barrault C, Garnier J, Lecron JC. (2012). Keratinocytes under Fire of Proinflammatory Cytokines: Bona Fide Innate Immune Cells Involved in the Physiopathology of Chronic Atopic Dermatitis and Psoriasis. *J Allergy (Cairo)*. 2012:718725.

Betz UA, Vosshenrich CA, Rajewsky K, Müller W. (1996). Bypass of lethality with mosaic mice generated by Cre-loxP-mediated recombination. *Curr Biol*. 6(10):1307-16.

Biddie SC, John S, Sabo PJ, Thurman RE, Johnson TA, Schiltz RL, Miranda TB, Sung MH, Trump S, Lightman SL, Vinson C, Stamatoyannopoulos JA, Hager GL. (2011). Transcription factor AP1 potentiates chromatin accessibility and glucocorticoid receptor binding. *Mol Cell*. 43:145–155

Boehncke WH, Schön MP. (2015). Psoriasis. *Lancet*. 386(9997):983-94.

Brahma PK, Zhang H, Murray BS, Shu FJ, Sidell N, Seli E, Kallen CB. (2012). The mRNA-binding protein Zfp36 is upregulated by β-adrenergic stimulation and represses IL-6 production in 3T3-L1 adipocytes. *Obesity (Silver Spring)*. 20(1):40-7.

Brooks SA, Blackshear PJ. (2013). Tristetraprolin (TTP): interactions with mRNA and proteins, and current thoughts on mechanisms of action. *Biochim Biophys Acta*. 1829(6-7):666-79.

Budunova IV, Kowalczyk D, Pérez P, Yao YJ, Jorcano JL, Slaga TJ. (2003). Glucocorticoid receptor functions as a potent suppressor of mouse skin carcinogenesis. *Oncogene*. 22(21):3279-87.

Cannarile L, Cuzzocrea S, Santucci L, Agostini M, Mazzon E, Esposito E, Muià C, Coppo M, Di Paola R, Riccardi C. (2009). Glucocorticoid-induced leucine zipper is protective in Th1-mediated models of colitis. *Gastroenterology*. 136(2):530-41.

Cannarile L, Zollo O, D'Adamio F, Ayroldi E, Marchetti C, Tabilio A, Bruscoli S, Riccardi C. (2001). Cloning, chromosomal assignment and tissue distribution of human GILZ, a glucocorticoid hormone-induced gene. *Cell Death Differ*. 8(2):201-3.

Cascallana JL, Bravo A, Donet E, Leis H, Lara MF, Paramio JM, Jorcano JL, Pérez P. (2005). Ectoderm-targeted overexpression of the glucocorticoid receptor induces hypohidrotic ectodermal dysplasia. *Endocrinology*. 146(6):2629-38.

Cheng Q, Morand E, Yang YH. (2014). Development of novel treatment strategies for inflammatory diseases- similarities and

divergence between glucocorticoids and GILZ. *Front Pharmacol*. 5:169.

Chinenov Y, Coppo M, Gupte R, Sacta MA, Rogatsky I. (2014). Glucocorticoid receptor coordinates transcription factor-dominated regulatory network in macrophages. *BMC Genomics*. 15:656.

Cordani N, Pozzi S, Martynova E, Fanoni D, Borrelli S, Alotto D, Castagnoli C, Berti E, Viganò MA, Mantovani R. (2011). Mutant p53 subverts p63 control over KLF4 expression in keratinocytes. *Oncogene.* 30(8):922-32.

D'Adamio F, Zollo O, Moraca R, Ayroldi E, Bruscoli S, Bartoli A, Cannarile L, Migliorati G, Riccardi C. (1997). A new dexamethasone-induced gene of the leucine zipper family protects T lymphocytes from TCR/CD3-activated cell death. *Immunity*. 7(6):803-12.

De Bosscher K, Haegeman G. (2009). Minireview: latest perspectives on antiinflammatory actions of glucocorticoids. *Mol Endocrinol*. 23(3):281-91.

Denecker G, Ovaere P, Vandenabeele P, Declercq W. (2008). Caspase-14 reveals its secrets. *J Cell Biol*. 180(3):451-8.

DiDonato JA, Mercurio F, Karin M. (2012). NF-κB and the link between inflammation and cancer. *Immunol Rev*. 246(1):379-400.

Esposito E, Bruscoli S, Mazzon E, Paterniti I, Coppo M, Velardi E, Cuzzocrea S, Riccardi C. (2012). Glucocorticoid-induced leucine zipper (GILZ) over-expression in T lymphocytes inhibits inflammation and tissue damage in spinal cord injury. *Neurotherapeutics*. 9(1):210-25.

Fanti PA, Dika E, Vaccari S, Miscial C, Varotti C. (2006). Generalized psoriasis induced by topical treatment of actinic keratosis with imiquimod. *Int J Dermatol*. 45(12):1464-5.

Flutter B, Nestle FO. (2013). TLRs to cytokines: mechanistic insights from the imiquimod mouse model of psoriasis. *Eur J Immunol.* 43(12):3138-46.

Foster KW, Liu Z, Nail CD, Li X, Fitzgerald TJ, Bailey SK, Frost AR, Louro ID, Townes TM, Paterson AJ, Kudlow JE, Lobo-Ruppert SM, Ruppert JM. (2005). Induction of KLF4 in basal keratinocytes blocks the proliferation-differentiation switch and initiates squamous epithelial dysplasia. *Oncogene*. 24(9):1491-500.

Fu M, Blackshear PJ. (2017). RNA-binding proteins in immune regulation: a focus on CCCH zinc finger proteins. *Nat Rev Immunol*. 17(2):130-143.

Fuchs E, Horsley V. (2008). More than one way to the skin…*Genes Dev*. 22(8):976-85.

Fuchs E, Raghavan S. (2002). Getting under the skin of epidermal morphogenesis. *Nat Rev Genet*. 3(3):199-209.

Ghaleb AM, Yang VW. (2017). Krüppel-like factor 4 (KLF4): What we currently know. *Gene*. 611:27-37.

Greb JE, Goldminz AM, Elder JT, Lebwohl MG, Gladman DD, Wu JJ, Mehta NN, Finlay AY, Gottlieb AB.(2016). Psoriasis. *Nat Rev Dis Primers*. 2:16082.

Grine L, Dejager L, Libert C, Vandenbroucke RE. (2015). An inflammatory triangle in psoriasis: TNF, type I IFNs and IL-17. *Cytokine Growth Factor Rev*. 26(1):25-33.

Grine L, Steeland S, Van Ryckeghem S, Ballegeer M, Lienenklaus S, Weiss S, Sanders NN, Vandenbroucke RE, Libert C. (2016). Topical imiquimod yields systemic effects due to unintended oral uptake. *Sci Rep.* 6:20134.

Guttman-Yassky E, Krueger JG, Lebwohl MG. (2017). Systemic immune mechanisms in atopic dermatitis and psoriasis with implications for treatment. *Exp Dermatol*. [Epub ahead of print].

Ha HL, Wang H, Pisitkun P, Kim JC, Tassi I, Tang W, Morasso MI, Udey MC, Siebenlist U. (2014). IL-17 drives psoriatic inflammation via distinct, target cell-specific mechanisms. *Proc Natl Acad Sci U S A*. 111(33):E3422-31.

Haines RL, Lane EB. (2012). Keratins and disease at a glance. *J Cell Sci*. 125(Pt 17):3923-8.

Han G, Li F, Singh TP, Wolf P, Wang XJ. (2012). The pro-inflammatory role of TGFβ1: a paradox? *Int J Biol Sci*. 8(2):228-35.

Härdle L, Bachmann M, Bollmann F, Pautz A, Schmid T, Eberhardt W, Kleinert H, Pfeilschifter J, Mühl H. (2015). Tristetraprolin regulation of interleukin-22 production. *Sci Rep*. 5:15112.

Hennings H, Michael D, Cheng C, Steinert P, Holbrook K, Yuspa SH. (1980). Calcium regulation of growth and differentiation of mouse epidermal cells in culture. *Cell.* 19(1):245-54.

Herrlich P. (2001). Cross-talk between glucocorticoid receptor and AP-1. *Oncogene*. 20(19):2465-75.

Hoppstädter J, Diesel B, Eifler LK, Schmid T, Brüne B, Kiemer AK. (2012). Glucocorticoid-induced leucine zipper is downregulated in human alveolar macrophages upon Toll-like receptor activation. *Eur J Immunol*. 42(5):1282-93.

Hoste E, Denecker G, Gilbert B, Van Nieuwerburgh F, van der Fits L, Asselbergh B, De Rycke R, Hachem JP, Deforce D, Prens EP, Vandenabeele P, Declercq W. (2013). Caspase-14-deficient mice are more prone to the development of parakeratosis. *J Invest Dermatol*. 133(3):742-50.

Hoste E, Kemperman P, Devos M, Denecker G, Kezic S, Yau N, Gilbert B, Lippens S, De Groote P, Roelandt R, Van Damme P, Gevaert K, Presland RB, Takahara H, Puppels G, Caspers P, Vandenabeele P, Declercq W. (2011). Caspase-14 is required for filaggrin degradation to natural moisturizing factors in the skin. *J Invest Dermatol*. 131(11):2233-41.

Hvid M, Johansen C, Deleuran B, Kemp K, Deleuran M, Vestergaard C. (2011). Regulation of caspase 14 expression in keratinocytes by inflammatory cytokines--a possible link between reduced skin barrier function and inflammation? *Exp Dermatol.* 20(8):633-6.

Imberg-Kazdan K, Ha S, Greenfield A, Poultney CS, Bonneau R, Logan SK, Garabedian MJ. (2013). A genome-wide RNA interference screen identifies new regulators of androgen receptor function in prostate cancer cells. *Genome Res*. 23(4):581-91.

Jackson B, Tilli CM, Hardman MJ, Avilion AA, MacLeod MC, Ashcroft GS, Byrne C. (2005). Late cornified envelope family in differentiating epithelia--response to calcium and ultraviolet irradiation. *J Invest Dermatol.* 124(5):1062-70.

Jaubert J, Cheng J, Segre JA. (2003). Ectopic expression of kruppel like factor 4 (Klf4) accelerates formation of the epidermal permeability barrier. *Development*. 130(12):2767-77.

Johnson-Huang LM, Lowes MA, Krueger JG. (2012). Putting together the psoriasis puzzle: an update on developing targeted therapies. *Dis Model Mech.* 5(4):423-33.

Jones SA, Perera DN, Fan H, Russ BE, Harris J, Morand EF. (2015). GILZ regulates Th17 responses and restrains IL-17-mediated skin inflammation. *J Autoimmun*. 61:73-80.

Kanemaru K, Matsuyuki A, Nakamura Y, Fukami K. (2015). Obesity exacerbates imiquimod-induced psoriasis-like epidermal hyperplasia and interleukin-17 and interleukin-22 production in mice. *Exp Dermatol.* 24(6):436-42.

Katz JP, Perreault N, Goldstein BG, Lee CS, Labosky PA, Yang VW, Kaestner KH. (2002). The zinc-finger transcription factor Klf4 is required for terminal differentiation of goblet cells in the colon. *Development*. 129(11):2619-28.

Keenan CR, Mok JS, Harris T, Xia Y, Salem S, Stewart AG. (2014). Bronchial epithelial cells are rendered insensitive to glucocorticoid transactivation by transforming growth factor-beta1. *Respir Res*. 15:55.

Kim J, Krueger JG. (2017). Highly Effective New Treatments for Psoriasis Target the IL-23/Type 17 T Cell Autoimmune Axis. *Annu Rev Med*. 68:255-269.

Knoedler JR, Denver RJ. (2014). Krüppel-like factors are effectors of nuclear receptor signaling. *Gen Comp Endocrinol*. 203:49-59.

Koster MI, Lu SL, White LD, Wang XJ, Roop DR. (2006). Reactivation of developmentally expressed p63 isoforms predisposes to tumor development and progression. *Cancer Res*. 66(8):3981-6.

Latorre V, Sevilla LM, Sanchis A, Pérez P. (2013). Selective ablation of glucocorticoid receptor in mouse keratinocytes increases susceptibility to skin tumorigenesis. *J Invest Dermatol*. 133(12):2771-9.

Lawlor KT, Kaur P. (2015). Dermal contributions to human interfollicular epidermal architecture and self-renewal. *Int J Mol Sci*. 16(12):28098-107.

Lee Y, Jang S, Min JK, Lee K, Sohn KC, Lim JS, Im M, Lee HE, Seo YJ, Kim CD, Lee JH. (2012). S100A8 and S100A9 are messengers in the crosstalk between epidermis and dermis modulating a psoriatic milieu in human skin. *Biochem Biophys Res Commun*. 423(4):647-53.

Leis H, Page A, Ramírez A, Bravo A, Segrelles C, Paramio J, Barettino D, Jorcano JL, Pérez P. (2004). Glucocorticoid Receptor Counteracts Tumorigenic Activity of Akt in Skin through Interference with the Phosphatidylinositol 3-Kinase Signaling Pathway. *Mol Endocrinol*. 18(2):303-11.

Li AG, Wang D, Feng XH, Wang XJ. (2004). Latent TGFbeta1 overexpression in keratinocytes results in a severe psoriasis-like skin disorder. *EMBO J*. 23(8):1770-81.

Liu J, Zhang M, Niu C, Luo Z, Dai J, Wang L, Liu E, Fu Z. (2013). Dexamethasone inhibits repair of human airway epithelial cells mediated by glucocorticoid-induced leucine zipper (GILZ). *PLoS One.* 8(4):e60705.

Melino G. (2011). p63 is a suppressor of tumorigenesis and metastasis interacting with mutant p53. *Cell Death Differ.* 18(9):1487-99.

Menon GK. (2002). New insights into skin structure: scratching the surface. *Adv Drug Deliv Rev*. 54 Suppl 1:S3-17

Menter A, Korman NJ, Elmets CA, Feldman SR, Gelfand JM, Gordon KB, Gottlieb A, Koo JY, Lebwohl M, Lim HW, Van Voorhees AS, Beutner KR, Bhushan R. (2009). Guidelines of care for the management of psoriasis and psoriatic arthritis. Section 3. Guidelines of care for the management and treatment of psoriasis with topical therapies. *J Am Acad Dermatol*. 60(4):643-59.

Miranda TB, Voss TC, Sung MH, Baek S, John S, Hawkins M, Grøntved L, Schiltz RL, Hager GL. (2013). Reprogramming the chromatin landscape: interplay of the estrogen and glucocorticoid receptors at the genomic level. *Cancer Res*. 73(16):5130-9.

Molle C, Zhang T, Ysebrant de Lendonck L, Gueydan C, Andrianne M, Sherer F, Van Simaeys G, Blackshear PJ, Leo O, Goriely S. (2013). Tristetraprolin regulation of interleukin 23 mRNA stability prevents a spontaneous inflammatory disease. *J Exp Med*. 210(9):1675-84.

Naito M, Ohashi A, Takahashi T. (2015). Dexamethasone inhibits chondrocyte differentiation by suppression of Wnt/β-catenin signaling in the chondrogenic cell line ATDC5. *Histochem Cell Biol*. 144(3):261-72.

Newton R. (2014). Anti-inflammatory glucocorticoids: changing concepts. *Eur J Pharmacol*. 724:231-6.

Ngo D, Beaulieu E, Gu R, Leaney A, Santos L, Fan H, Yang Y, Kao W, Xu J, Escriou V, Loiler S, Vervoordeldonk MJ, Morand EF. (2013a). Divergent effects of endogenous and exogenous glucocorticoid-induced leucine zipper in animal models of inflammation and arthritis. *Arthritis Rheum*. 65(5):1203-12.

Ngo D, Cheng Q, O'Connor AE, DeBoer KD, Lo CY, Beaulieu E, De Seram M, Hobbs RM, O'Bryan MK, Morand EF. (2013b). Glucocorticoid-induced leucine zipper (GILZ) regulates testicular

FOXO1 activity and spermatogonial stem cell (SSC) function. *PLoS One*. 8(3):e59149.

Nyabi O, Naessens M, Haigh K, Gembarska A, Goossens S, Maetens M, De Clercq S, Drogat B, Haenebalcke L, Bartunkova S, De Vos I, De Craene B, Karimi M, Berx G, Nagy A, Hilson P, Marine JC, Haigh JJ. (2009). Efficient mouse transgenesis using Gateway-compatible ROSA26 locus targeting vectors and F1hybrid ES cells. *Nucleic Acids Res*. 37(7):e55.

Oakley RH, Cidlowski JA. (2013). The biology of the glucocorticoid receptor: new signaling mechanisms in health and disease. *J Allergy Clin Immunol*. 132(5):1033-44.

Patel S, Xi ZF, Seo EY, McGaughey D, Segre JA. (2006). Klf4 and corticosteroids activate an overlapping set of transcriptional targets to accelerate in utero epidermal barrier acquisition. *Proc Natl Acad Sci U S A*. 103(49):18668-73.

Patial S, Curtis AD 2nd, Lai WS, Stumpo DJ, Hill GD, Flake GP, Mannie MD, Blackshear PJ. (2016). Enhanced stability of tristetraprolin mRNA protects mice against immune-mediated inflammatory pathologies. *Proc Natl Acad Sci U S A*. 113(7):1865-70.

Pearson R, Fleetwood J, Eaton S, Crossley M, Bao S. (2008). Krüppel-like transcription factors: a functional family. *Int J Biochem Cell Biol*. 40(10):1996-2001.

Pérez P. (2011). Glucocorticoid receptors, epidermal homeostasis and hair follicle differentiation. *Dermatoendocrinol*. 3(3):166-74.

Pinheiro I, Dejager L, Petta I, Vandevyver S, Puimège L, Mahieu T, Ballegeer M, Van Hauwermeiren F, Riccardi C, Vuylsteke M, Libert C. (2013). LPS resistance of SPRET/Ei mice is mediated by Gilz, encoded by the Tsc22d3 gene on the X chromosome. *EMBO Mol Med.* 5(3):456-70.

Ramamoorthy S, Cidlowski JA. (2016). Corticosteroids: Mechanisms of Action in Health and Disease. *Rheum Dis Clin North Am*. 42(1):15-31, vii.

Rashmi P, Colussi G, Ng M, Wu X, Kidwai A, Pearce D. (2017). Glucocorticoid-induced leucine zipper protein regulates sodium and potassium balance in the distal nephron. *Kidney Int*. pii: S0085-2538(16)30654-8.

Raychaudhuri SP, Raychaudhuri SK. (2009). Biologics: target-specific treatment of systemic and cutaneous autoimmune diseases. *Indian J Dermatol*. 54(2):100-9.

Rizzo JM, Oyelakin A, Min S, Smalley K, Bard J, Luo W, Nyquist J, Guttman-Yassky E, Yoshida T, De Benedetto A, Beck LA, Sinha S, Romano RA. (2016). ΔNp63 regulates IL-33 and IL-31 signaling in atopic dermatitis. *Cell Death Differ*. 23(6):1073-85.

Romano RA, Smalley K, Magraw C, Serna VA, Kurita T, Raghavan S, Sinha S. (2012). ΔNp63 knockout mice reveal its indispensable role as a master regulator of epithelial development and differentiation. *Development*. 139(4):772-82.

Ronchetti S, Migliorati G, & Riccardi C. (2015). GILZ as a Mediator of the Anti-Inflammatory Effects of Glucocorticoids. *Frontiers in Endocrinology*. 6: 170.

Rowland BD, Peeper DS. (2006). KLF4, p21 and context-dependent opposing forces in cancer. *Nat Rev Cancer*. 6(1):11-23.

Sacta MA, Chinenov Y, Rogatsky I. (2016). Glucocorticoid Signaling: An Update from a Genomic Perspective. *Annu Rev Physiol*. 78:155-80.

Sano S, Chan KS, Carbajal S, Clifford J, Peavey M, Kiguchi K, Itami S, Nickoloff BJ, DiGiovanni J. (2005). Stat3 links activated keratinocytes and immunocytes required for development of psoriasis in a novel transgenic mouse model. *Nat Med*. 11(1):43-9.

Schöne S, Jurk M, Helabad MB, Dror I, Lebars I, Kieffer B, Imhof P, Rohs R, Vingron M, Thomas-Chollier M, Meijsing SH. (2016). Sequences flanking the core-binding site modulate glucocorticoid receptor structure and activity. *Nat Commun.* 7:12621.

Segre J. (2003). Complex redundancy to build a simple epidermal permeability barrier. *Curr Opin Cell Biol*. 15(6):776-82.

Segre JA, Bauer C, Fuchs E. (1999). Klf4 is a transcription factor required for establishing the barrier function of the skin. *Nat Genet*. 22(4):356-60.

Sen GL, Boxer LD, Webster DE, Bussat RT, Qu K, Zarnegar BJ, Johnston D, Siprashvili Z, Khavari PA. (2012). ZNF750 is a p63 target gene that induces KLF4 to drive terminal epidermal differentiation. *Dev Cell*. 22(3):669-77.

Sen GL, Reuter JA, Webster DE, Zhu L, Khavari PA. (2010). DNMT1 maintains progenitor function in self-renewing somatic tissue. *Nature*. 463(7280):563-7.

Sen GL, Webster DE, Barragan DI, Chang HY, Khavari PA. (2008). Control of differentiation in a self-renewing mammalian tissue by the histone demethylase JMJD3. *Genes Dev*. 22(14):1865-70.

Sevilla LM, Bayo P, Latorre V, Sanchis A, Pérez P. (2010). Glucocorticoid receptor regulates overlapping and differential gene subsets in developing and adult skin. *Mol Endocrinol*. 24(11):2166-78.

Sevilla LM, Latorre V, Sanchis A, Pérez P. (2013). Epidermal inactivation of the glucocorticoid receptor triggers skin barrier defects and cutaneous inflammation. *J Invest Dermatol*. 133(2):361-70.

Shi X, Hamrick M, Isales CM. (2007). Energy Balance, Myostatin, and GILZ: Factors Regulating Adipocyte Differentiation in Belly and Bone. *PPAR Res*. 2007:92501.

Shiraishi K, Yamasaki K, Nanba D, Inoue H, Hanakawa Y, Shirakata Y, Hashimoto K, Higashiyama S. (2007). Pre-B-cell leukemia transcription factor 1 is a major target of promyelocytic leukemia zinc-

finger-mediated melanoma cell growth suppression. *Oncogene*. 26(3):339-48.

Slominski A, Zbytek B, Nikolakis G, Manna PR, Skobowiat C, Zmijewski M, Li W, Janjetovic Z, Postlethwaite A, Zouboulis CC, Tuckey RC. (2013). Steroidogenesis in the skin: implications for local immune functions. *J Steroid Biochem Mol Biol*. 137:107-23.

Smoak K, Cidlowski JA. (2006). Glucocorticoids regulate tristetraprolin synthesis and posttranscriptionally regulate tumor necrosis factor alpha inflammatory signaling. *Mol Cell Biol*. 26(23):9126-35.

Soundararajan R, Wang J, Melters D, Pearce D. (2007). Differential activities of glucocorticoid-induced leucine zipper protein isoforms. *J Biol Chem*. 282(50):36303-13.

Srinivasan M, Janardhanam S. (2011). Novel p65 binding glucocorticoid-induced leucine zipper peptide suppresses experimental autoimmune encephalomyelitis. *J Biol Chem*. 286(52):44799-810.

Stojadinovic O, Lee B, Vouthounis C, Vukelic S, Pastar I, Blumenberg M, Brem H, Tomic-Canic M. (2007). Novel genomic effects of glucocorticoids in epidermal keratinocytes: inhibition of apoptosis, interferon-gamma pathway, and wound healing along with promotion of terminal differentiation. *J Biol Chem*. 282(6):4021-34.

Suarez PE, Rodriguez EG, Soundararajan R, Mérillat AM, Stehle JC, Rotman S, Roger T, Voirol MJ, Wang J, Gross O, Pétrilli V, Nadra K, Wilson A, Beermann F, Pralong FP, Maillard M, Pearce D, Chrast R, Rossier BC, Hummler E. (2012). The glucocorticoid-induced leucine zipper (gilz/Tsc22d3-2) gene locus plays a crucial role in male fertility. *Mol Endocrinol.* 26(6):1000-13.

Suárez-Fariñas M, Li K, Fuentes-Duculan J, Hayden K, Brodmerkel C, Krueger JG. (2012). Expanding the psoriasis disease profile: interrogation of the skin and serum of patients with moderate-to-severe psoriasis. *J Invest Dermatol.* 132(11):2552-64.

Surjit M, Ganti KP, Mukherji A, Ye T, Hua G, Metzger D, Li M, Chambon P. (2011). Widespread negative response elements mediate direct repression by agonist-liganded glucocorticoid receptor. *Cell*. 145(2):224-41.

Takahashi K, Tanabe K, Ohnuki M, Narita M, Ichisaka T, Tomoda K, Yamanaka S. (2007). Induction of pluripotent stem cells from adult human fibroblasts by defined factors. *Cell*. 131(5):861-72.

Tarutani M, Cai T, Dajee M, Khavari PA. (2003). Inducible actvation of Ras and Raf in adult epidermis. *Cancer Res.* 63(2):319-23.

Truong AB, Kretz M, Ridky TW, Kimmel R, Khavari PA. (2006). P63 regulates proliferation and differentiation of developmentally mature keratinocytes. *Genes Dev.* 20(22):3185-97.

Van Belle AB, de Heusch M, Lemaire MM, Hendrickx E, Warnier G, Dunussi-Joannopoulos K, Fouser LA, Renauld JC, Dumoutier L. (2012). IL-22 is required for imiquimod-induced psoriasiform skin inflammation in mice. *J Immunol*. 188(1):462-9.

Vago JP, Tavares LP, Garcia CC, Lima KM, Perucci LO, Vieira ÉL, Nogueira CR, Soriani FM, Martins JO, Silva PM, Gomes KB, Pinho V, Bruscoli S, Riccardi C, Beaulieu E, Morand EF, Teixeira MM, Sousa LP. (2015). The role and effects of glucocorticoid-induced leucine zipper in the context of inflammation resolution. *J Immunol*. 194(10):4940-50.

Vanbokhoven H, Melino G, Candi E, Declercq W. (2011). p63, a story of mice and men. *J Invest Dermatol*. 131(6):1196-207.

Van der Fits L, Mourits S, Voerman JS, Kant M, Boon L, Laman JD, Cornelissen F, Mus AM, Florencia E, Prens EP, Lubberts E. (2009). Imiquimod-induced psoriasis-like skin inflammation in mice is mediated via the IL-23/IL-17 axis. *J Immunol*. 182(9):5836-45.

Wagner EF, Schonthaler HB, Guinea-Viniegra J, Tschachler E. (2010). Psoriasis: what we have learned from mouse models. *Nat Rev Rheumatol*. 6(12):704-14.

Wasim M, Carlet M, Mansha M, Greil R, Ploner C, Trockenbacher A, Rainer J, Kofler R. (2010). PLZF/ZBTB16, a glucocorticoid response gene in acute lymphoblastic leukemia, interferes with glucocorticoid-induced apoptosis. *J Steroid Biochem Mol Biol*. 120(4-5):218-27.

Weikum ER, Knuesel MT, Ortlund EA, Yamamoto KR. (2017). Glucocorticoid receptor control of transcription: precision and plasticity via allostery. *Nat Rev Mol Cell Biol*. 18(3):159-174.

Wolk K, Witte E, Wallace E, Döcke WD, Kunz S, Asadullah K, Volk HD, Sterry W, Sabat R. (2006). IL-22 regulates the expression of genes responsible for antimicrobial defense, cellular differentiation, and mobility in keratinocytes: a potential role in psoriasis. *Eur J Immunol.* 36(5):1309-23.

Wrone-Smith T, Nickoloff BJ. (1996). Dermal injection of immunocytes induces psoriasis. *J Clin Invest*. 98(8):1878-87.

Yang A, Schweitzer R, Sun D, Kaghad M, Walker N, Bronson RT, Tabin C, Sharpe A, Caput D, Crum C, McKeon F. (1999). p63 is essential for regenerative proliferation in limb, craniofacial and epithelial development. *Nature*. 398(6729):714-8.

Yano S, Okochi H. (2005). Long-term culture of adult murine epidermal keratinocytes. *Br J Dermatol*. 153(6):1101-4.

Yoon HK, Li ZJ, Choi DK, Sohn KC, Lim EH, Lee YH, Kim S, Im M, Lee Y, Seo YJ, Lee JH, Kim CD. (2014). Glucocortioid receptor enhances involucrin expression of keratinocyte in a ligand-independent manner. *Mol Cell Biochem.* 390(1-2):289-95.

Zenz R, Eferl R, Kenner L, Florin L, Hummerich L, Mehic D, Scheuch H, Angel P, Tschachler E, Wagner EF. (2005). Psoriasis-like skin disease and arthritis caused by inducible epidermal deletion of Jun proteins. *Nature*. 437(7057):369-75.

Zhang Y, Meng XM, Huang XR, Wang XJ, Yang L, Lan HY. (2014). Transforming growth factor-β1 mediates psoriasis-like lesions via a Smad3-dependent mechanism in mice. *Clin Exp Pharmacol Physiol*. 41(11):921-32.

Annex

Supplementary table 1. Identification of genes by GR ChIP-seq in MPKs after treatment with Dex for 2 h. Gene symbol, chromosomal location with start and end coordinates, p-value, fold enrichment and over-represented GRE, KLF and AP-1 motifs in the genomic sequences are shown. Genome build: NCBI37/mm9.

Gene symbol	Chromosome	Start	End	Rangers p-value	Fold enrichment	GRE MOTIF	KLF4 MOTIF	AP-1 MOTIF
Nuak2	chr1	134232118	134232317	9,72E-06	4.32	GGCGGGATCATGATGTTCTT		TGAGGCAC
Per2	chr1	93332943	93333187	1,37E-05	4.38	GTGTACAGAATGTTCCTGGC	ACCCTCCCAACACA	
AK017125	chr1	174479923	174480155	9,72E-06	6.00	AGGGACAGAGAGTTCCTCAC	TTCGACCACACCCC	
Ralb	chr1	121406141	121406412	1,12E-05	6.19	AGGGACAGAGAGTCCAGGAC		CTGACTCA
Gpr161	chr1	167221724	167222033	1,14E-07	7.65		GGCCTGGGGCAGAG	
Itgb6	chr2	60538127	60538554	4,22E-17	11.46	CTGTACATTCTGTGCTGCTT	TGAGTGAGGAGAGG	
4921504E06Rik	chr2	19501545	19501811	4,18E-06	4.39	AGACAGAATGCTCTGTTCAG		GTGACTCA
Bcl2l1	chr2	152646064	152646334	7,15E-06	5.60	TGAAGGGACACTGTGTTCCC		
Camk1d	chr2	5300192	5300558	1,51E-09	5.87			
Tcp11l1	chr2	104545592	104545927	1,36E-08	5.94	GGGAACAATTTGTGCTTTAG		
Pax8	chr2	24295623	24295932	2,13E-06	6.87	GGAGGGCACATGATGTACAA		
Pxmp3	chr3	5860465	5860933	3,61E-31	3.76			
S100a10	chr3	93359908	93360134	1,49E-06	4.92	TAGCACAAAGGGTTCCTGGA	TGGGTGTGGCCTAG	GTGACTCA
Zbtb7b	chr3	89182446	89182778	4,11E-10	5.89	AGGAACAAGACATTCCCTGC		TGAGTCA
Wars2	chr3	98953903	98954240	4,22E-06	6.33			

Pdlim5	chr3	142035411	142035782	7,57E-10	6.62	AGGAACAGAATGTCCCAGAC		
4930503B20Rik	chr3	146320314	146320626	3,47E-08	9.59	AGGTACACAATGTTCCAGCA		ATGACTGA
Kif17	chr4	137834299	137834582	1,08E-10	12.67	GGCAGGGACATCATGTTCTT		GTGACTCA
Ror1	chr4	100074338	100075124	2,90E-09	2.88			
Errfi1	chr4	150156225	150156530	4,18E-06	3.03		TCCAGCCCCTTCCA	
Fblim1	chr4	141125922	141126201	9,65E-06	3.60	GCCCAGCACCTTCTGTTCCT	ACCAACCCCACTCC	
H6pd	chr4	149353824	149354095	9,71E-07	5.65		ATTTCCCCCACACT	
Trnp1	chr4	133047772	133048085	1,23E-07	6.06	AGCAGGAATGGAATGTTCCT	CCCTCCCCCACCCC	
Clic4	chr4	134842823	134843144	2,10E-09	7.04	CCGCAGAACGCCCTGTACCG	CTCTGCCCTACCCA	
BC051525	chr4	120289310	120289634	1,80E-08	8.91	GGGAACACAGAGTCCTGGGC	GGGGTGGGGACCTG	
MRPL33	chr5	31936399	31936639	2,32E-06	4.78	TAGAACAGAACATCCCTGGG		
Cdk8	chr5	147072423	147073058	1,80E-37	5.07			
Tgfbr3	chr5	107553054	107553284	4,22E-06	5.48	TAAGAGCACTGGCTGTTCTA	TAGGAGGGGCTGGA	ATGACTCA
Myo1h	chr5	114806670	114806890	1,37E-05	6.25	TGCAGGAATGGTATGTACCC		
Dok7	chr5	35480769	35481005	1,49E-06	6.85	CAGAGGCACGGAATGTTCCA		TGAGTCTC
Tead4	chr6	128232125	128232410	2,32E-06	5.11	GCAAAGAACTGTCTGTTCCT		
Hipk2	chr6	38785363	38785603	3,08E-06	5.40			ATTACTCA
Tra2a	chr6	49186327	49186699	2,02E-09	5.93			
D6Mm5e	chr6	82977825	82978166	9,71E-09	6.25	GCTGGGAACTCCCTGTACTT		
Klf13	chr7	71041798	71042157	3,81E-19	16.41	GGCGGGAACAGCATGTTCTC	TCTTGCCCAAGCCA	

Nr2f2	chr7	77181883	77182166	2,32E-06	3.91	CAAAAGAACAAGCTCTACTT		CTGACTCA
AK005418	chr7	117260441	117260742	2,44E-06	4.56	TAGTACATTTTGTACTGTAC	TGGGTGGGGAGAGA	
Hif3a	chr7	17643520	17643811	1,28E-06	5.71	GAGGACATTCCGTCCTGTAC	AGGGTGGGGGTAGG	
Adam12	chr7	141429168	141429410	1,23E-07	5.80			
Copb1	chr7	121346411	121346696	3,83E-07	5.87	AGGGAGCACAGTATGTTCCA		TGAGTAAC
Zfp36	chr7	29161349	29161679	5,12E-09	7.03	CCGCACATTCCGTCCTCGCC	CCCCGCCCCACCCC	
Abhd2	chr7	86481591	86481932	1,80E-08	9.93	AGGAACACCATGTCTTGGAG		AGTGACTCA
Hpgd	chr8	58899521	58899885	1,55E-08	4.81	ATGTACATTCTGTTCTATCC		TGACTCA
Banp	chr8	124552173	124552452	6,17E-08	8.42	AAGAACAGGCTGTGCTTGGT		TGAGTCAG
Rpl29	chr9	106314587	106314875	9,65E-06	4.35			
Zbtb16	chr9	48545557	48545850	1,27E-05	4.83	GGGTACAGTGTGTTCTTGGA		
2610002I17Rik	chr9	110183639	110183998	2,78E-06	5.34		AGCGTGGGGACCAT	
Gcnt3	chr9	69895676	69895947	2,13E-06	6.59	TTGTACATGCAGTCCCTGCA	CCCTGCCCAGCCCT	
Lars2	chr9	123370921	123371313	4,84E-14	6.89			
Rdx	chr9	51913510	51913850	8,86E-08	7.50	TGCAAGAACCAAATGTTCTC		CTGACTCA
Cadm1	chr9	47170423	47170735	2,31E-10	8.04	GGCCAGTACAATTTGTTCCT	TGGGAGGGGTTAAA	TGAGGCAG
Zbtb16	chr9	48531743	48532054	1,14E-07	8.22	GGCCAGCACTGCGTGTTCCT		
Lrrc20	chr10	60927817	60928113	2,70E-09	10.56	GCAGGGCACTCTGTGTACCC	TCGGGCCACACCCA	
Anapc16	chr10	59436847	59437177	1,13E-13	12.25	AGCCAGAACACAATGTTCTC	TGAGAGGGGAGCAG	
Unc5b	chr10	60268187	60268411	9,72E-06	4.74			

Mthfd1l	chr10	6240677	6240908	7,01E-07	5.20	ACACAGCACATAGTGTTCCT	AGTGTCTGGGAAGG	
Moxd1	chr10	24115898	24116160	6,54E-08	7.50	TCAGAGGACAGTATGTACTG		
Mknk2	chr10	80127345	80127590	1,23E-07	9.73	AGGAACAGCTCGTCCTAGGA		
Cdkn2aipnl	chr11	51729492	51729896	3,77E-20	15.48	CAGGACACCCAGTCCTTGGC	ATGGGCCTCACACC	
Krt42	chr11	100148262	100148483	2,82E-06	3.48		CCGCACCCCACCCA	
Sphk1	chr11	116394968	116395251	7,62E-06	4.13			
Spred2	chr11	19749912	19750178	2,32E-06	5.13			
Bahcc1	chr11	120114112	120114325	3,08E-06	5.45		GGGGTGGGGCAGAA	
Axin2	chr11	108872822	108873495	1,20E-37	5.56		ACGTGCCCCTCTCT	
Per1	chr11	68910392	68910729	3,69E-12	9.11	AGAACACGATGTTCC	CCCTGCCCCACATT	
Rin3	chr12	103566346	103566603	1,37E-05	3.65	AAGTACATTGTGTCCTTTGA	AGGGTGGGGGTGGG	
Tmx1	chr12	71725393	71725689	4,22E-06	3.70		AGGGTGTGGCCAGG	
Sel1l	chr12	93117331	93117677	2,83E-08	5.80	ACGAACATTCTGTCCCAGAA		ATGACTCA
Fntb	chr12	77984857	77985096	3,34E-08	7.25	AGGATCAGAATGTTCTGTAG	AGGGTGAGGCCCAG	
Id2	chr12	25854574	25854878	5,42E-07	8.06	CCTGAGCACTCGGTGTTCCT		GTGACTCA
Klf6	chr13	5840671	5840954	1,55E-08	4.56		ACCTTCCACTCCCT	
AK144747	chr13	90653450	90653801	3,83E-07	4.78	TCCCAGCACGGGGTGTTCTT		ATGACTCA
Gadd45g	chr13	52001484	52001729	2,09E-07	5.19		CCCAGCCCTACACT	
Jarid2	chr13	44964828	44965532	1,20E-11	5.23			
Hexb	chr13	97960356	97960722	2,32E-10	6.51	TCTCAGGACCGACTGACCCA		

Edn1	chr13	42469698	42470010	9,53E-12	8.60	AGCAGGGACACTGTGTTCCA	CACTTCCCCTCCCT	
AK014969	chr13	52345015	52345280	1,80E-08	8.61	ATGAACACGATGTTCCCTGA		
AK163289	chr15	61439750	61440210	1,41E-06	3.39			
Azin1	chr15	38386962	38387374	6,46E-06	3.70			
Micall1	chr15	78961912	78962221	6,46E-06	5.00	AGTCACAGAATGTCCTTGGC		GTGACTGA
Krt6a	chr15	101527943	101528370	3,20E-11	5.18	GCACTGCTCACTTTGTTCCC		
Eif3h	chr15	51562278	51562693	9,67E-15	8.55			
Grhl2	chr15	37122539	37122902	6,84E-09	8.81	GGGAACACTGTGTCCTTGTA		ATGACTCA
AK029404	chr16	31598964	31599440	1,81E-07	3.67	AGGTACATCCAGTCCTGAGC		
Cldn1	chr16	26249109	26249392	1,28E-06	4.78	TAGAACATTGTATTCTTGGC		TGAGTCAT
Cblb	chr16	52094783	52095062	4,34E-07	5.00	AAGTACAGACTGTCCCAGGA		TGAGTCTC
Gm608	chr16	44233196	44233452	5,46E-06	5.19	TGGTACAATTTGTGCCTGGT		TGAGTCAC
Zc3h7a	chr16	11144006	11144412	3,08E-18	6.39		GGCGTCGGGACCGG	
N6amt1	chr16	87268098	87268539	3,19E-15	6.47	GTCTGGCACTCACTCATCCA	TCCTGCCTGTCCCC	GTGACCCA
Filip1l	chr16	57391446	57391936	6,85E-34	7.16			
AK053957	chr16	25059331	25059626	1,55E-08	7.17		CCGGGCCCCTCCCA	
Parn	chr16	13507025	13507296	6,54E-08	7.42		ACTTGCCCCACCCA	
Gnb1l	chr16	18548113	18548426	1,51E-09	8.90			TGAGTCA
BC099513	chr16	95463156	95463451	9,73E-09	9.41	TCACGGAACATATTGTACCT		
Ets2	chr16	95881100	95881395	4,33E-10	9.69			

Mir715	chr17	39979802	39985914	0,00E+00	2.32			
AK138323	chr17	36368050	36368683	1,69E-09	6.43		CCCTCTCCCTCCCC	
Hsf2bp	chr17	32049262	32049584	1,29E-07	9.75	GGGAACATTCCGTCTCGGAA		
Mc2r	chr18	68851604	68851972	1,49E-09	3.87			
AK009639	chr19	5850058	5850453	9,03E-19	13.12	AGGTACATTCCGTTCCAGGC	TGGGCTGGGCCGGG	
Hoga1	chr19	42132954	42133253	6,17E-08	8.76	GGCCATCACACCGTGTTCCT		GTGACTCA
Tsc22d3	chrX	137063762	137064002	7,62E-06	7.67	GCAAAAAACAGAATGTTCAG	AGGGAGGGGCAGGA	TGAGTAAT
Frmd7	chrX	48321734	48321979	9,72E-06	7.88	GACAAGCACAGGCTGTTCTT		
Il1rapl1	chrX	84483537	84483912	1,21E-06	8.17			

List of figures

Chapter I: Introduction

Chapter IV: Results and Discussion

Part I

Part II